UNIVERSITY OF SOUTHAMPTON

School of Electronics and Computer Science

Faculty of Physical Sciences and Engineering

Mobile Social Networking Aided Content Dissemination in Heterogeneous Networks

by

Jie Hu

Draft thesis for the fulfilment of the PhD study in the subject of Wireless Communications

July 2013

SUPERVISORs:

Professor Lie-Liang Yang

Professor Lajos Hanzo

University of Southampton

Southampton SO17 1BJ

United Kingdom

Contents

Chapter 3

Stochastic Geometry In The Cellular Networks

3.1 Introduction

3.1.1 Background and Related Works

Nowadays, the global communication communities pay much attention to the network-level design for the cellular communication. In order to digest a huge amount of tele-traffic in the near future, heterogeneous networks [1] emerge as one of the key technique in the 5G system [2]. The heterogeneous networks consist of different sizes of cells, which include macro-cells providing a large coverage in the rural area, and pico-cells strengthening communication qualities in the urban area, as well as the femto-cell supporting the communication in homes or offices. Furthermore, apart from cellular communication, other communication techniques, which are operated on the unlicensed frequency bands, such as IEEE 802.11 protocol [3] aided Wi-Fi hotspots, can also be incorporated into the landscape of heterogeneous networks. All these centralised infrastructures can be jointly scheduled in order to provide high reliability and high quality of communication services.

There are two key issues attracting the most attention from both the academic and industrial communities. The first one is the user association issue [4] [5]. Since a lot of centralised infrastructure is deployed, a user may simultaneously appear within the technical coverage of many base stations (BSs). However, the qualities of the channels connecting the user to these BSs are different from each other. Even more, some BSs might reject the access of the user due to the congestions. Therefore, the network operator should jointly schedule all these BSs, analyse the qualities of the channels and finally make an optimal decision on which BS the user should be connected to, so as to optimise the communication performance. The second one is the tele-traffic offloading issue [6] [7]. In order to reduce the maintenance cost and increase the profit, network operators

always encourage their subscribers to give a higher priority to the low-cost IEEE 802.11 networks supported by numerous Wi-Fi hotspots. Making full exploitation of the Wi-Fi hotspots, network operators are capable of offloading a huge amount of tele-traffic from the congested cellular networks to the IEEE 802.11 networks, which may further improve their profits while accommodating more tele-traffic demand.

However, both the user association issue and the tele-traffic offloading issue are dominated by the geometrical positions of users. When the path loss (PL) is regarded as the only factor that attenuates the channel, a BS or a Wi-Fi hotspot, which is geometrically closest to the user, have to be employed by network operators for the sake of fulfilling the communication demand of the user. Even when the stochastic attenuation factors, such as shadowing and multipath fading, are taken into account, the closest centralised infrastructure are still more likely to be employed than their counterparts. As a result, stochastic geometry has been widely investigated in the context of heterogeneous networks. A commonly-accepted mathematical tool for modelling the geometric positions of the users around a transmitter is Poisson-Point-Process (PPP). The PPP is characterised by the following properties [8]:

- The number of isolated points falling within two regions A and B are independent random variables, if A and B do not intersect each other.
- The expected number of isolated points falling within a region A is the measure of the region A. This "measure" is often proportional to the area or volume of A, but some times more elaborate measures are used. The measure must be defined in such a way that the measure of the union of regions that do not intersect each other is simply the sum of their measures.

As a result, the probability of the number of X isolated nodes falling into region A is modelled by a Poisson distribution, which is expressed as

$$\Pr(X = x) = \frac{(\mu S_A)^x \mathrm{e}^{-\mu S_A}}{x!}. \tag{3.1}$$

Here, if A is regarded as a two-dimensional region, S_A in Eq.(3.1) is the area of the region A and μ is the points density. In the research of the heterogeneous networks, the region A is often modelled as a circular area, whose centre is a transmitter (e.g. BS or Wi-Fi hotspot) and whose radius is the transmission range of this transmitter. The number of receivers (e.g. mobile users) in this circular area is modelled by the PPP, while their positions are modelled by the *independent uniform distribution* in the circular area studied. As a result, the statistical properties of the random distance between the BS, which is at the centre of the circular area, and the MU, which roams within the circular area, are exploited for evaluating the downlink transmission performance at the receiver

end [9] [10] and for quantifying the uplink interference imposed on the transmitter end by these receivers [11] [12]. However, this common assumption in the current research ignores some other realistic scenarios. For example, the movement of mobile users (MUs) does not cover an area as large as the complete coverage of the BS. Realistically, their movements are always bounded by a specific region, such as an office or a building, and the BS can be at any arbitrary position inside or outside these bounded areas. Hence, it is vital for us to study the distance variation between the BS and the MU in these scenarios as well.

Apart from the heterogeneous networks, which are based on centralised infrastructure, direct communication amongst MUs can also be exploited in order to further improve the quality and the reliability of communication services. Direct communication amongst MUs can be realised by distributed IEEE 802.11 technique [13], the Bluetooth technique [14], and the LTE-aided device-to-device technique [15]. With the aid of direct communication amongst MUs, the distance between the transmitter and the receiver is significantly shortened, which remarkably reduces the adverse channel attenuation incurred by the PL. Direct communication amongst MUs are also capable of offloading the tele-traffic from the congested centralised infrastructure. In order to precisely analyse direct communication amongst MUs, it is crucial for us to study the distance variation between a pair of MUs, both of which move within a bounded area.

3.1.2 Novel Contributions and Chapter Organisations

In this chapter, the movement of MUs is characterised by the following uniform mobility model:

Definition 3.1 (Uniform mobility model)**.** *The position of the $i-th$ MSN users during the $t-th$ time interval is denoted by $\mathbf{P}_i(t)$, which obeys a stationary and ergodic process with a stationary uniform distribution in a bounded area. Moreover, the positions of different MUs are independent and identically distributed (i.i.d.).*

This mobility model has been widely used for analysing the relevant performance metrics in the mobile ad hoc networks [16] [17].

The main contribution and the structure of this chapter are summarised as below:

- In Section 3.2, we recall the distance distribution between the BS and the MU, when the BS is at the centre of a circular cell, while the MU roam within the circular area by following the uniform mobility model. Furthermore, we also provide the cdf and the pdf in closed-form formulas for the random distance between the BS and the MU, when the cell is modelled by a *l*-sided regular polygon.

- In Section 3.3, we obtain the cdfs and the pdfs of the random distance between the BS and the MU in closed-form formulas, when the BS is at an arbitrary position, outside/inside a bounded area, while the MU roams within the bounded area by obeying the uniform mobility model. The bounded area is modelled as a circular and a square area, respectively.
- In Section 3.4, we analyse the cdfs and the pdfs of the random distance between a pair of MUs, both of which roam within a circular/square area.
- In Section 3.5, by exploiting the derived distance distribution, we characterise the statistical properties of the time-variant PL, and the spectral efficiency of the single-hop transmission, as well as the spectral efficiency of the multicast transmission.
- In Section 3.6, numerical results are provided for validating the accuracy of our theoretical analysis and for revealing some insights on network design.
- Finally, we conclude this chapter in Section 3.7.

3.2 Distance distribution between BS and MU roaming in a cell

In this scenario, a BS is assumed to be located at the centre of a cell, while MUs associated with this BS may appear at any locations of this specific cell with equal probability. Let us first discuss the distribution of the random distance between the BS and a MU for this scenario. This distance distribution heavily depends on a specific shape of the cellular area. Apart from the maximum allowable transmit power of the BS, the size and the shape of the cellular area are determined by the minimum strength of the received signal, which is required by a MU in order to successfully recover the contaminated signal induced by various channel attenuations. Theoretically speaking, when only path loss is considered, the coverage of a cell should be a circular area, as shown in Figure 1(a), because there are not any uncertainties affecting the range of the BS. However, when uncertainties are introduced by shadowing and multipath fading, the coverage of a cell should be in an irregular shape, as shown in Figure 1(b). Concerning the realistic implementation of cellular networks, regular hexagon is invoked for modelling the coverage a specific cell, as shown in Figure 1(c).

In this scenario, the MU obeys the uniform mobility model given by Definition 3.1 within a bounded cellular area, while the BS is at the centre of the studied cellular area. Two basic shapes model the coverage area of a cell, namely circle and l-sided regular polygon. The statistical properties of the random distance between the BS and the MU are given by the following theorems:

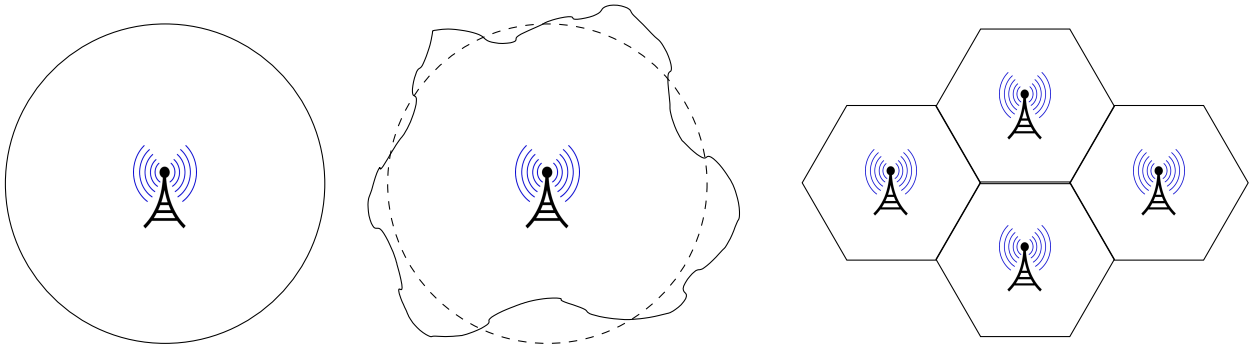

(a) Circular coverage (b) Irregular coverage (c) Hexagon for realistic implementation

Figure 3.1: Various shapes of coverage area of a cell

Theorem 3.1 (Circular cell)**.** *If a cell is modelled by a circular area having a radius of r, the cumulative distribution function (cdf) of the random distance Y_b between the centre-positioned BS and a MU obeying the uniform mobility model is given by*

$$F_{Y_b}(y_b) = \begin{cases} \frac{y_b^2}{r^2}, & 0 \leq y_b \leq r, \\ 1, & y_b > r. \end{cases} \tag{3.2}$$

Furthermore, the corresponding probability density function (pdf) can be derived as

$$f_{Y_b}(y_b) = \begin{cases} \frac{y_b^2}{r^2}, & 0 \leq y_b \leq r, \\ 0, & \textit{otherwise}. \end{cases} \tag{3.3}$$

Proof. Please refer to Section 3.A.1 for the detailed proof. □

Furthermore, integrating Y_b over the pdf (3.3), the average distance can be derived as

$$E[Y_b] = \int_{y_b} y_b f_{Y_b}(y_b) dy_b = \int_0^r y_b \cdot \frac{2y_b}{r^2} dy_b = \frac{2}{3} r. \tag{3.4}$$

The cdf and the pdf given by Theorem 3.1 have already been widely adopted by the communication communities for the path loss analysis [], for the interference analysis [], as well as for the wireless multicast/broadcast outage analysis [].

Theorem 3.2. *If a cell is modelled by a l-sided ($l \geq 3$) regular polygon having r as its radius*[1]*, the cdf of the random distance Y_b between the centre-positioned BS and a MU obeying the uniform*

[1]The radius of a l-sided regular polygon is the distance from the centre to one of the vertices.

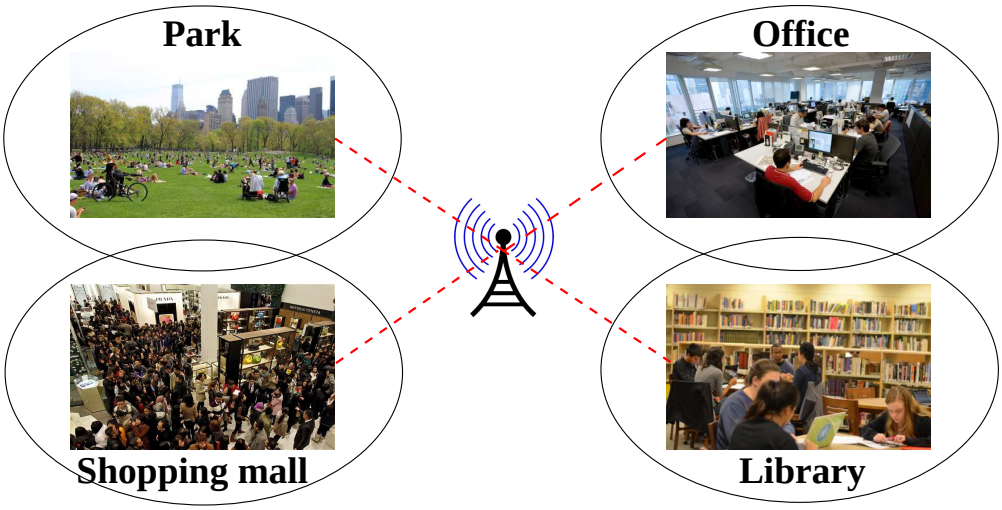

Figure 3.2: MUs move within some bounded areas

mobility model is given by

$$F_{Y_b}(y_b) = \begin{cases} \dfrac{\pi}{l\tan\theta}\left(\dfrac{y_b}{r\cos\theta}\right)^2, & 0 \le y_b \le r\cos\theta, \\ \dfrac{1}{l\tan\theta}\left(\dfrac{y_b}{r\cos\theta}\right)^2\left(\pi - l\arccos\left(\dfrac{y_b}{r\cos\theta}\right)^{-1}\right) & \\ \quad + \dfrac{1}{\tan\theta}\sqrt{\left(\dfrac{y_b}{r\cos\theta}\right)^2 - 1}, & r\cos\theta < y_b \le r \\ 1, & \textit{otherwise}. \end{cases} \tag{3.5}$$

Furthermore, the corresponding pdf can be derived as

$$f_{Y_b}(y_b) = \begin{cases} \dfrac{2\pi}{lr\sin\theta}\cdot\dfrac{y_b}{r\cos\theta}, & 0 \le y_b \le r\cos\theta, \\ \dfrac{2}{lr\sin\theta}\dfrac{y_b}{r\cos\theta}\left(\pi - l\arccos\left(\dfrac{y_b}{r\cos\theta}\right)^{-1}\right), & r\cos\theta < y_b \le r, \\ 0, & \textit{otherwise}. \end{cases} \tag{3.6}$$

Proof. Please refer to Section 3.A.2 for the detailed proof. □

3.3 Random distance between BS and MU roaming in a bounded area

Sometimes the assumption that MUs may appear at any positions of the cell is not quite realistic because in some real scenarios, the movement of a MU is bounded within a specific area. As shown in Figure 3.2, we list some typical bounded area as examples. Families and friends may

enjoy the beautiful sunshine, have picnics and do sports in a park on weekends. In this scenario, movements of people are bounded within the territory of a park. Employees work in their offices every day, have routine meetings with their colleagues in meeting rooms and enjoy their short break in entertaining rooms. In this scenario, movements of people are bounded within the building where their company is located. Students walk between shelves of a library in order to find their interested books, they watch some multimedia materials in multimedia rooms, and they take some breath in the cafe bar. In this scenario, movements of people are bounded within the building where a library is located. Before Christmas, people wanders in the shopping mall in order to find some attractive deals and to prepare Christmas gifts for their friends and relatives. In this scenario, movements of people are also bounded within the building of the shopping mall. As a result, for the sake of further analysing and predicting the performance of wireless communication between a BS and a MU, it is vital for us to obtain the statistical properties of the random distance between a BS and a MU when the movement of the MU is restricted within a specific area.

Corresponding to the aforementioned realistic scenarios, we assume that a MU roams within a bounded area by following the uniform mobility model. Without loss of generality, we model the bounded area as a circular area and a square area, and derive the cdfs or pdfs of the random distance Y_b between a BS and a MU for these two scenarios, respectively.

3.3.1 Mobile users roam in a circular area

First of all, we model the bounded area by a circular area having point O as its centre and having r meters as its radius. We denote this circular area as $\odot(O, r)$. A BS is located at point B, which is d metres away from the centre O of the circular area. A MU roams within the circular area $\odot(O, r)$ by obeying the uniform mobility model. In the following two theorems, we provide the cdfs and pdfs of the random distance Y_b between the BS and the MU for the scenario that the BS is outside the circular area $\odot(O, r)$ and the scenario that the BS is inside the circular area $\odot(O, r)$, respectively.

Theorem 3.3. *If the BS is outside the studied circular area $\odot(O, r)$, namely $d > r$, the cdf of the*

random distance Y_b between the BS and the MU is expressed as

$$F_{Y_b}(y_b) = \begin{cases} 0, & 0 \le y_b \le d-r, \\ \frac{1}{\pi}\left[\arccos\left(\frac{r^2+d^2-y_b^2}{2rd}\right) + \frac{y_b^2}{r^2}\arccos\left(\frac{y_b^2+d^2-r^2}{2y_bd}\right)\right. & \\ \quad \left. -\frac{1}{2r^2}\sqrt{4r^2d^2-(r^2+d^2-y_b^2)^2}\right], & d-r < y_b \le d+r, \\ 1, & y_b > d+r. \end{cases} \tag{3.7}$$

Furthermore, the corresponding pdf can be derived as

$$f_{Y_b}(y_b) = \begin{cases} \frac{2y_b}{\pi r^2}\arccos\left(\frac{y_b^2+d^2-r^2}{2y_bd}\right), & d-r \le y_b \le d+r, \\ 0, & \textit{otherwise}. \end{cases} \tag{3.8}$$

Proof. Please refer to Appendix 3.B.1 for the detailed proof. □

Theorem 3.4. *If the BS is inside the studied circular area $\odot(O,r)$, namely $d \le r$, the cdf of the random distance Y_b between the BS and the MU is expressed as*

$$F_{Y_b}(y_b) = \begin{cases} \frac{y_b^2}{r^2}, & 0 \le y_b \le r-d, \\ \frac{1}{\pi}\left[\arccos\left(\frac{r^2+d^2-y_b^2}{2rd}\right) + \frac{y_b^2}{r^2}\arccos\left(\frac{y_b^2+d^2-r^2}{2y_bd}\right)\right. & \\ \quad \left. -\frac{1}{2r^2}\sqrt{4r^2d^2-(r^2+d^2-y_b^2)^2}\right], & r-d < y_b \le r+d, \\ 1, & y_b > d+r. \end{cases} \tag{3.9}$$

Furthermore, the corresponding pdf can be derived as

$$f_{Y_b}(y_b) = \begin{cases} \frac{2y_b}{r^2}, & 0 \le y_b \le r-d, \\ \frac{2y_b}{\pi r^2}\arccos\left(\frac{y_b^2+d^2-r^2}{2y_bd}\right), & r-d < y_b \le d+r, \\ 0, & \textit{otherwise}. \end{cases} \tag{3.10}$$

For the special case of $d = 0$, the BS is at the centre of the studied circular area $\odot(O,r)$. Hence, the cdf and the pdf of the random distance Y_b are the same as Theorem 3.1.

Proof. Please refer to Appendix 3.B.2 for the detailed proof. □

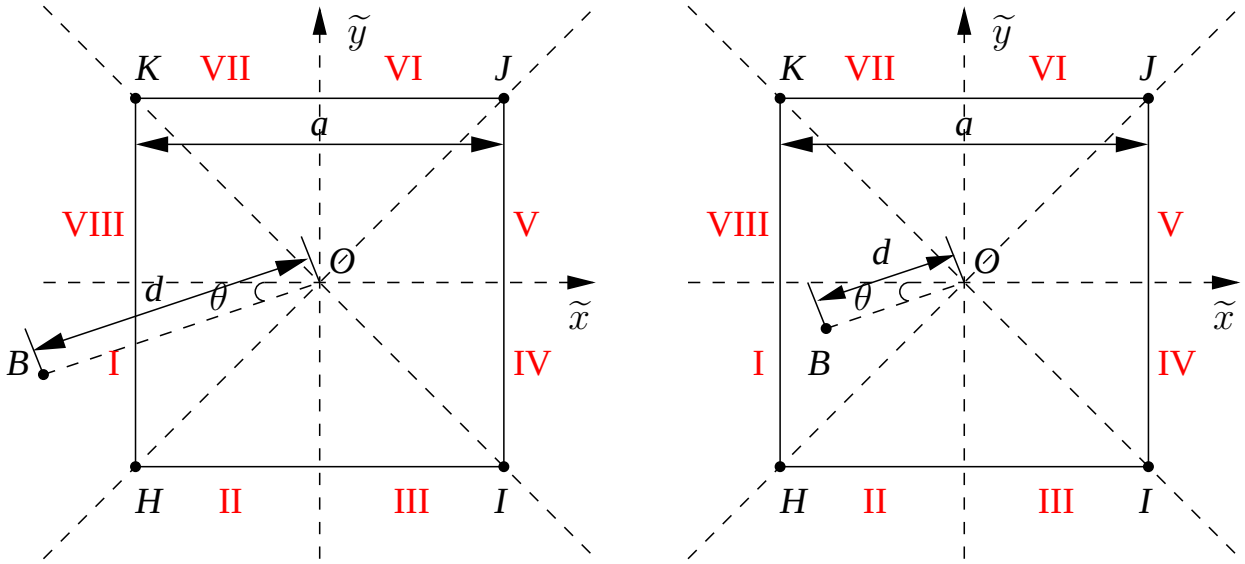

(a) BS is outside the square: $d\cos\theta > \frac{a}{2}$

(b) BS is inside the square: $d\cos\theta \leq \frac{a}{2}$

Figure 3.3: A square area

3.3.2 Mobile users roam in a square area

Let us model the bounded area as a square having point O as its centre and having a as its side-length. This square area is denoted by $\square HIJK$, as shown in Figure 3.3(a)(b). The area of the studied square is $S_{\square HIJK} = \overline{HI}^2 = a^2$. As shown in Figure 3.3(a)(b), we divide the whole space into eight subspaces from I to VIII. Due to the symmetrical property of the square area, if the BS finds a position in a specific subspace, it can also find corresponding symmetrical positions within the other subspaces, respectively. The random distances between the roaming MU and these symmetrical positions of the BS share the same statistical properties. As a result, we only have to study the scenario that the BS is located in a specific subspace, say space I, as shown in Figure 3.3(a)(b). The derived cdf or pdf of the random distance Y_b is capable of generalising the statistical characteristics for Y_b, regardless of which specific subspace the BS is in.

A BS is located at point B, as shown in Figure 3.3(a)(b). The position of point B is determined by a tuple (d, θ), where d is the distance between point B and the centre O of $\square HIJK$ and θ is the angle between the straight line $\overline{OB}$ and the horizontal line, as shown in Figure 3.3(a)(b). In order to make sure that the BS is located in subspace I, the angle θ should be in the range of $[0, \pi/4]$. No matter where the BS is, its position can be equivalently converted to a tuple (d, θ) and the corresponding subspace can be converted to subspace I. Let us consider a two dimensional surface $\widetilde{x}O\widetilde{y}$, as shown in Figure 3.3(a)(b). The centre O of the square $\square HIJK$ is also the origin of the

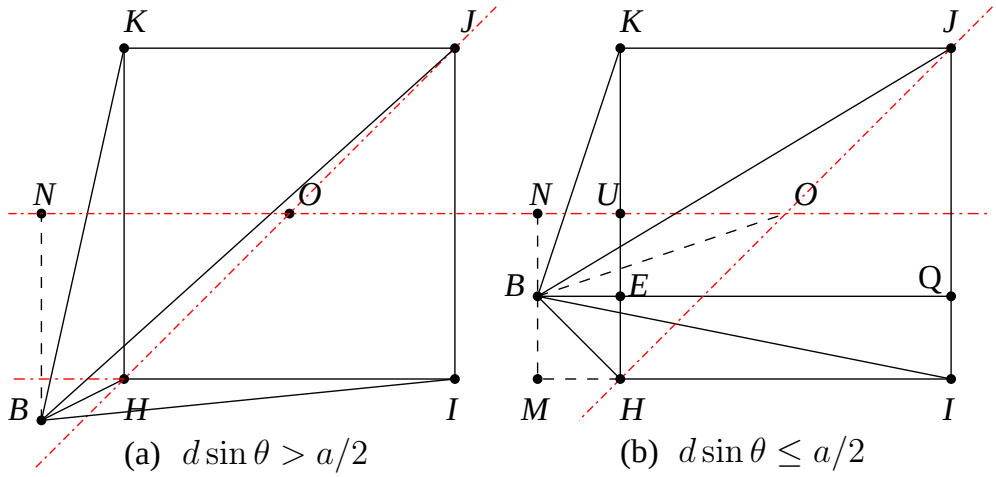

Figure 3.4: BS is outside the bounded square area

surface $\widetilde{x}O\widetilde{y}$. Given an arbitrary position of the BS, which is denoted as the coordinates $(\widetilde{x}_B, \widetilde{y}_B)$, we can convert the conventional coordinates into a tuple (d, θ) associated with $\theta \in [0, \pi/4]$, which are expressed as the following equations:

$$d = \sqrt{\widetilde{x}_B^2 + \widetilde{y}_B^2},\ \cos\theta = \frac{\max\{|\widetilde{x}_B|, |\widetilde{y}_B|\}}{\sqrt{\widetilde{x}_B^2 + \widetilde{y}_B^2}},\ \sin\theta = \frac{\min\{|\widetilde{x}_B|, |\widetilde{y}_B|\}}{\sqrt{\widetilde{x}_B^2 + \widetilde{y}_B^2}} \tag{3.11}$$

Furthermore, the horizontal distance between point B and the centre O is derived as $d\cos\theta$. If we have $d\cos\theta > \overline{HI}/2 = a/2$, as shown in Figure 3.3(a), the position B of the BS is outside the studied square area $\square HIJK$. If we have $d\cos\theta \leq \overline{HI}/2 = a/2$, as shown in Figure 3.3(b), the position B of the BS is inside the studied square area $\square HIJK$ or on its boundary. A MU moves within $\square HIJK$ by obeying the uniform mobility model. In the following sections, we will discuss the statistical properties of the random distance Y_b between the BS and the MU for the scenarios that the BS is outside the square area and that the BS is inside the square area, respectively.

3.3.2.1 The BS is outside the square area

Let us first consider the scenario that the BS is outside the square area. In this scenario, the horizontal distance from point B to the centre O is longer than the half of the side length, say $\overline{ON} = d\cos\theta > \overline{HI}/2 = a/2$, as shown in Figure 3.4(a)(b). However, we have to consider two different cases for the vertical distance from point B to the centre O, which is expressed as $\overline{BN} = d\sin\theta$. If the vertical distance is longer than the half of the side length, say $d\sin\theta > a/2$, the position B of the BS is below the horizontal line $\overline{HI}$, as shown in Figure 3.4(a). In contrast, if the vertical distance is shorter than the half of the side length, say $d\sin\theta \leq a/2$, the position B

of the BS is above the horizontal line $\overline{HI}$, as shown in Figure 3.4(b). In this section, we focus on the derivation of the cdf or the pdf of the random distance Y_b for the case $d\sin\theta \leq a/2$, as shown in Figure 3.4(b). Before taking any further actions, we have to obtain some important geometrical properties of the studied scenario, namely the distances from point B to all the vertices as well as to all the sides of $\square HIJK$. Note that the formulas derived for $d\sin\theta \leq a/2$ are also capable of expressing the corresponding distances for $d\sin\theta > a/2$.

As shown in Figure 3.4(b), given the position of point B, which is defined by the tuple (d,θ), the horizontal distance from point B to the centre O is $\overline{ON} = d\cos\theta$, and the corresponding vertical distance is $\overline{BN} = d\sin\theta$. As a result, the distance from B to the side $\overline{KH}$ is $\overline{BE} = \overline{NU} = \overline{ON} - \overline{OU} = d\cos\theta - a/2$. The distance from B to the side $\overline{HI}$ is $\overline{BM} = \overline{NM} - \overline{NB} = a/2 - d\sin\theta$. The distance from B to the side $\overline{IJ}$ is $\overline{BQ} = \overline{BE} + \overline{EQ} = \overline{BE} + \overline{HI} = d\cos\theta + a/2$. The distance from B to the side JK is derived as $\overline{EK} = \overline{KU} + \overline{UE} = \overline{KU} + \overline{BN} = a/2 + d\sin\theta$.

Furthermore, Pythagorean theorem is invoked for calculating the distances from point B to all the vertices of $\square HIJK$. The distance from B to vertex H is expressed as

$$\begin{aligned}\overline{BH} &= \sqrt{\overline{BM}^2 + \overline{MH}^2} = \sqrt{\overline{BM}^2 + \overline{BE}^2} \\ &= \sqrt{\left(\frac{a}{2} - d\sin\theta\right)^2 + \left(d\cos\theta - \frac{a}{2}\right)^2} \\ &= \sqrt{a^2/2 + d^2 - ad(\sin\theta + \cos\theta)}. \end{aligned} \tag{3.12}$$

The distance from B to vertex I is expressed as

$$\begin{aligned}\overline{BI} &= \sqrt{\overline{BM}^2 + \overline{MI}^2} = \sqrt{\overline{BM}^2 + \overline{BQ}^2} \\ &= \sqrt{\left(\frac{a}{2} - d\sin\theta\right)^2 + \left(\frac{a}{2} + d\cos\theta\right)^2} \\ &= \sqrt{a^2/2 + d^2 + ad(\cos\theta - \sin\theta)}. \end{aligned} \tag{3.13}$$

The distance from B to vertex J is expressed as

$$\begin{aligned}\overline{BJ} &= \sqrt{\overline{BQ}^2 + \overline{QJ}^2} = \sqrt{\overline{BQ}^2 + \overline{EK}^2} \\ &= \sqrt{\left(\frac{a}{2} + d\cos\theta\right)^2 + \left(\frac{a}{2} + d\sin\theta\right)^2} \\ &= \sqrt{a^2/2 + d^2 + ad(\cos\theta + \sin\theta)}. \end{aligned} \tag{3.14}$$

The distance from B to vertex K is expressed as

$$\begin{aligned}\overline{BK} &= \sqrt{\overline{BE}^2 + \overline{EK}^2} \\ &= \sqrt{\left(d\cos\theta - \frac{a}{2}\right)^2 + \left(\frac{a}{2} + d\sin\theta\right)^2} \\ &= \sqrt{a^2/2 + d^2 - ad(\cos\theta - \sin\theta)}. \end{aligned} \tag{3.15}$$

Based on these geometrical properties, the cdf $F_{Y_b}(y_b)$ is given by the following theorem:

Theorem 3.5. *If the position B of the BS is outside the square area $\square HIJK$ and is above the horizontal line $\overline{HI}$, namely $d\sin\theta \le a/2 \le d\cos\theta$, within which the MU roams by obeying the uniform mobility model, as shown in Figure 3.4(b), the cdf of the random distance Y_b between the BS and the MU is expressed by the following equation:*

$$F_{Y_b}(y_b) = \begin{cases} F^{I}_{Y_b}(y_b), & 0 \le y_b \le d\cos\theta - \frac{a}{2}, \\ F^{II}_{Y_b}(y_b), & d\cos\theta - \frac{a}{2} < y_b \le \sqrt{a^2/2 + d^2 - ad(\sin\theta + \cos\theta)}, \\ F^{III}_{Y_b}(y_b), & \sqrt{a^2/2 + d^2 - ad(\sin\theta + \cos\theta)} < y_b \le \sqrt{a^2/2 + d^2 - ad(\cos\theta - \sin\theta)}, \\ F^{IV}_{Y_b}(y_b), & \sqrt{a^2/2 + d^2 - ad(\cos\theta - \sin\theta)} < y_b \le d\cos\theta + \frac{a}{2}, \\ F^{V}_{Y_b}(y_b), & d\cos\theta + \frac{a}{2} < y_b \le \sqrt{a^2/2 + d^2 + ad(\cos\theta - \sin\theta)}, \\ F^{VI}_{Y_b}(y_b), & \sqrt{a^2/2 + d^2 + ad(\cos\theta - \sin\theta)} < y_b \le \sqrt{a^2/2 + d^2 + ad(\cos\theta + \sin\theta)}, \\ F^{VII}_{Y_b}(y_b), & y_b > \sqrt{a^2/2 + d^2 + ad(\cos\theta + \sin\theta)}. \end{cases} \tag{3.16}$$

where $F^{I}_{Y_b}(y_b) = 0$ and $F^{VII}_{Y_b}(y_b) = 1$, while $F^{II}_{Y_b}(y_b)$ to $F^{VI}_{Y_b}(y_b)$ are given by Eqs.(3.109), (3.125), (3.141), (3.150), and (3.169), respectively. Please refer to Appendix 3.B.3 for the exact expressions.

Proof. Please refer to Appendix 3.B.3 for the detailed proof. □

After differentiating $F_{Y_b}(y_b)$ given by Eq.(3.16) in each region, we can obtain the pdf of the random distance Y_b. Due to its complexity, here we choose not to present the pdf in this chapter.

Moreover, by following the same methodology as presented in Appendix 3.B.3, we are able to derive the cdf of the random distance Y_b for $d\sin\theta > a/2$. We do not have to consider as many different y_b values as we discussed for $d\sin\theta \le a/2$. If we have $0 \le y_b \le \overline{BH}$, the cdf of Y_b is zero. For $\overline{BH} < y_b \le \overline{BK}$, the cdf of Y_b can be formulated by $F^{III}_{Y_b}(y_b)$ that is derived in Eq.(3.125). If we have $\overline{BK} < y_b \le \overline{BI}$, the cdf of Y_b can be expressed by $F^{IV}_{Y_b}(y_b)$ that is derived in Eq.(3.141). For $\overline{BI} < y_b \le \overline{BJ}$, the cdf of Y_b can be formulated by $F^{VI}_{Y_b}(y_b)$ that is derived in Eq.(3.169). Finally, if $y_b > \overline{BJ}$, the cdf of Y_b is equal to unity.

3.3.2.2 The BS is inside the square area

Now, let us consider the scenario that the position B of the BS, which is denoted by the tuple (d, θ), is inside the square area $\square HIJK$. The centre of $\square HIJK$ is located at the origin $(0, 0)$ of the two-dimensional surface $\widetilde{x}O\widetilde{y}$. Without loss of generality, we assume that B is located in subspace I, as shown in Figure 3.3(b). Hence, the coordinate $(\widetilde{x}_B, \widetilde{y}_B)$ of point B can be expressed by the tuple (d, θ), namely $\widetilde{x}_B = -d\cos\theta$ and $\widetilde{y}_B = -d\sin\theta$, where we thus have $\theta \in [0, \frac{\pi}{4}]$ and $d\cos\theta \geq d\sin\theta$ because B is located in subspace I, whereas we also have $d\cos\theta \leq \frac{a}{2}$ because point B is in side the square area $\square HIJK$. Given a random position $(\widetilde{X}, \widetilde{Y})$ of a MU, the random distance Y_b between this MU and the BS is derived as

$$Y_b = \sqrt{(\widetilde{X} - \widetilde{x}_B)^2 + (\widetilde{Y} - \widetilde{y}_B)^2} = \sqrt{(\widetilde{X} + d\cos\theta)^2 + (\widetilde{Y} + d\sin\theta)^2}. \tag{3.17}$$

In order to derive the cdf or pdf for the random distance Y_b, the following steps are proposed relying on Eq.(3.17):

- Confirm the pdfs for the random coordinates $\widetilde{X}$ and $\widetilde{Y}$.
- Define new random variables, namely $\Delta_x = \widetilde{X} + d\cos\theta$ and $\Delta_y = \widetilde{Y} + d\sin\theta$, and derive their pdfs, respectively.
- Define new random variables, namely $Z_x = \Delta_x^2$ and $Z_y = \Delta_y^2$, and derive their pdfs, respectively.
- Given the pdfs of Z_x and Z_y, we are capable of deriving the cdf for the random distance Y_b, which is defined as $Y_b = \sqrt{Z_x + Z_y}$.

Now let us start the derivation of the cdf for the random distance Y_b according to the above-mentioned steps. First of all, we have the following lemma:

Lemma 3.1. *The pdfs for the random coordinates $\widetilde{X}$ and $\widetilde{Y}$ are expressed as*

$$f_{\widetilde{X}}(\widetilde{x}) = \begin{cases} \frac{1}{a}, & -\frac{a}{2} \leq \widetilde{x} \leq \frac{a}{2}, \\ 0, & \textit{otherwise}, \end{cases} \qquad f_{\widetilde{Y}}(\widetilde{y}) = \begin{cases} \frac{1}{a}, & -\frac{a}{2} \leq \widetilde{x} \leq \frac{a}{2}, \\ 0, & \textit{otherwise}. \end{cases} \tag{3.18}$$

Proof. Since the MU's movement is restricted within $\square HIJK$ by obeying the uniform mobility model, $\widetilde{X}$ and $\widetilde{Y}$ are both uniformly distributed random variables in the region $[-\frac{a}{2}, \frac{a}{2}]$. As a result, this lemma is readily proven. □

For the second step, the pdfs of the random variable Δ_x and Δ_y are provided by the following lemma:

Lemma 3.2. *Given $\Delta_x = \widetilde{X} + d\cos\theta$, the pdf of the random variable Δ_x is expressed as*

$$f_{\Delta_x}(\delta_x) = \begin{cases} \frac{1}{a}, & -\frac{a}{2} + d\cos\theta \le \delta_x \le \frac{a}{2} + d\cos\theta, \\ 0, & \textit{otherwise}. \end{cases} \tag{3.19}$$

Similarly, given $\Delta_y = \widetilde{Y} + d\sin\theta$, the pdf of the random variable Δ_y is expressed as

$$f_{\Delta_y}(\delta_y) = \begin{cases} \frac{1}{a}, & -\frac{a}{2} + d\sin\theta \le \delta_y \le \frac{a}{2} + d\sin\theta, \\ 0, & \textit{otherwise}. \end{cases} \tag{3.20}$$

Proof. This lemma is readily proven according since the sum of a uniformly distributed random variable and a constant is still uniformly distributed. □

For the third step, the pdfs of the random variable Z_x and Z_y are provided by the following lemma:

Lemma 3.3. *Given $Z_x = \Delta_x^2$, the pdf of the random variable Z_x is expressed as*

$$f_{Z_x}(z_x) = \begin{cases} \frac{1}{a\sqrt{z_x}}, & 0 < z_x < (\frac{a}{2} - d\cos\theta)^2 \\ \frac{1}{2a\sqrt{z_x}}, & (\frac{a}{2} - d\cos\theta)^2 < z_x < (\frac{a}{2} + d\cos\theta)^2 \\ 0, & \textit{otherwise}. \end{cases} \tag{3.21}$$

Similarly, given $Z_y = \Delta_y^2$, the pdf of the random variable Z_y is expressed as

$$f_{Z_y}(z_y) = \begin{cases} \frac{1}{a\sqrt{z_y}}, & 0 < z_y < (\frac{a}{2} - d\sin\theta)^2 \\ \frac{1}{2a\sqrt{z_y}}, & (\frac{a}{2} - d\sin\theta)^2 < z_y < (\frac{a}{2} + d\sin\theta)^2 \\ 0, & \textit{otherwise}. \end{cases} \tag{3.22}$$

Proof. Please refer to Appendix 3.B.4 for the detailed proof. □

In the last step, we should derive the cdf for the random variable $Y_b = \sqrt{Z_x + Z_y}$. Specifically, the cdf of Y_b can be expressed as

$$\begin{aligned} F_{Y_b}(y_b) &= \Pr(Y_b \le y_b) = \Pr(\sqrt{Z_x + Z_y} \le y_b) = \Pr(Z_x + Z_y \le y_b^2) \\ &= \iint_{\mathcal{S}} f_{Z_x Z_y}(z_x, z_y) dz_x dz_y, \end{aligned} \tag{3.23}$$

where $f_{Z_x Z_y}(z_x, z_y)$ is a joint pdf of random variables Z_x and Z_y and $\mathcal{S}$ is a two-dimensional integral area jointly determined by the domain of $f_{Z_x Z_y}(z_x, z_y)$ and the straight line $z_x + z_y = y_b^2$. According to Eqs.(3.21) and (3.22), the domain of the joint pdf $f_{Z_x Z_y}(z_x, z_y)$ is denoted as the rectangular $\square OBHF$ in Figure 3.5. Furthermore, since Z_x and Z_y are independent random variables, their joint pdf can be expressed as $f_{Z_x Z_y}(z_x, z_y) = f_{Z_x}(z_x) \cdot f_{Z_y}(z_y)$. However, given a pair of values (z_x, z_y) in different regions, namely region I, II, III and IV, as shown in Figure 3.5, we have different expressions for $f_{Z_x Z_y}(z_x, z_y)$, which is presented as the following equations:

$$f_{Z_x Z_y}(z_x, z_y) = \begin{cases} f^{(I)}_{Z_x Z_y}(z_x, z_y) = \frac{1}{a^2 \sqrt{z_x z_y}}, & 0 < z_x < (\frac{a}{2} - d\cos\theta)^2 \\ & 0 < z_y < (\frac{a}{2} - d\sin\theta)^2, \\ f^{(II)}_{Z_x Z_y}(z_x, z_y) = \frac{1}{2a^2 \sqrt{z_x z_y}}, & (\frac{a}{2} - d\cos\theta)^2 < z_x < (\frac{a}{2} + d\cos\theta)^2 \\ & 0 < z_y < (\frac{a}{2} - d\sin\theta)^2, \\ f^{(III)}_{Z_x Z_y}(z_x, z_y) = \frac{1}{2a^2 \sqrt{z_x z_y}}, & 0 < z_x < (\frac{a}{2} - d\cos\theta)^2 \\ & (\frac{a}{2} - d\sin\theta)^2 < z_y < (\frac{a}{2} + d\sin\theta)^2, \\ f^{(IV)}_{Z_x Z_y}(z_x, z_y) = \frac{1}{4a^2 \sqrt{z_x z_y}}, & (\frac{a}{2} - d\cos\theta)^2 < z_x < (\frac{a}{2} + d\cos\theta)^2 \\ & (\frac{a}{2} - d\sin\theta)^2 < z_y < (\frac{a}{2} + d\sin\theta)^2. \end{cases} \tag{3.24}$$

We denote the points on the boundaries between different regions by their corresponding coordinates in axes $z_x O z_y$, as shown in Figure 3.5. The coordinate of point A is $((\frac{a}{2} - d\cos\theta)^2, 0)$, and the coordinates of points B, C, D and E are given by $((\frac{a}{2} + d\cos\theta)^2, 0)$, $((\frac{a}{2} + d\cos\theta)^2, (\frac{a}{2} - d\sin\theta)^2)$, $((\frac{a}{2} - d\cos\theta)^2, (\frac{a}{2} - d\sin\theta)^2)$ and $(0, (\frac{a}{2} - d\sin\theta)^2)$, respectively. Moreover, the coordinates of points F, G, and H are given by $(0, (\frac{a}{2} + d\sin\theta)^2)$, $((\frac{a}{2} - d\cos\theta)^2, (\frac{a}{2} + d\sin\theta)^2)$, and $((\frac{a}{2} + d\cos\theta)^2, (\frac{a}{2} + d\sin\theta)^2)$, respectively.

Furthermore, we must obtain the sum of each point's z_x-coordinate and z_y-coordinate. For example, we denote the sum of point A's z_x-coordinate and z_y-coordinate as $\widetilde{z}_A = z_{A,x} + z_{A,y} = (\frac{a}{2} - d\cos\theta)^2$. As shown in Eq.(3.24), we have different expressions for the joint pdf of Z_x and Z_y in different regions of Figure.3.5. In order to further derive the double integral of Eq.(3.23), we must first sort the array $\{\widetilde{z}_i | i \in \{A, B, C, D, E, F, G, H\}\}$ in an ascending order. The ascending sort of the array $\{\widetilde{z}_i | i \in \{A, B, C, D, E, F, G, H\}\}$ is determined by the ascending sort of another

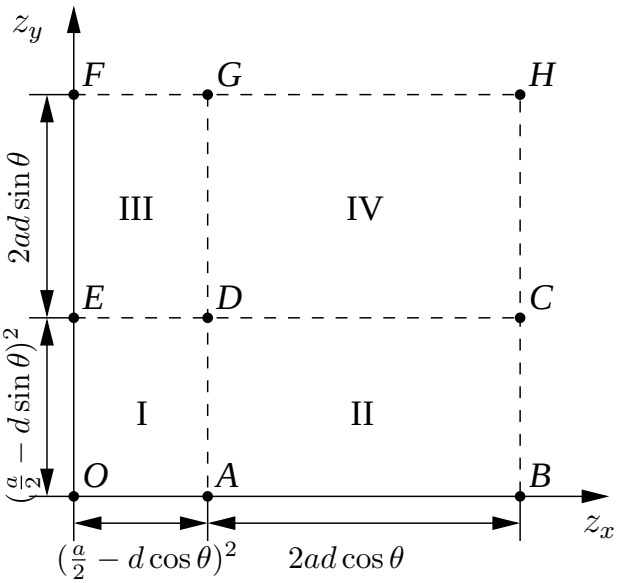

Figure 3.5: The domain of the joint pdf $f_{Z_xZ_y}(z_x, z_y)$.

array $\{\overline{OA}, \overline{OB}, \overline{AB}, \overline{OE}, \overline{OF}, \overline{EF}\}$, where $\overline{OA} = (\frac{a}{2} - d\cos\theta)^2$ is the distance between points O and A, as shown in Figure 3.5, $\overline{OB} = (\frac{a}{2} + d\cos\theta)^2$ is the distance between points O and B, and $\overline{AB} = (\frac{a}{2} + d\cos\theta)^2 - (\frac{a}{2} - d\cos\theta)^2 = 2ad\cos\theta$ is the distance between points A and B, whereas $\overline{OE} = (\frac{a}{2} - d\sin\theta)^2$ is the distance between points O and E, $\overline{OF} = (\frac{a}{2} + d\sin\theta)^2$ is the distance between points O and F, and $\overline{EF} = (\frac{a}{2} + d\sin\theta)^2 - (\frac{a}{2} - d\sin\theta)^2 = 2ad\sin\theta$ is the distance between points E and F. Obviously, since the angle θ is in the region $\theta \in [0, \frac{\pi}{4}]$, we have $d\cos\theta \geq d\sin\theta$. Furthermore, since the BS is located within the square area, we have $d\cos\theta \leq \frac{a}{2}$. As a result, we have several apparent inequalities, which are $\overline{OA} \leq \overline{OE}$, $\overline{EF} \leq \overline{AB}$, $\overline{OA} \leq \overline{OB}$ and $\overline{AB} \leq \overline{OB}$, as well as $\overline{OE} \leq \overline{EF}$, $\overline{EF} \leq \overline{OF}$, and $\overline{OF} \leq \overline{OB}$. In order to fulfil these inequalities, we might have eight possible ascending sorts for the array $\{\overline{OA}, \overline{OB}, \overline{AB}, \overline{OE}, \overline{OF}, \overline{EF}\}$, which are presented as: i) $\overline{OA} \leq \overline{OE} \leq \overline{EF} \leq \overline{OF} \leq \overline{AB} \leq \overline{OB}$, if the BS's location is within the red area, as shown in Figure 3.6; ii)$\overline{OA} \leq \overline{OE} \leq \overline{EF} \leq \overline{AB} \leq \overline{OF} \leq \overline{OB}$, if the BS's location is within the green area, as shown in Figure 3.6; iii) $\overline{OA} \leq \overline{EF} \leq \overline{OE} \leq \overline{OF} \leq \overline{AB} \leq \overline{OB}$, if the BS's location is within the magenta area, as shown in Figure 3.6; iv) $\overline{OA} \leq \overline{EF} \leq \overline{OE} \leq \overline{AB} \leq \overline{OF} \leq \overline{OB}$, if the BS's location is within the blue area, as shown in Figure 3.6; v) $\overline{EF} \leq \overline{OA} \leq \overline{OE} \leq \overline{OF} \leq \overline{AB} \leq \overline{OB}$, if the BS's location is within the cyan area, as shown in Figure 3.6; vi) $\overline{EF} \leq \overline{OA} \leq \overline{OE} \leq \overline{AB} \leq \overline{OF} \leq \overline{OB}$, if the BS's location is within the white area, as shown in Figure 3.6; vii) $\overline{EF} \leq \overline{OA} \leq \overline{AB} \leq \overline{OE} \leq \overline{OF} \leq \overline{OB}$, if the BS's location is within the black area, as shown in Figure 3.6; viii) $\overline{EF} \leq \overline{AB} \leq \overline{OA} \leq \overline{OE} \leq \overline{OF} \leq \overline{OB}$, if the BS's location is within the yellow area, as shown in Figure 3.6.

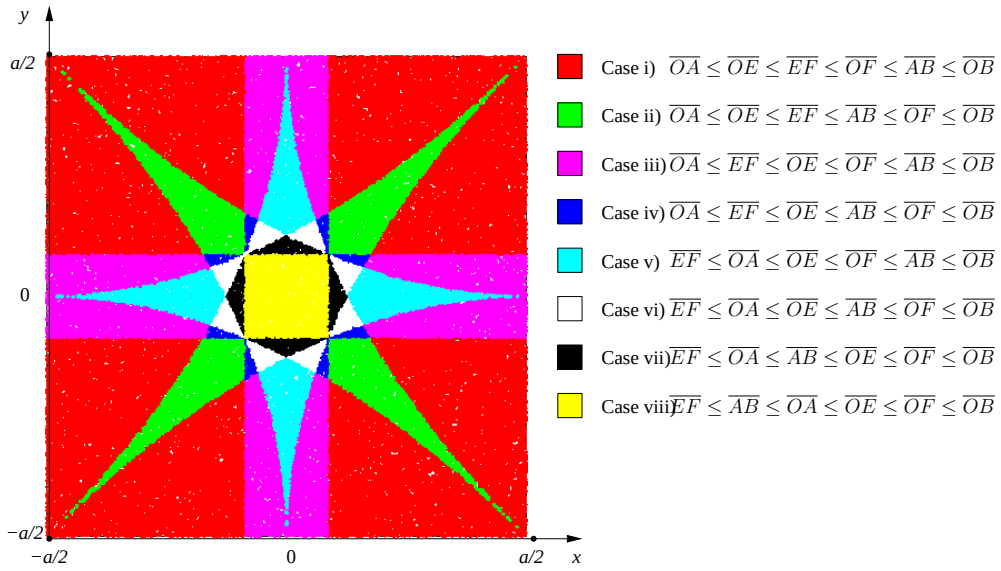

Figure 3.6: Different positions of the BS result in different cases.

According to Figure 3.6, we found that if we uniformly throw a BS into a square area, case i) $\overline{OA} \le \overline{OE} \le \overline{EF} \le \overline{OF} \le \overline{AB} \le \overline{OB}$ is most likely to happen with a probability of 59.5%. As a result, in order to show the methodology of solving the double integral of Eq.(3.23), we will take case i as an example.

Theorem 3.6. *Given a specific position of the BS (d, θ), the following inequalities are assumed $\overline{OA} \le \overline{OE} \le \overline{EF} \le \overline{OF} \le \overline{AB} \le \overline{OB}$. The cdf of the random distance Y_b between the BS inside the square area and the MU roaming within the same area can be expressed as*

$$F_{Y_b}(y_b) = \begin{cases} F_{Y_b}^{(1)}(y_b), & 0 \le y_b \le \frac{a}{2} - d\cos\theta, \\ F_{Y_b}^{(2)}(y_b), & \frac{a}{2} - d\cos\theta < y_b \le \frac{a}{2} - d\sin\theta \\ F_{Y_b}^{(3)}(y_b), & \frac{a}{2} - d\sin\theta < y_b \le \sqrt{a^2/2 + d^2 - ad(\cos\theta + \sin\theta)}, \\ F_{Y_b}^{(4)}(y_b), & \sqrt{a^2/2 + d^2 - ad(\cos\theta + \sin\theta)} < y_b \le \frac{a}{2} + d\sin\theta, \\ F_{Y_b}^{(5)}(y_b), & \frac{a}{2} + d\sin\theta < y_b \le \frac{a}{2} + d\cos\theta, \\ F_{Y_b}^{(6)}(y_b), & \frac{a}{2} + d\cos\theta < y_b \le \sqrt{a^2/2 + d^2 - ad(\cos\theta - \sin\theta)}, \\ F_{Y_b}^{(7)}(y_b), & \sqrt{a^2/2 + d^2 - ad(\cos\theta - \sin\theta)} y_b \le \sqrt{a^2/2 + d^2 + ad(\cos\theta - \sin\theta)}. \\ F_{Y_b}^{(8)}(y_b), & \sqrt{a^2/2 + d^2 + ad(\cos\theta - \sin\theta)} < y_b \le \sqrt{a^2/2 + d^2 + ad(\cos\theta + \sin\theta)}. \\ F_{Y_b}^{(9)}(y_b), & y_b > \sqrt{a^2/2 + d^2 + ad(\cos\theta + \sin\theta)}. \end{cases} \tag{3.25}$$

where the exact expressions for $F_{Y_b}^{(1)}(y_b)$ to $F_{Y_b}^{(9)}(y_b)$ are provided by Eqs.(3.176) to (3.184), as presented in Appendix 3.B.5.

Proof. Please refer to Appendix 3.B.5 for the detailed proof. □

The calculations of Eq.(3.23) for the rest seven cases can be completed by following the same methodology, as presented in Appendix 3.B.5, which are omitted because of space limit.

3.4 Random distance between a pair of MUs roaming in a bounded area

In the past two sections, we discuss the random distance between a BS and a MU in different scenarios, where the BS is a static node and the MU is a moving node. Generally speaking, various distance distributions derived in the previous sections can be invoked for evaluating the performance of wireless links connecting a static node and a moving node. In realistic wireless communications, only centralised infrastructure, e.g. BSs and Wi-Fi hotspots, are often modelled as static nodes. As a result, distance distributions derived in previous sections are only capable of evaluating the performance of centralised wireless links, e.g. cellular links connecting MUs to a BS and Wi-Fi links connecting MUs to a Wi-Fi hotspot.

However, as the rapid development of multi-functional mobile devices, direct communications between a pair of MUs and its peer attracts much attention from both academic and industrial communities. There are several techniques supporting direct communication between a pair of MUs. Bluetooth and infrared transmission modes has been installed on mobile phones for decades, their pairwise nature enables direct communication between a MU and its neighbour. However, due to their short transmission range, it is impossible for these two techniques to deliver the information to a far end. Apart from centralised communication between a MU and a access point, the family of 802.11 protocols [28] is also capable of supporting purely distributed communication between a pair of MUs. From the route establishment in network layer to the resource allocation in medium-access-control layer, all the actions are completed by the direct or multi-hop communications amongst MUs equipped with Wi-Fi transmission modules without any aid of centralised infrastructure. However, a purely distributed way of routing and resource allocation may impose more overhead signalling and power dissipation, which might reduce the efficiency of the transmission of the desired data. As a result, in order to improve the efficiency of route finding and resource allocation, recently, cellular device to device communication [15] is becoming a more favourite choice for realising direct communication between a pair of MUs. In the cellular device to device communication, all the overhead signalling for route finding and resources scheduling is carried out by the BS of the cell. After a pair of MUs fetch free resource and a direct link between them is established, the transmitter may directly convey the required data to the receiver.

As a result, the distance distribution between a static node and a mobile node is not capable

of evaluating the performance of a direct link between a pair of MUs due to the mobile nature of both the transmitter and the receiver. Hence, in this section, we will characterise the distance distribution between a pair of MUs in different scenarios in order to provide a more precise tool for studying the link performance between a pair of mobile nodes.

3.4.1 Mobile users roam in a circular area

Let us first consider the scenario that a pair of MUs move within a circular area $\odot(O, r)$ having point O as its centre and having r metres as its radius. The movements of this MU pair obey the uniform mobility model, as introduced in Definition 3.1. However, it is difficult for us to reflect the uniform-distributed characteristics of MUs within circular area $\odot(O, r)$ by invoking the Cartesian coordinate system. People may argue that, why not try polar coordinate system? We will also show the difficulties of deriving the random distance between a pair of MUs when the polar coordinate system is invoked. The polar coordinate of MU_i is given by (D_i, Θ_i), where D_i is the radial coordinate and Θ_i is the angular coordinate. We are able to convert the polar coordinates into the Cartesian coordinates on the two-dimensional plane $\widetilde{x}O\widetilde{y}$ by invoking the following two relationships: $\widetilde{X}_i = D_i \cos\Theta_i$ and $\widetilde{Y}_i = D_i \sin\Theta_i$. As a result, the Euclidean distance between a pair of MUs is expressed as

$$Y_s = \sqrt{(\widetilde{X}_1 - \widetilde{X}_2)^2 + (\widetilde{Y}_1 - \widetilde{Y}_2)^2} = \sqrt{D_1^2 + D_2^2 - 2D_1D_2\cos(\Theta_1 - \Theta_2)}. \tag{3.26}$$

In order to characterise the cdf or pdf of Y_s expressed as Eq.(3.26), apart from the pdf of D_1^2 and D_2^2, we have to obtain the pdf for $2D_1D_2\cos(\Theta_1 - \Theta_2)$. Unfortunately, these three random variables are not independent of one another, which makes the cdf derivation of Y_s extremely hard.

However, we may readily derive the cdf or pdf of the random distance Y_s between a pair of MUs with the aid of Crofton's mean value and fixed points theorems. Before introducing these two theorems, we firstly provide the definitions of a $\sigma-$algebra and of a measure in the probability theory.

Definition 3.2 (A $\sigma-$algebra)**.** *A $\sigma-$algebra on a set $\mathcal{S}$ is a collection of subsets of $\mathcal{S}$ that is closed under countable-fold set operations (complement, union of countably many sets and intersection of countably many sets).*

Definition 3.3 (A measure on a set)**.** *Let $\mathcal{S}$ be a set and let $\Psi_{\mathcal{S}}$ be a $\sigma-$algebra over set $\mathcal{S}$. A function defined as $\varphi : \Psi \to \mathbb{R}$, where $\mathbb{R}$ is the extended real number system, is called a measure if it satisfies the following properties:*

- *Non-negativity: For any subset $\mathcal{A}$ of $\mathcal{S}$ that belongs to $\Psi_{\mathcal{S}}$, we have $\varphi(\mathcal{A}) \geq 0$;*
- *Null empty set: For a null set ϕ, we have $\varphi(\phi) = 0$;*
- *Countable additivity: For all countable collections $\{\mathcal{A}_i, i = 1, 2, \cdots, N\}$ of pairwise disjoint sets in $\Psi_{\mathcal{S}}$, we have $\varphi(\bigcup_{i=1}^{N} \mathcal{A}_i) = \sum_{i=1}^{N} \varphi(\mathcal{A}_i)$.*

Now, let us define a points set $\mathcal{S}$, whose $\sigma-$algebra is denoted as $\Psi_{\mathcal{S}}$. A measure over a subset $\mathcal{A}$ that belongs to $\Psi_{\mathcal{S}}$ is defined as $\varphi_{\mathcal{S}} : \Psi_{\mathcal{S}} \rightarrow \mathbb{R}$. Specifically, if $\mathcal{S}$ is a point sets on two-dimensional plane, the measure $\varphi_{\mathcal{S}}(\mathcal{A})$ is the area covered by a points subset $\mathcal{A}$. If $\mathcal{S}$ is a point sets on three-dimensional space, the measure $\varphi_{\mathcal{S}}(\mathcal{A})$ is defined as the volume of a points subset $\mathcal{A}$. Based on the definition of a measure on a point set, if the probability of an event, which depends on the positions of the points within $\mathcal{A}$, is of interest, the Crofton's fixed points theorem is defined as

Theorem 3.7 (Fixed points theorem)**.** *Given a points set $\mathcal{S}$, whose $\sigma-$algebra is $\Psi_{\mathcal{S}}$, we let n points $\{\epsilon_i, i = 1, 2, ..., n\}$ be randomly distributed in a points subset $\mathcal{A}$ that belongs to $\Psi_{\mathcal{S}}$. We define $\mathcal{H}$ as an event depending on the positions of these nodes. Let $\mathcal{A}'$ be a subset belonging to $\Psi_{\mathcal{S}}$, which is slightly smaller than $\mathcal{A}$ but contained within it, say $\mathcal{A}' \subset \mathcal{A}$. We also let $\delta\mathcal{A}$ be the part of $\mathcal{A}$, which is not within $\mathcal{A}'$. Then the following relationships can be invoked for calculating the probability of the event $\mathcal{H}$ occurring:*

$$dPr(\mathcal{H}) = n(Pr(\mathcal{H}|\epsilon_1 \in \delta\mathcal{A}) - Pr(\mathcal{H}))\left[\varphi(\mathcal{A})\right]^{-1} d\varphi(\mathcal{A}), \tag{3.27}$$

where $\varphi(\mathcal{A})$ is a measure of the points subset $\mathcal{A}$.

Furthermore, if the mean value of a random variable, which is determined by the positions of the points within $\mathcal{A}$, is of interest, the Crofton's mean value theorem is defined as

Theorem 3.8 (Mean value theorem)**.** *Given a points set $\mathcal{S}$, whose $\sigma-$algebra is $\Psi_{\mathcal{S}}$, we let n points $\{\epsilon_i, i = 1, 2, ..., n\}$ be randomly distributed in a points subset $\mathcal{A}$ that belongs to $\Psi_{\mathcal{S}}$. Let X be a random variable determined by the positions of these n points. Moreover, let $\mathcal{A}'$ be a subset belonging to $\Psi_{\mathcal{S}}$, which is slightly smaller than $\mathcal{A}$ but contained within it, say $\mathcal{A}' \subset \mathcal{A}$. We also let $\delta\mathcal{A}$ be the part of $\mathcal{A}$, which is not within $\mathcal{A}'$. Then we have the following relationship for calculating the mean value of the random variable X:*

$$dE(X) = n(E[X|\epsilon_1 \in \delta\mathcal{A}] - E[X])\left[\varphi(\mathcal{A})\right]^{-1} d\varphi(\mathcal{A}), \tag{3.28}$$

where $\varphi(\mathcal{A})$ is a measure of the points subset $\mathcal{A}$.

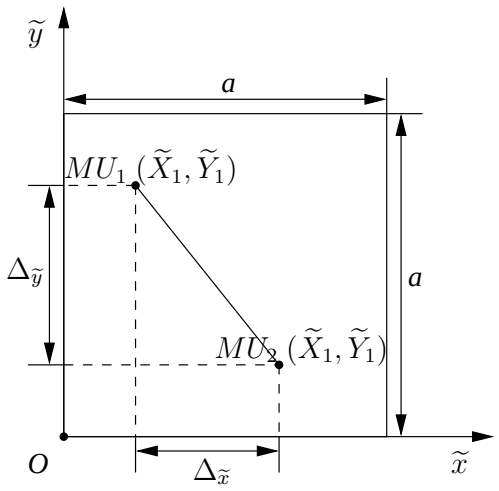

Figure 3.7: The Cartesian coordinate system for calculating the cdf of the random distance Y_s

With the aid of the Crofton's fixed points theorem and the mean value theorem, we arrive at the following theorem:

Theorem 3.9. *When a pair of MUs roam within a circular area having a radius r by obeying the uniform mobility model, the pdf of the random distance Y_s between this pair of MUs is expressed as*

$$f_{Y_s}(y_s) = \frac{8}{\pi r} \cdot \frac{y_s}{2r} \left[\arccos \frac{y_s}{2r} - \frac{y_s}{2r} \sqrt{1 - \left(\frac{y_s}{2r}\right)^2} \right], \tag{3.29}$$

for $0 \leq y_s \leq 2r$. Furthermore, integrating the above-derived $f_{Y_s}(y_s)$ over the region $[0, y_s]$, we may obtain the cdf $F_{Y_s}(y_s)$ as

$$F_{Y_s}(y_s) = \frac{2}{\pi} \left\{ 4 \left(\frac{y_s}{2r}\right)^2 \arccos\left(\frac{y_s}{2r}\right) + \arcsin\left(\frac{y_s}{2r}\right) - \left[\frac{y_s}{2r} + 2\left(\frac{y_s}{2r}\right)^3 \right] \sqrt{1 - \left(\frac{y_s}{2r}\right)^2} \right\}. \tag{3.30}$$

Proof. Please refer to Appendix 3.C.1 for the detailed proof. □

3.4.2 Mobile users roam in a square area

In this scenario, we consider that a pair of MUs move within a square area by obeying the uniform mobility model, as introduced in Definition 3.1. In order to derive the cdf or the pdf of the random distance Y_s between a pair of MUs roaming in the square area, the two-dimensional Cartesian coordinate system $\widetilde{x}O\widetilde{y}$ is invoked. The left bottom corner of the square area considered is placed at the origin O and the side length of the square area is a, as shown in Figure 3.7.

Let the Cartesian coordinate of MU_1 be $(\widetilde{X}_1, \widetilde{Y}_1)$ and let that of MU_2 be $(\widetilde{X}_2, \widetilde{Y}_2)$, where all these random variables, namely $\widetilde{X}_1$, $\widetilde{X}_2$, $\widetilde{Y}_1$, $\widetilde{Y}_2$ are independent by obeying an identical uniform distribution defined in the region $[0, a]$. For example, the pdf of the random variable $\widetilde{X}_1$ can be expressed as

$$f_{\widetilde{X}_1}(\widetilde{x}_1) = \begin{cases} \frac{1}{a}, & 0 \leq \widetilde{x}_1 \leq a, \\ 0, & \text{otherwise.} \end{cases} \tag{3.31}$$

Thus, the random distance Y_s between MU_1 and MU_2 can be expressed as

$$Y_s = \sqrt{(\widetilde{X}_1 - \widetilde{X}_2)^2 + (\widetilde{Y}_1 - \widetilde{Y}_2)^2}. \tag{3.32}$$

In order to derive the cdf and pdf of the random distance Y_s, the following steps are needed:

- We define two new random variable as $\Delta_{\widetilde{x}} = \widetilde{X}_1 - \widetilde{X}_2$ and $\Delta_{\widetilde{y}} = \widetilde{Y}_1 - \widetilde{Y}_2$. Obviously, $\Delta_{\widetilde{x}}$ and $\Delta_{\widetilde{y}}$ are independent and identical random variables. We will firstly derive the pdfs for both the $\Delta_{\widetilde{x}}$ and $\Delta_{\widetilde{y}}$.

- Then, we define another two random variables as $Z_{\widetilde{x}} = \Delta_{\widetilde{x}}^2$ and $Z_{\widetilde{y}} = \Delta_{\widetilde{y}}^2$. Obviously, $Z_{\widetilde{x}}$ and $Z_{\widetilde{y}}$ are independent of each other and share an identical distribution. We will secondly derive the pdfs for both the $Z_{\widetilde{x}}$ and $Z_{\widetilde{y}}$.

- Now, the random distance Y_s can be expressed as $Y_s = \sqrt{Z_{\widetilde{x}} + Z_{\widetilde{y}}}$. Given the pdfs of $Z_{\widetilde{x}}$ and $Z_{\widetilde{x}}$, we may finally arrive at the cdf and pdf of the random distance Y_s between a pair of MUs roaming within a square area.

First of all, the pdfs of the random variables $\Delta_{\widetilde{x}}$ and $\Delta_{\widetilde{y}}$ are provided by the following lemma:

Lemma 3.4. *Given that $\Delta_{\widetilde{x}} = \widetilde{X}_1 - \widetilde{X}_2$ and both $\widetilde{X}_1$ and $\widetilde{X}_2$ are i.i.d. random variables, whose pdfs are given by Eq.(3.31), the pdf of the random variable $\Delta_{\widetilde{x}}$ can be expressed as*

$$f_{\Delta_{\widetilde{x}}}(\delta_{\widetilde{x}}) = \begin{cases} \frac{\delta_{\widetilde{x}} + a}{a^2}, & -a \leq \delta_{\widetilde{x}} < 0 \\ \frac{a - \delta_{\widetilde{x}}}{a^2}, & 0 \leq \delta_{\widetilde{x}} \leq a \\ 0, & \textit{otherwise}. \end{cases} \tag{3.33}$$

Apparently, $\Delta_{\widetilde{y}} = \widetilde{Y}_1 - \widetilde{Y}_2$ shares the identical pdf with $\Delta_{\widetilde{x}}$.

Proof. Please refer to Appendix 3.C.2 for the detailed proof. □

For the second step, the pdfs of the random variables $Z_{\widetilde{x}}$ and $Z_{\widetilde{y}}$ are provided by the following lemma:

Lemma 3.5. *Given $Z_{\widetilde{x}} = \Delta_{\widetilde{x}}^2$, the pdf of the random variable $Z_{\widetilde{x}}$ can be expressed as*

$$f_{Z_{\widetilde{x}}}(z_{\widetilde{x}}) = \begin{cases} \dfrac{1}{a\sqrt{z_{\widetilde{x}}}} - \dfrac{1}{a^2}, & 0 \leq z_x \leq a^2 \\ 0, & \textit{otherwise}. \end{cases} \tag{3.34}$$

Moreover, the random variable $Z_{\widetilde{y}} = \Delta_{\widetilde{y}}^2$ shares the same pdf with $Z_{\widetilde{x}}$.

Proof. Please refer to Appendix 3.C.3 for the detailed proof. □

Finally, with the aid of Lemma 3.4 and Lemma 3.5, the cdf and the pdf of the random distance Y_b are provided by the following theorem:

Theorem 3.10. *The cdf of the random distance Y_s, which is defined as $Y_s = \sqrt{Z_{\widetilde{x}} + Z_{\widetilde{y}}}$, between a pair of MU roaming within a square area having a as its side length can be expressed as*

$$F_{Y_s}(y_s) = \begin{cases} \dfrac{1}{a^2}\left(\pi y_s^2 - \dfrac{8y_s^3}{3a} + \dfrac{y_s^4}{2a^2}\right), & 0 \leq y_s < a \\ \dfrac{1}{a^2}\left[2y_s^2 \arcsin\dfrac{2a^2 - y_s^2}{y_s^2} + \left(\dfrac{4}{3}a + \dfrac{8}{3a}y_s^2\right)\sqrt{y_s^2 - a^2}\right. & \\ \qquad \left. -2y_s^2 - \dfrac{y_s^4}{2a^2} + \dfrac{a^2}{3}\right], & a < y_s \leq \sqrt{2}a \\ 1, & y_s > \sqrt{2}a. \end{cases} \tag{3.35}$$

After differentiating $F_{Y_s}(y_s)$ in each region with respect to y_s, we arrive at the pdf of the random distance Y_s, which is expressed as

$$f_{Y_s}(y_s) = \begin{cases} \dfrac{1}{a^2}\left(2\pi y_s - \dfrac{8y_s^2}{a} + \dfrac{2y_s^3}{a^2}\right), & 0 \leq y_s < a \\ \dfrac{1}{a^2}\left(4y_s \arcsin\dfrac{2a^2 - y_s^2}{y_s^2} + \dfrac{8y_s}{a}\sqrt{y_s^2 - a^2} - 4y_s - \dfrac{2y_s^3}{a^2}\right), & a < y_s \leq \sqrt{2}a \\ 0, & \textit{otherwise}. \end{cases} \tag{3.36}$$

Proof. Please refer to Appendix 3.C.4 for the detailed proof. □

3.5 Application of distance distribution in cellular networks

In wireless communications, long-distance between a transmitter and receiver pair imposes significant channel attenuation, which is regarded as the path loss (PL). The PL is normally considered as a deterministic parameter in the following scenarios:

- Both transmitters and receivers in the studied wireless network are static nodes. The variation of the channel gain is mainly incurred by the stochastic shadowing effect and multipath fading.

- The distance variations incurred by the movement of both transmitters and receivers are much slower than the variations of the stochastic shadowing effect and multipath fading. In this scenario, the varying PL incurred by the slow movements of the nodes are ignored by the performance evaluation of the wireless link

When mobility pattern of the MUs is taken into consideration, most of research focus on the connectivities of wireless links, such as the link life time [], link change rate [] and link arrival rate []. Apart from these issues in terms of network topology, MUs' mobility may also influence the physical-layer performance of wireless links in the following scenarios:

- The distance between a transmitter and receiver pair is significantly changed between two successive transmission blocks. As a result, the variation of the PL keeps the same pace with the variations of the stochastic shadowing effect and multipath fading [].

- When the single-transmitter-multiple receiver transmission mode, namely broadcast and multicast transmission, are taken into consideration, the positions of the single transmitter and multiple receivers may get refreshed for different transmission blocks []. For the sake of discussing the multicast spectral efficiency and the statistical properties of the number of outage MUs in the broadcast context, we have to consider the varying PL in addition to the shadowing and multipath fading.

In this section, by considering the distance variation incurred by the MUs' mobility, we present a list of applications in performance analysis of the wireless channel in mobile cellular networks. With the aid of the various distance distribution, we first study the statistical properties of the time-varying PL, then analyse the spectral efficiency for a single hop link and further evaluate the statistical properties of the number of outage MUs in the cellular broadcast. Finally, we analyse the multicast spectral efficiency.

3.5.1 Time-varying PL

Given a specific distance y_l between a transmitter-receiver pair, which is assumed to be longer than the reference distance d_0 determining the edge of the near-field, the PL model is defined by the following equation

$$\omega_l = \frac{P_{l,0}}{P_r} = \left(\frac{y_l}{d_0}\right)^{\kappa}, \; y_l \geq d_0, \tag{3.37}$$

where P_r is the power received at the receiver y_l m away from the transmitter, $P_{l,0}$ is the power received at the reference point that is d_0 m away from the transmitter and κ is the PL exponent. Note that the index 'l' is a generic subscript, which represents 'b' when the BS is the transmitter, while it represents 's' when a MU is the transmitter. In the rest of this chapter, subscripts 'l', 'b' and 's' hold the same meaning. The free-space PL model [18] is exploited for calculating the PL from the transmitter to the reference point, which is expressed as

$$\omega_{l,0} = \frac{P_l}{P_{l,0}} = \frac{(4\pi)^2 d_0^2}{\lambda_l^2} = \left(\frac{4\pi d_0}{c/f_{l,c}}\right)^2, \tag{3.38}$$

where $\lambda_l = c/f_{c,l}$ is the wave-length, c is the speed of light, $f_{c,l}$ is the carrier frequency, and P_l is the transmit power. Thus, the received reference power $P_{l,0}$ is obtained as $P_{l,0} = P_l/\omega_{l,0}$. Unfortunately, Eq.(3.38) is invalid for calculating the PL in the near-field of the transmit antenna. As a result, we assume that, when the distance y_l between the transmitter and receiver is shorter than d_0, the received power P_r is approximated to be the received reference power $P_{l,0}$ at the reference distance d_0. This assumption is reasonable and it provides an accurate approximation when the reference distance d_0 is far shorter than the size of the bounded area within which the MUs move by obeying the uniform mobility model. In a nutshell, given an arbitrary distance y_l, the PL model is defined as

$$\omega_l = \frac{P_l}{P_r} = \begin{cases} \omega_{l,0}, & 0 \leq y_l \leq d_0, \\ \omega_{l,0}\left(\frac{y_l}{d_0}\right)^{\kappa}, & y_l > d_0, \end{cases} \tag{3.39}$$

where the path loss $\omega_{l,0}$ at the reference distance d_0 is given by Eq.(3.38).

According to the uniform mobility model, as introduced in Definition 3.1, the position of a MU is a stationary stochastic process by obeying the uniform distribution. Thus, the distance Y_l between the transmitter and the receiver is also a stochastic process given that at least the receiver is a MU. As shown in Eq.(3.39), the path loss ω_l is a function with respect to the distance y_l. As a result, the path loss Ω_l is also a stochastic process. The cdf of the time-varying PL Ω_l is defined as

the probability of Ω_l being lower than ω_l. Let us now discuss the cdf $F_{\Omega_l}(\omega_l)$ for the time variant path loss Ω_l given different value of ω_l.

According to Eq.(3.39), the minimum value for Ω_l is $\omega_{l,0}$. As a result, Ω_l could not take a value lower than $\omega_{l,0}$. Hence, if we have $\omega_l < \omega_{l,0}$, the cdf of Ω_l is $F_{\Omega_l}(\omega_l) = 0$.

However, if we have $\omega_l \geq \omega_{l,0}$, the cdf of the time-varying PL Ω_l can be expressed as

$$F_{\Omega_l}(\omega_l) = \Pr(\Omega_l \leq \omega_l) = \Pr\left(\omega_{l,0}\left(\frac{y_l}{d_0}\right)^{\kappa} \leq \omega_l\right) = \Pr\left(y_l \leq d_0 \sqrt[\kappa]{\frac{\omega_l}{\omega_{l,0}}}\right) \tag{3.40}$$

$$= F_{Y_l}\left(d_0 \sqrt[\kappa]{\frac{\omega_l}{\omega_{l,0}}}\right). \tag{3.41}$$

In a nut shell, the cdf of the time-varying PL Ω_l between a transmitter and a receiver can be expressed as

$$F_{\Omega_l}(\omega_l) = \Pr(\Omega_l \leq \omega_l) = \begin{cases} 0, & \omega_l < \omega_{l,0} \\ F_{Y_l}\left(d_0 \sqrt[\kappa]{\frac{\omega_l}{\omega_{l,0}}}\right), & \omega_l \geq \omega_{l,0}. \end{cases} \tag{3.42}$$

Apparently, the cdf $F_{\Omega_l}(\omega_l)$ derived in Eq.(3.42) is not a continuous function because $\lim_{\omega_l \to \omega_{l,0}^+} = F_{Y_l}(d_0) \neq 0$. However, if d_0 is quite shorter than the size of the area studied, $F_{Y_l}(d_0)$ is very close to zero. In order to maintain the continuity of $F_{\Omega_l}(\omega_l)$, we may normalise the pdf $f_{Y_l}(y_l)$ of the random distance Y_l by $(1 - F_{Y_l}(d_0))$. The consequent cdf $\widetilde{F}_{Y_l}(y_l)$ can be expressed as $\widetilde{F}_{Y_l}(y_l) = (F_{Y_l}(y_l) - F_{Y_l}(d_0))/(1 - F_{Y_l}(d_0))$ for $y_l \geq d_0$. Obviously, we have $\widetilde{F}_{Y_l}(d_0) = 0$. This slight revision on the original cdf $F_{Y_l}(y_l)$ may not change its statistical property a lot if $F_{Y_l}(d_0)$ is very close to zero.

If we differentiate Eq.(3.42) with respect to ω_l in the region $\omega_l \in [\omega_{l,0}, +\infty)$, we arrive at the pdf of the time-varying PL Ω_l, which is expressed as

$$f_{\Omega_l}(\omega_l) = \frac{d}{d\omega_l} F_{Y_l}\left(d_0 \sqrt[\kappa]{\frac{\omega_l}{\omega_{l,0}}}\right) = \frac{d_0}{\kappa\omega_l} \sqrt[\kappa]{\frac{\omega_l}{\omega_{l,0}}} \cdot f_{Y_l}\left(d_0 \sqrt[\kappa]{\frac{\omega_l}{\omega_{l,0}}}\right), \omega_l \geq \omega_{l,0}. \tag{3.43}$$

By substituting the corresponding cdf $F_{Y_b}(y_b)$ and pdf $f_{Y_b}(y_b)$ into Eqs.(3.42) and (3.43), we may arrive at the cdf and the pdf of the time-variant PL between the BS and a MU. Let us consider the scenario that a cell is modelled by a circular area having r as its radius and the BS is at the centre of this circular area, while the MU moves within the circular cell by obeying the uniform mobility model. Note that since the maximum value for the random distance Y_b is the radius r, the corresponding maximum value for the time-varying PL Ω_b is $\omega_{b,0}(r/d_0)^{\kappa}$. As a result, by

substituting $F_{Y_b}(y_b)$ of Eq.(3.2) into Eq.(3.42), the cdf of Ω_b is expressed as

$$F_{\Omega_b}(\omega_b) = \frac{d_0^2}{r^2} \cdot \sqrt[\kappa]{\left(\frac{\omega_b}{\omega_{b,0}}\right)^2}, \quad 1 \leq \frac{\omega_b}{\omega_{b,0}} \leq \left(\frac{r}{d_0}\right)^\kappa, \tag{3.44}$$

Moreover, we have $F_{\Omega_b}(\omega_b) = 0$ for $\omega_b/\omega_{b,0} < 1$, while $F_{\Omega_b}(\omega_b) = 1$ for $\omega_b/\omega_{b,0} > (r/d_0)^\kappa$. Furthermore, by substituting $f_{Y_b}(y_b)$ of Eq.(3.3) into Eq.(3.43), the pdf of Ω_b is expressed as

$$f_{\Omega_b}(\omega_b) = \begin{cases} \dfrac{2}{\kappa\omega_b}\left(\dfrac{d_0}{r}\sqrt[\kappa]{\dfrac{\omega_b}{\omega_{b,0}}}\right)^2, & 1 \leq \dfrac{\omega_b}{\omega_{b,0}} \leq \left(\dfrac{r}{d_0}\right)^\kappa, \\ 0, & \text{otherwise.} \end{cases} \tag{3.45}$$

Then, Let us consider the scenario that a pair of MUs both move within a circular area having r as its radius by obeying the uniform mobility model. We note that the maximum value for the random distance Y_s is the diameter $2r$ and the corresponding maximum value for the time-variant PL Ω_s is $\omega_{s,0}(2r/d_0)^\kappa$. As a result, by substituting $F_{Y_s}(y_s)$ of Eq.(3.30) into Eq.(3.42), the cdf of Ω_s is expressed as

$$\begin{aligned} F_{\Omega_s}(\omega_s) = \frac{2}{\pi}\Bigg\{ & 4\left(\frac{d_0}{2r}\sqrt[\kappa]{\frac{\omega_b}{\omega_{b,0}}}\right)^2 \arccos\left(\frac{d_0}{2r}\sqrt[\kappa]{\frac{\omega_b}{\omega_{b,0}}}\right) + \arcsin\left(\frac{d_0}{2r}\sqrt[\kappa]{\frac{\omega_b}{\omega_{b,0}}}\right) \\ & - \left[\frac{d_0}{2r}\sqrt[\kappa]{\frac{\omega_b}{\omega_{b,0}}} + 2\left(\frac{d_0}{2r}\sqrt[\kappa]{\frac{\omega_b}{\omega_{b,0}}}\right)^3\right]\sqrt{1-\left(\frac{d_0}{2r}\sqrt[\kappa]{\frac{\omega_b}{\omega_{b,0}}}\right)^2}\Bigg\}, 1 \leq \frac{\omega_s}{\omega_{s,0}} \leq \left(\frac{2r}{d_0}\right)^\kappa \end{aligned} \tag{3.46}$$

Moreover, we have $F_{\Omega_s}(\omega_s) = 0$ for $\omega_s/\omega_{s,0} < 1$, while $F_{\Omega_s}(\omega_s) = 1$ for $\omega_s/\omega_{s,0} > (2r/d_0)^\kappa$. Furthermore, by substituting $f_{Y_s}(y_s)$ of Eq.(3.29) into Eq.(3.43), the pdf of Ω_s is expressed as

$$f_{\Omega_s}(\omega_s) = \begin{cases} \dfrac{4}{\pi\kappa\omega_b}\left(\dfrac{d_0}{r}\sqrt[\kappa]{\dfrac{\omega_b}{\omega_{b,0}}}\right)^2 \Bigg[\arccos\left(\dfrac{d_0}{2r}\sqrt[\kappa]{\dfrac{\omega_s}{\omega_{s,0}}}\right) \\ \qquad\qquad -\dfrac{d_0}{2r}\sqrt[\kappa]{\dfrac{\omega_s}{\omega_{s,0}}}\sqrt{1-\left(\dfrac{d_0}{2r}\sqrt[\kappa]{\dfrac{\omega_s}{\omega_{s,0}}}\right)^2}\Bigg], 1 \leq \dfrac{\omega_s}{\omega_{s,0}} \leq \left(\dfrac{2r}{d_0}\right)^\kappa \\ 0, \quad \text{otherwise.} \end{cases} \tag{3.47}$$

3.5.2 Ergodic Spectral efficiency for a single hop link

In [19], the authors discussed the time scale of a MU's mobility and that of an information transmission. In line with [19], we assume the slotted ALOHA [20] as the medium-access-control (MAC) protocol. We first portray the mobility time slot in Figure 3.8(a), from which we can ob-

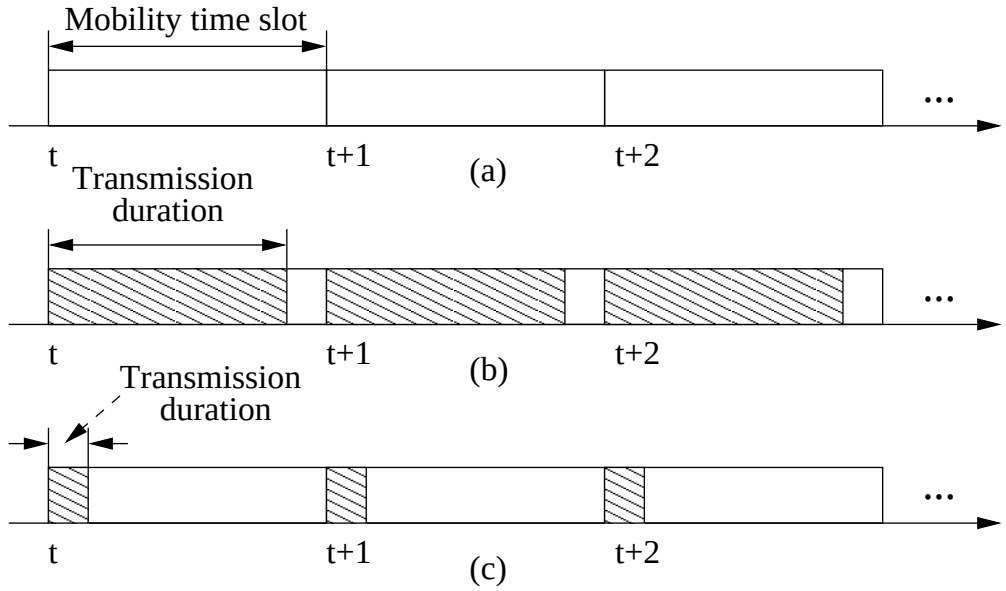

Figure 3.8: Mobility and transmission time scales [19].

serve that the performance of the information transmission during the t^{th} mobility time slot varies from that during the $(t+1)^{\text{th}}$ mobility time slot due to the time-variant PL incurred by the mobility of the transmitter and the receiver. As shown in both Figures 3.8(b) and (c), we assume an information transmission starts at the beginning of a mobility time slot and completes before the end of the mobility time slot. Then, the next information transmission starts at the beginning of the subsequent mobility time slot.

In the following two scenarios, the multipath fading effect does not need to be considered for deriving the ergodic spectral efficiency for a single hop link:

- In broadband communications, various advanced diversity techniques are employed at the receiver end, such as selective combining technique, maximum ratio combining technique and equal-gain combining technique, so as to counteract the adverse effect of the multipath fading.

- In narrowband communications, if the information transmission duration is comparable to the duration of a mobility time slot, as shown in Figure 3.8(b), the information transmission duration may include numerous multipath fading block. According to the law of large numbers, the channel amplitude during the entire transmission duration may converge to the average value of the multipath fading. Hence, the stochastic properties of the multipath fading do not influence the channel in this scenario.

Bn contrast, in the next scenario, we have to jointly consider both the multipath fading effect and the time-varying PL effect on the ergodic channel spectral efficiency:

- In narrowband communications, if the information transmission duration is much shorter than the duration of a mobility time slot, the channel fluctuation during the t^{th} information transmission duration are quite different from that during the $(t+1)^{\text{th}}$ information transmission duration, as shown in Figure 3.8(c), due to the joint effect of the stochastic multipath fading and the time-varying PL.

According to the information theory [21], the channel capacity is defined as the upper bound of the information rate that can be achieved with arbitrarily small error probability. As a result, in the presence of the noise, the spectral efficiency, which is defined as the information rates per bandwidth, can be expressed as

$$C_l = \log_2(1+\text{SNR}_l) = \log_2\left(1+\frac{P_l|h_l|^2}{N_0 B_l \cdot \Omega_l}\right) = \log_2\left(1+\frac{\overline{P}_l|h_l|^2}{\Omega_l}\right), \tag{3.48}$$

where $|h_l|^2$ is the power amplitude of the random multipath fading having a unity average value and Ω_l is the time-varying PL incurred by the mobility of both the transmitter and the receiver, whereas N_0 is the power spectrum density of the noise and B_l is the communication bandwidth, whereas $\overline{P}_l$ is the normalisation of the actual transmit power P_l by the noise power $N_0 B_l$.

Then we will discuss the statistical properties for the spectral efficiency C_l defined in Eq.(3.48) with and without considering the multipath fading effect.

3.5.2.1 Spectral efficiency without the multipath fading effect

In this scenario, the power amplitude $|h_l|^2$ of the multipath fading is a deterministic constant which is equal to a unity. The spectral efficiency C_l is dominated by the time-varying PL Ω_l. Since the time-varying PL Ω_l is caused by the distance variation, the spectral efficiency thus depends on the statistical properties of the random distance Y_l between the transmitter and the receiver. The cdf $F_{C_l}(c_l)$ of the spectral efficiency C_l is defined as the probability of C_l being lower than a specific realisation c_l, which is further expressed as

$$\begin{aligned} F_{C_l}(c_l) &= \text{Pr}(C_l \le c_l) = \text{Pr}\left[\log_2\left(1+\frac{\overline{P}_l}{\Omega_l}\right) \le c_l\right] = \text{Pr}\left(\Omega_l \ge \frac{\overline{P}_l}{2^{c_l}-1}\right) \\ &= 1 - F_{\Omega_l}\left(\frac{\overline{P}_l}{2^{c_l}-1}\right), \end{aligned} \tag{3.49}$$

where $F_{\Omega_l}(\cdot)$ is the cdf of the time-variant PL, whose generic expression is given by Eq.(3.42). According to the PL model proposed in Eq.(3.39), the minimum PL value is $\omega_{l,0}$, which further

produces the maximum possible value for the random spectral efficiency C_l:

$$c_{l,\max} = \log_2\left(1 + \frac{\overline{P}_l}{\omega_{l,0}}\right). \tag{3.50}$$

Similar to the derivation of Eq.(3.42), the cdf $F_{C_l}(c_l)$ has a different expression given a specific value of c_l. We omit the derivation process here and directly present the generic expression for the cdf of the random spectral efficiency C_l:

$$F_{C_l}(c_l) = \begin{cases} 1 - F_{Y_l}\left(d_0 \sqrt[\kappa]{\dfrac{\overline{P}_l}{\omega_{l,0}(2^{c_l}-1)}}\right), & 0 < c_l \le c_{l,\max}, \\ 1, & c_l > c_{l,\max}, \end{cases} \tag{3.51}$$

where $F_{Y_l}(\cdot)$ is the cdf of the random distance Y_l. Note that the complementary cumulative distribution function (ccdf) $(1 - F_{C_l}(c_l))$ is normally invoked for outage analysis of the channel, where c_l often takes the value of the minimum acceptable spectral efficiency. After differentiating $F_{C_l}(c_l)$ of Eq.(3.51) with respect to c_l in the region $(0, c_{l,\max}]$, we arrive at the pdf of the random spectral efficiency, which is expressed as

$$f_{C_l}(c_l) = \frac{d_0}{\kappa} \cdot \frac{2^{c_l}\ln 2}{2^{c_l}-1} \cdot \sqrt[\kappa]{\frac{\overline{P}_l}{\omega_{l,0}(2^{c_l}-1)}} \cdot f_{Y_l}\left(d_0 \sqrt[\kappa]{\frac{\overline{P}_l}{\omega_{l,0}(2^{c_l}-1)}}\right), \quad 0 < c_l \le c_{l,\max}, \tag{3.52}$$

and $f_{C_l}(c_l) = 0$, otherwise, where $f_{Y_l}(\cdot)$ is the pdf of the random distance Y_l.

By substituting the corresponding cdf $F_{Y_b}(y_b)$ and pdf $f_{Y_b}(y_b)$ into Eqs.(3.51) and (3.52), we may arrive at the cdf and the pdf of the random spectral efficiency C_b between the BS and a MU. Let us first consider the scenario that a cell is modelled by a circular area and the BS is at the centre of this circular area, while the MU moves within the circular cell by obeying the uniform mobility model. We note that since the maximum value for the random distance Y_b is the radius r, the corresponding minimum value for the random spectral efficiency C_b is

$$c_{b,\min} = \log_2\left[1 + \frac{\overline{P}_b}{\omega_{b,0}}\left(\frac{d_0}{r}\right)^{\kappa}\right] \tag{3.53}$$

As a result, by substituting $F_{Y_b}(y_b)$ of Eq.(3.2) into Eq.(3.51), the cdf of Ω_b is expressed as

$$F_{C_b}(c_b) = \begin{cases} 0, & 0 < c_b < c_{b,\min}, \\ 1 - \left(\dfrac{d_0}{r} \sqrt[\kappa]{\dfrac{\overline{P}_b}{\omega_{b,0}(2^{c_b}-1)}} \right)^2, & c_{b,\min} \le c_b \le c_{b,\max}, \\ 1, & c_b > c_{b,\max}, \end{cases} \tag{3.54}$$

where $c_{b,\max}$ is derived by substituting $\overline{P}_b$ and $\omega_{b,0}$ into Eq.(3.50). Furthermore, by substituting $f_{Y_b}(y_b)$ of Eq.(3.3) into Eq.(3.52), the pdf of the random spectral efficiency C_b is expressed as

$$f_{C_b}(c_b) = \frac{2^{c_b+1}\ln 2}{\kappa(2^{c_b}-1)} \cdot \left(\frac{d_0}{r} \sqrt[\kappa]{\frac{\overline{P}_b}{\omega_{b,0}(2^{c_b}-1)}} \right)^2, \quad c_{b,\min} < c_b \le c_{b,\max}, \tag{3.55}$$

and $f_{C_b}(c_b) = 0$, otherwise.

Second, we consider the scenario that a pair of MUs both move within a circular area having r as its radius by obeying the uniform mobility model. We note that since the maximum value for the random distance Y_s is the diameter $2r$, the corresponding minimum value for the random spectral efficiency C_s is

$$c_{s,\min} = \log_2 \left[1 + \frac{\overline{P}_s}{\omega_{s,0}} \left(\frac{d_0}{2r} \right)^{\kappa} \right] \tag{3.56}$$

As a result, by substituting $F_{Y_s}(y_s)$ of Eq.(3.30) into Eq.(3.51), the cdf of the random spectral efficiency C_s is expressed as

$$\begin{aligned} F_{C_s}(c_s) = 1 + \frac{2}{\pi} \Bigg\{ & \left[\frac{d_0}{2r} \sqrt[\kappa]{\frac{\overline{P}_s}{\omega_{s,0}(2^{c_s}-1)}} + 2 \left(\frac{d_0}{2r} \sqrt[\kappa]{\frac{\overline{P}_s}{\omega_{s,0}(2^{c_s}-1)}} \right)^3 \right] \sqrt{1 - \left(\frac{d_0}{2r} \sqrt[\kappa]{\frac{\overline{P}_s}{\omega_{s,0}(2^{c_s}-1)}} \right)^2} \\ & - 4 \left(\frac{d_0}{2r} \sqrt[\kappa]{\frac{\overline{P}_s}{\omega_{s,0}(2^{c_s}-1)}} \right)^2 \arccos \left(\frac{d_0}{2r} \sqrt[\kappa]{\frac{\overline{P}_s}{\omega_{s,0}(2^{c_s}-1)}} \right) \\ & - \arcsin \left(\frac{d_0}{2r} \sqrt[\kappa]{\frac{\overline{P}_s}{\omega_{s,0}(2^{c_s}-1)}} \right) \Bigg\}, c_{s,\min} \le c_s \le c_{s,\max}, \end{aligned} \tag{3.57}$$

where $c_{s,\max}$ is derived by substituting $\overline{P}_s$ and $\omega_{s,0}$ into Eq.(3.50). We also have $F_{C_s}(c_s) = 0$ if $0 < c_s < c_{s,\min}$, while $F_{C_s}(c_s) = 1$ if $c_s > c_{s,\max}$. Furthermore, by substituting $f_{Y_s}(y_s)$ of

Eq.(3.29) into Eq.(3.52), the pdf of the spectral efficiency C_s is expressed as

$$f_{C_s}(c_s) = \frac{2^{c_s+2}\ln 2}{\pi\kappa(2^{c_l}-1)} \left(\frac{d_0}{r}\sqrt[\kappa]{\frac{\overline{P}_s}{\omega_{s,0}(2^{c_s}-1)}}\right)^2 \left[-\frac{d_0}{2r}\sqrt[\kappa]{\frac{\overline{P}_s}{\omega_{s,0}(2^{c_s}-1)}}\sqrt{1-\left(\frac{d_0}{2r}\sqrt[\kappa]{\frac{\overline{P}_s}{\omega_{s,0}(2^{c_s}-1)}}\right)^2}\right.$$
$$\left. + \arccos\left(\frac{d_0}{2r}\sqrt[\kappa]{\frac{\overline{P}_s}{\omega_{s,0}(2^{c_s}-1)}}\right)\right], c_{s,\min} \le c_s \le c_{s,\max}, \quad (3.58)$$

and $f_{C_s}(C_s) = 0$, otherwise.

3.5.2.2 Spectral efficiency with the multipath fading

We assume that the amplitude h_l of the channel gain follows the uncorrelated Rayleigh fading associated with a unity mean. As a result, the power amplitude $X = |h_l|^2$ of the channel gain obeys the exponential distribution associated with a unity mean, whose pdf and cdf are given by $f_X(x) = \mathrm{e}^{-x}$ and $F_X(x) = 1 - \mathrm{e}^{-x}$, respectively. In the scenario, which is shown in Figure 3.8(c), the spectral efficiency C_l is dominated by both the time-varying PL Ω_l and the random multipath fading $|h_l|^2$. The cdf $F_{C_l}(c_l)$ of the spectral efficiency C_l is defined as the probability of C_l being lower than a specific realisation c_l, which is further expressed

$$F_{C_l}(c_l) = \mathrm{Pr}(C_l \le c_l) = \mathrm{Pr}\left[\log_2\left(1 + \frac{\overline{P}_l}{\Omega_l}\cdot|h_l|^2\right) \le c_l\right]. \quad (3.59)$$

Given a specific realisation $\Omega_l = \omega_l$ of the time-varying PL, the conditional cdf of the spectral efficiency C_l is expressed as

$$F_{C_l}(c_l|\Omega_l = \omega_l) = \mathrm{Pr}(C_l \le c_l|\Omega_l = \omega_l) = \mathrm{Pr}\left[|h_l|^2 \le (2^{c_l}-1)\frac{\omega_l}{\overline{P}_l}\Big|\Omega_l = \omega_l\right]$$
$$= 1 - \mathrm{e}^{-(2^{c_l}-1)\omega_l/\overline{P}_l}. \quad (3.60)$$

According to Bayesian principle [22], by exploiting the generic expression of the pdf of the time-varying PL Ω_l of Eq.(3.43), the cdf $F_{C_l}(c_l)$ of the spectral efficiency can be further derived as

$$F_{C_l}(c_l) = \int_{\omega_l} F_{C_l}(c_l|\Omega_l = \omega_l) f_{\Omega_l}(\omega_l) d\omega_l$$
$$= \int_{\omega_{l,0}}^{+\infty} \left(1 - \mathrm{e}^{-(2^{c_l}-1)\omega_l/\overline{P}_l}\right) \cdot \frac{d_0}{\kappa\omega_l}\sqrt[\kappa]{\frac{\omega_l}{\omega_{l,0}}} \cdot f_{Y_l}\left(d_0\sqrt[\kappa]{\frac{\omega_l}{\omega_{l,0}}}\right) d\omega_l, \;\; c_l > 0, \quad (3.61)$$

where $f_{Y_l}(y_l)$ is the pdf of the random distance Y_l between the transmitter and the receiver. By differentiating $F_{Y_l}(y_l)$ with respect to c_l, we arrive at the pdf of the spectral efficiency C_l, which is expressed as

$$f_{C_l}(c_l) = \int_{\omega_{l,0}}^{+\infty} 2^{c_l} \mathrm{e}^{-(2^{c_l}-1)\omega_l/\overline{P}_l} \cdot \frac{d_0 \ln 2}{\kappa \overline{P}_l} \cdot \sqrt[\kappa]{\frac{\omega_l}{\omega_{l,0}}} \cdot f_{Y_l}\left(d_0 \sqrt[\kappa]{\frac{\omega_l}{\omega_{l,0}}}\right) d\omega_l, \quad c_l > 0, \tag{3.62}$$

Note that when the multipath fading is not taken into consideration, the spectral efficiency C_l cannot exceed its upper bound $c_{l,\max}$ because the minimum value for the PL is $\omega_{l,0}$ according to the PL model expressed in Eq.(3.39) considered in this chapter. However, if the multipath fading effect is considered, the uncertainty of the channel's power amplitude might greatly fluctuate the spectral efficiency C_l and make it possibly take any value larger than zero.

Unfortunately, we are not able to derive the close-form formulas for the statistical properties of the random spectral efficiency C_l by considering both the time-varying PL and the multipath fading effect. Alternatively, we express both the cdf and the pdf of C_l in terms of a single integral, as shown in Eqs.(3.61) and (3.62) which can be easily solved by numerical algorithms, such as the *adaptive quadrature* algorithm [23].

By substituting the corresponding pdf $f_{Y_b}(y_b)$ into Eqs.(3.61) and (3.62), we may arrive at the cdf and the pdf of the random spectral efficiency C_b between the BS and a MU. Let us first consider the scenario that a cell is modelled by a circular area associated with a radius of r and the BS is at the centre of this circular area, while the MU moves within the circular cell by obeying the uniform mobility model. Note that since the maximum value for the random distance Y_b is the radius r, the corresponding maximum PL is $\omega_{b,\max} = \omega_{b,0}(r/d_0)^{\kappa}$. As a result, by substituting $f_{Y_b}(y_b)$ of Eq.(3.3) into Eq.(3.61), the cdf $F_{C_b}(c_b)$ can be expressed as

$$F_{C_b}(c_b) = \int_{\omega_{b,0}}^{\omega_{b,\max}} \left(1 - \mathrm{e}^{-(2^{c_b}-1)\omega_b/\overline{P}_b}\right) \cdot \frac{2}{\kappa \omega_b} \cdot \left(\frac{d_0}{r} \sqrt[\kappa]{\frac{\omega_b}{\omega_{b,0}}}\right)^2 d\omega_b, \quad c_b > 0. \tag{3.63}$$

Similarly, by substituting $f_{Y_b}(y_b)$ of Eq.(3.3) into Eq.(3.62), the pdf $f_{C_b}(c_b)$ can be expressed as

$$f_{C_b}(c_b) = \int_{\omega_{b,0}}^{\omega_{b,\max}} 2^{c_b+1} \mathrm{e}^{-(2^{c_b}-1)\omega_l/\overline{P}_b} \cdot \frac{\ln 2}{\kappa \overline{P}_b} \cdot \left(\frac{d_0}{r} \sqrt[\kappa]{\frac{\omega_b}{\omega_{b,0}}}\right)^2 d\omega_b, \quad c_b > 0. \tag{3.64}$$

By substituting the corresponding pdf $f_{Y_s}(y_s)$ into Eqs.(3.61) and (3.62), we may arrive at the cdf and the pdf of the random spectral efficiency C_s between a pair of MUs. Let us consider the scenario that both the transmitter and the receiver move within a circular area having a radius of r by obeying the uniform mobility model. We note that since the maximum value for the random

distance Y_s is the diameter $2r$, the corresponding maximum PL is $\omega_{s,\max} = \omega_{s,0}(2r/d_0)^\kappa$. As a result, by substituting $f_{Y_s}(y_s)$ of Eq.(3.29) into Eq.(3.61), the cdf $F_{C_s}(c_s)$ can be expressed as

$$F_{C_s}(c_s) = \int_{\omega_{s,0}}^{\omega_{s,\max}} \left(1 - \mathrm{e}^{-\frac{(2^{c_s}-1)\omega_s}{\overline{P}_s}}\right) \cdot \frac{16}{\pi\kappa\omega_s} \left(\frac{d_0}{2r}\sqrt[\kappa]{\frac{\omega_s}{\omega_{s,0}}}\right)^2 \left[\arccos\left(\frac{d_0}{2r}\sqrt[\kappa]{\frac{\omega_s}{\omega_{s,0}}}\right) - \frac{d_0}{2r}\sqrt[\kappa]{\frac{\omega_s}{\omega_{s,0}}}\sqrt{1 - \left(\frac{d_0}{2r}\sqrt[\kappa]{\frac{\omega_s}{\omega_{s,0}}}\right)^2}\right] d\omega_s, \quad c_s > 0. \quad (3.65)$$

Similarly, by substituting $f_{Y_s}(y_s)$ of Eq.(3.29) into Eq.(3.62), the pdf $f_{C_s}(c_s)$ can be expressed as

$$f_{C_s}(c_s) = \int_{\omega_{s,0}}^{\omega_{s,\max}} 2^{c_s+4}\mathrm{e}^{-\frac{(2^{c_s}-1)\omega_s}{\overline{P}_s}} \cdot \frac{\ln 2}{\pi\kappa\overline{P}_s} \cdot \left(\frac{d_0}{2r}\sqrt[\kappa]{\frac{\omega_s}{\omega_{s,0}}}\right)^2 \left[\arccos\left(\frac{d_0}{2r}\sqrt[\kappa]{\frac{\omega_s}{\omega_{s,0}}}\right) - \frac{d_0}{2r}\sqrt[\kappa]{\frac{\omega_s}{\omega_{s,0}}}\sqrt{1 - \left(\frac{d_0}{2r}\sqrt[\kappa]{\frac{\omega_s}{\omega_{s,0}}}\right)^2}\right] d\omega_s, \quad c_s > 0. \quad (3.66)$$

3.5.3 Broadcast outage event

In the broadcast scenario, a transmitter broadcasts a series of messages in a broadcast channel. All the receivers that are interested in these messages tune their radio front to this broadcast channel so as to receive the messages. However, the broadcast technique is quite different from both the point-to-point and multicast communication techniques, where the transmitter aware the existence of the all the receivers. The broadcaster does not have any knowledge of the receivers. As a result, no additional techniques, such as retransmission, are adopted for guarantee the reliability of the message reception at a specific receiver end. Once the receiver is in the outage state during the transmission of a packet, it may never receive this packet afterwards.

We first consider the BS-based broadcast, where the transmitter is a static node. In a specific area, either the whole coverage of a cell or other bounded area, N receivers move independently by obeying the uniform mobility model. As a result, each link connecting the broadcaster to a specific receiver is independent of all the other links in the broadcast scenario since the positions of the receivers are independently distributed in the studied area. In this section, we consider the scenario that the BS is at the centre of a circular cell, whose radius is r m, while the N receivers move within this circular cell by following independent uniform mobility model.

If the ergodic spectral efficiency of a link connecting the broadcaster to a specific receiver is lower than a pre-defined threshold C_{th}, this receiver falls into the outage state. Given the closed-form cdf of the ergodic spectral efficiency in a single hop link, whose generic equation are ex-

pressed as Eq.(3.51) for no multipath fading case and expressed as Eq.(3.61) for multipath fading case, we may further derive the probability P_{out} of a specific receiver staying in the outage state during a packet transmission.

Since the distances between N receivers and the broadcaster are independent of each other, the discrete random variable $\mathcal{N}$ representing the number of receivers that are in the outage state can be modelled by a binomial distribution. As a result, the probability mass function (pmf) of $\mathcal{N}$ can be expressed as

$$\Pr(\mathcal{N} = n) = \binom{N}{n} P_{out}^{n}(1 - P_{out})^{N-n}, \tag{3.67}$$

When only the path loss between the broadcaster and the receiver is taken into account, P_{out} in Eq.(3.67) is obtained by substituting c_{th} into Eq.(3.54). When both the path loss and the multipath fading is jointly considered, P_{out} in Eq.(3.67) is obtained by substituting c_{th} into Eq. (3.63).

Note that Eq.(3.67) is derived based on the fact that when the broadcaster is a static node, the random distances between this broadcaster to any other receivers are independent random variables. As a result, the cdf of the joint distance distribution from the broadcaster to N receivers can be formulated as $F_{Y_{b,1},\cdots,Y_{b,N}}(y_{b,1},\cdots,y_{b,N}) = \prod_{n=1}^{N} F_{Y_{b,n}}(y_{b,n})$. However, this fact is not true if the broadcaster is also a mobile node since the independence amongst the random distances from the receivers to the broadcaster is damaged according to the relevant research in [25] and [26]. For example, if we consider that the broadcaster and N receivers all move in a $a \times a$ square area by following the uniform mobility model, the joint distance distribution should be formulated as

$$F_{Y_{s,1},\cdots,Y_{s,N}}(y_{s,1},\cdots,y_{s,N}) = \frac{1}{a^2}\int_0^a dx \int_0^a dy \prod_{n=1}^{N} F_{Y_b}(y_{s,n}|(x,y)), \tag{3.68}$$

where $F_{Y_b}(y_{s,n}|(x,y))$ is the cdf of the random distance between the broadcaster, which is located at a given reference point (x,y), and the n^{th} receiver, which is uniformly distributed in the square area. $F_{Y_b}(y_{s,n}|(x,y))$ can be derived by following the methodology developed in Section 3.2.2. However, as shown in Section 3.2.2, $F_{Y_b}(y_{s,n}|(x,y))$ is too complicated to be exploited for further deriving the joint distribution $F_{Y_{s,1},\cdots,Y_{s,N}}(y_{s,1},\cdots,y_{s,N})$, which makes the derivation of the pmf $\Pr(\mathcal{N} = n)$ even more difficult. Hence, in this section, we only consider the scenario that the broadcaster is a static node.

3.5.4 Spectral efficiency for multicast transmissions

In the multicast transmissions, a multicaster has to multicast the same message to multiple re-

ceivers, which produces multiple links for delivering the message of common interest. Here, we assume that N receivers independently move within a certain region of the plane by following the uniform mobility model and they are all connected to the multicaster. Different from the broadcast technique, in the multicast scenario, the multicaster is aware of all the receivers and it has to guarantee every single packet successfully delivered to all the receivers. Hence, in the multicast transmission, both the outage and the retransmission events are dominated by the receiver, who has the weakest link with the multicaster. As a result, we define the spectral efficiency (channel capacity) for the multicast transmission as the spectral efficiency of the weakest link [24], which is expressed as

$$C_{l,m} = \min_{n=1,\cdots,N} \left\{ \log_2 \left(1 + \frac{P_l |h_n|^2}{N_0 B_l \cdot \Omega_{l,n}} \right) \right\} = \min_{n=1,\cdots,N} \left\{ \log_2 \left(1 + \frac{\overline{P}_l |h_n|^2}{\Omega_{l,n}} \right) \right\}, \tag{3.69}$$

where $|h_n|^2$ is the power amplitude caused by the multipath fading of the link connecting the n^{th} receiver to the multicaster and $\Omega_{l,n}$ is the time-varying PL of the same link incurred by the movement of both the n^{th} receiver and the multicaster, whereas $\overline{P}_l$ is derived by normalising the transmit power P_l by the noise power $N_0 B_l$.

3.5.4.1 Spectral efficiency for multicast transmission without the multipath fading

In this scenario, the power amplitudes $\{|h_n|^2 | n = 1, \cdots, N\}$ for the N receivers are all deterministic constants equal to a unity. As a result, the multicast spectral efficiency can be simplified as

$$C_{l,\mathcal{M}} = \min_{n=1,\cdots,N} \{C_{l,n}\} = \min_{n=1,\cdots,N} \left\{ \log_2 \left(1 + \frac{\overline{P}_l}{\Omega_{l,n}} \right) \right\}, \tag{3.70}$$

where $C_{l,n}$ is the spectral efficiency for a single-hop link from the multicaster to the n^{th} receiver. Since the positions of these N receivers are independently and identically distributed in the area considered, according to the relationships between the distance variation and the time-varying PL, as derived in Section 3.5.1, the PLs $\{\Omega_{l,n} | n = 1, \cdots, N\}$ between the multicaster and the N receivers are also independent and identical random variables. According to Eq.(3.70), in this scenario, the multicast spectral efficiency $C_{l,m}$ only depends on the time-varying PL. The cdf of

the multicast spectral efficiency is expressed as

$$\begin{aligned} F_{C_{l,\mathcal{M}}}(c_{l,\mathcal{M}}) &= \Pr(C_{l,\mathcal{M}} \le c_{l,\mathcal{M}}) = \Pr\left[\min_{n=1,\cdots,N}\left\{\log_2\left(1+\frac{\overline{P}_l}{\Omega_{l,n}}\right)\right\} \le c_{l,\mathcal{M}}\right] \\ &= 1-\prod_{n=1}^{N}\Pr\left[\log_2\left(1+\frac{\overline{P}_l}{\Omega_{l,n}}\right) \ge c_{l,\mathcal{M}}\right] = 1-\prod_{n=1}^{N}\Pr\left(\Omega_{l,n} \le \frac{\overline{P}_l}{2^{c_{l,\mathcal{M}}}-1}\right) \\ &= 1-\prod_{n=1}^{N}F_{\Omega_{l,n}}\left(\frac{\overline{P}_l}{2^{c_{l,\mathcal{M}}}-1}\right) = 1-\left[F_{\Omega_l}\left(\frac{\overline{P}_l}{2^{c_{l,\mathcal{M}}}-1}\right)\right]^N. \end{aligned} \tag{3.71}$$

where $F_{\Omega_l}(\cdot)$ is the cdf of the time-varying PL, whose generic expression is given by Eq.(3.42). According to the PL model proposed in Eq.(3.39), the minimum PL value for a single-hop link is $\omega_{l,0}$. When the PLs between the multicaster and all the receivers are equal to $\omega_{l,0}$, the maximum possible value for the multicast spectral efficiency $C_{l,\mathcal{M}}$ is achieved, which is expressed as:

$$c_{l,\mathcal{M}}^{\max} = \log_2\left(1+\frac{\overline{P}_l}{\omega_{l,0}}\right). \tag{3.72}$$

As a result, by substituting $F_{\Omega_l}(\cdot)$ of Eq.(3.42) into Eq.(3.71), we arrive at the generic formula for the cdf of the multicast spectral efficiency without the multipath fading effect:

$$F_{C_{l,\mathcal{M}}}(c_{l,\mathcal{M}}) = \begin{cases} 1-\left[F_{Y_l}\left(d_0\sqrt[\kappa]{\dfrac{\overline{P}_l}{\omega_{l,0}(2^{c_{l,\mathcal{M}}}-1)}}\right)\right]^N, & 0 < c_{l,\mathcal{M}} \le c_{l,\mathcal{M}}^{\max}, \\ 1, & c_{l,\mathcal{M}} > c_{l,\mathcal{M}}^{\max}, \end{cases} \tag{3.73}$$

where $F_{Y_l}(\cdot)$ is the cdf of the random distance Y_l between a transmitter and a receiver. Note that if we let $c_{l,\mathcal{M}}$ be a specific spectral efficiency threshold for the multicast links connecting the multicaster to the receivers, the cdf $F_{C_{l,\mathcal{M}}}(c_{l,\mathcal{M}})$ represents the outage probability of the multicast transmission. By differentiating the cdf $F_{C_{l,\mathcal{M}}}(c_{l,\mathcal{M}})$ with respect to $c_{l,\mathcal{M}}$, the pdf of the multicast spectral efficiency $C_{l,\mathcal{M}}$ can be expressed as

$$\begin{aligned} f_{C_{l,\mathcal{M}}}(c_{l,\mathcal{M}}) = {} & \frac{N\cdot 2^{c_{l,\mathcal{M}}}\ln 2}{\kappa\cdot(2^{c_{l,\mathcal{M}}}-1)}\cdot d_0\sqrt[\kappa]{\frac{\overline{P}_l}{\omega_{l,0}(2^{c_{l,\mathcal{M}}}-1)}}\cdot f_{Y_l}\left(d_0\sqrt[\kappa]{\frac{\overline{P}_l}{\omega_{l,0}(2^{c_{l,\mathcal{M}}}-1)}}\right) \\ & \cdot\left[F_{Y_l}\left(d_0\sqrt[\kappa]{\frac{\overline{P}_l}{\omega_{l,0}(2^{c_{l,\mathcal{M}}}-1)}}\right)\right]^{N-1}, \quad \text{for } 0 < c_{l,\mathcal{M}} \le c_{l,\mathcal{M}}^{\max}, \end{aligned} \tag{3.74}$$

and $f_{C_{l,\mathcal{M}}}(c_{l,\mathcal{M}}) = 0$, otherwise.

By substituting the corresponding cdf $F_{Y_b}(y_b)$ and pdf $f_{Y_b}(y_b)$ into Eqs.(3.73) and (3.74), we may arrive at the cdf and the pdf of the multicast spectral efficiency $C_{b,\mathcal{M}}$ between the BS and multiple MUs, where the BS plays the role of the multicaster. We assume that a cell is modelled by a circular area having a radius of r and the BS is at the centre of this circular area, while N MUs move within the circular cell independently by obeying the uniform mobility model. Note that since the maximum value for the random distance Y_b is r, the corresponding maximum PL is $\omega_{b,\max} = \omega_{b,0}(r/d_0)^{\kappa}$. When the PLs between the BS and all the N MUs are equal to $\omega_{b,\max}$, the following minimum multicast spectral efficiency is achieved:

$$c_{b,\mathcal{M}}^{\min} = \log_2\left(1 + \frac{\overline{P}_b}{\omega_{b,\max}}\right) = \log_2\left[1 + \frac{\overline{P}_b}{\omega_{b,0}}\left(\frac{d_0}{r}\right)^{\kappa}\right]. \tag{3.75}$$

As a result, by substituting $F_{Y_b}(y_b)$ of Eq.(3.2) into Eq.(3.80), the cdf $F_{C_{b,\mathcal{M}}}(c_{b,\mathcal{M}})$ can be expressed as

$$F_{C_{b,\mathcal{M}}}(c_{b,\mathcal{M}}) = \begin{cases} 0, & 0 < c_{b,\mathcal{M}} < c_{b,\mathcal{M}}^{\min} \\ 1 - \left(\dfrac{d_0}{r}\sqrt[\kappa]{\dfrac{\overline{P}_b}{\omega_{b,0}(2^{c_{b,\mathcal{M}}}-1)}}\right)^{2N}, & c_{b,\mathcal{M}}^{\min} \le c_{b,\mathcal{M}} \le c_{b,\mathcal{M}}^{\max}, \\ 1, & c_{b,\mathcal{M}} > c_{b,\mathcal{M}}^{\max}, \end{cases} \tag{3.76}$$

where $c_{b,\mathcal{M}}^{\max}$ is derived by substituting P_b and $\omega_{b,0}$ into Eq.(3.72).

By substituting both $F_{Y_b}(y_b)$ of Eq.(3.2) and $f_{Y_b}(y_b)$ of Eq.(3.3) into Eq.(3.74), the pdf of the multicast spectral efficiency $C_{b,\mathcal{M}}$ can be formulated as

$$f_{C_{b,\mathcal{M}}}(c_{b,\mathcal{M}}) = \frac{2N \cdot 2^{c_{b,\mathcal{M}}} \ln 2}{\kappa \cdot (2^{c_{b,\mathcal{M}}}-1)} \cdot \left(\frac{d_0}{r}\sqrt[\kappa]{\frac{\overline{P}_b}{\omega_{b,0}(2^{c_{b,\mathcal{M}}}-1)}}\right)^{2N}, c_{b,\mathcal{M}}^{\min} \le c_{b,\mathcal{M}} \le c_{b,\mathcal{M}}^{\max}, \tag{3.77}$$

and $f_{C_{b,\mathcal{M}}}(c_{b,\mathcal{M}}) = 0$, otherwise.

Similar to the broadcast scenario, if the multicaster also moves within the area studied, the distances between the multicaster to the N receivers are no longer independent random variables. Due to its extreme complexity, we thus omit the derivation of the cdf and pdf for the multicast spectral efficiency.

3.5.4.2 Spectral efficiency for multicast transmission with the multipath fading

We model the amplitude h_l of the channel gain by the uncorrelated Rayleigh fading associated with a unity mean. As a result, the power amplitude $X_n = |h_n|^2$ of the channel gain between the

multicaster and the n^{th} receiver obeys the exponential distribution associated with a unity mean, whose pdf and cdf are given by $f_{X_n}(x_n) = \mathrm{e}^{-x_n}$ and $F_{X_n}(x_n) = 1 - \mathrm{e}^{-x_n}$, respectively. If the multicaster is a static node, the multicast spectral efficiency C_l is dominated by the independent time-varying PLs $\{\Omega_{l,n}|n = 1, \cdots, N\}$ and the random multipath fading $\{|h_n|^2|n = 1, \cdots, N\}$. Since the time-varying PLs $\{\Omega_{l,n}|n = 1, \cdots, N\}$ are incurred by the distance variations, the multicast spectral efficiency thus depends on the statistical properties of the random distance Y_l between the multicaster and the receiver. The cdf $F_{C_{l,\mathcal{M}}}(c_{l,\mathcal{M}})$ of the multicast spectral efficiency $C_{l,\mathcal{M}}$ is defined as the probability of $C_{l,\mathcal{M}}$ being lower than a specific realisation $c_{l,\mathcal{M}}$, which is further expressed as

$$\begin{aligned} F_{C_{l,\mathcal{M}}}(c_{l,\mathcal{M}}) &= \mathrm{Pr}(C_{l,\mathcal{M}} \leq c_{l,\mathcal{M}}) = \mathrm{Pr}\left[\min_{n=1,\cdots,N}\left\{\log_2\left(1 + \frac{\overline{P}_l|h_n|^2}{\Omega_{l,n}}\right)\right\} \leq c_{l,\mathcal{M}}\right] \\ &= 1 - \prod_{n=1}^{N} \mathrm{Pr}\left[\log_2\left(1 + \frac{\overline{P}_l|h_n|^2}{\Omega_{l,n}}\right) \geq c_{l,\mathcal{M}}\right]. \end{aligned} \tag{3.78}$$

Substituting a vector of specific PLs' realisation $\{\Omega_{l,n} = \omega_{l,n}|n = 1, \cdots, N\}$ into Eq.(3.78), the conditional cdf for the multicast spectral efficiency $C_{l,\mathcal{M}}$ can be further derived as

$$F_{C_{l,\mathcal{M}}}(c_{l,\mathcal{M}}|\omega_1, \cdots, \omega_N) = 1 - \prod_{n=1}^{N} \mathrm{Pr}\left(|h_n|^2 \geq \frac{\omega_{l,n}(2^{c_{l,\mathcal{M}}} - 1)}{\overline{P}_l}\right) = 1 - \prod_{n=1}^{N} \mathrm{e}^{-\frac{\omega_{l,n}(2^{c_{l,\mathcal{M}}} - 1)}{\overline{P}_l}}. \tag{3.79}$$

Since the time-varying PLs $\{\Omega_{l,n}|n = 1, \cdots, N\}$ are independent random variables, the joint pdf of $\{\Omega_{l,n}|n = 1, \cdots, N\}$ can be expressed as $f_{\Omega_{l,1}\cdots\Omega_{l,2}}(\omega_{l,1}, \cdots, \omega_{l,N}) = \prod_{n=1}^{N} f_{\Omega_{l,n}}(\omega_{l,n})$. According to Bayesian principle [22], the cdf of the multicast spectral efficiency $C_{l,\mathcal{M}}$ can be finally derived as

$$\begin{aligned} F_{C_{l,\mathcal{M}}}(c_{l,\mathcal{M}}) &= \int_{\omega_{l,1}} d_{\omega_{l,1}} \cdots \int_{\omega_{l,N}} F_{C_{l,\mathcal{M}}}(c_{l,\mathcal{M}}|\omega_{l,1}, \cdots, \omega_{l,N}) f_{\Omega_{l,1}\cdots\Omega_{l,2}}(\omega_{l,1}, \cdots, \omega_{l,N}) d_{\omega_{l,N}} \\ &= 1 - \prod_{n=1}^{N} \int_{\omega_{l,0}}^{+\infty} \mathrm{e}^{-\frac{\omega_{l,n}(2^{c_{l,\mathcal{M}}} - 1)}{\overline{P}_l}} f_{\Omega_{l,n}}(\omega_{l,n}) d\omega_{l,n} \\ &= 1 - \prod_{n=1}^{N} \int_{\omega_{l,0}}^{+\infty} \mathrm{e}^{-\frac{\omega_{l,n}(2^{c_{l,\mathcal{M}}} - 1)}{\overline{P}_l}} \cdot \frac{d_0}{\kappa\omega_{l,n}} \sqrt[\kappa]{\frac{\omega_{l,n}}{\omega_{l,0}}} \cdot f_{Y_l}\left(d_0 \sqrt[\kappa]{\frac{\omega_{l,n}}{\omega_{l,0}}}\right) d\omega_{l,n} \\ &= 1 - \left[\int_{\omega_{l,0}}^{+\infty} \mathrm{e}^{-\frac{\omega_l(2^{c_{l,\mathcal{M}}} - 1)}{\overline{P}_l}} \cdot \frac{d_0}{\kappa\omega_l} \sqrt[\kappa]{\frac{\omega_l}{\omega_{l,0}}} \cdot f_{Y_l}\left(d_0 \sqrt[\kappa]{\frac{\omega_l}{\omega_{l,0}}}\right) d\omega_l\right]^N, \end{aligned} \tag{3.80}$$

for $c_{l,\mathcal{M}} > 0$, where $f_{Y_l}(\cdot)$ is the pdf of the random distance Y_l between a transmitter and receiver pair, and $F_{C_{l,\mathcal{M}}}(c_{l,\mathcal{M}}) = 0$, otherwise. The second equality of Eq.(3.80) is obtained due to the independence of the random variables $\{\Omega_{l,n}|n = 1, \cdots, N\}$. The third equality of Eq.(3.80) is derived by substituting Eq.(3.43) into the second line. Finally, we arrive at the fourth equality of Eq.(3.80) since random variables $\{\Omega_{l,n}|n = 1, \cdots, N\}$ have identical distributions, where the generic symbol ω_l replaces the specific symbol $\omega_{l,n}$.

By differentiating $F_{C_{l,\mathcal{M}}}(c_{l,\mathcal{M}})$ of Eq.(3.80) with respect to $c_{l,\mathcal{M}}$, the pdf of the multicast spectral efficiency can be formulated as

$$f_{C_{l,\mathcal{M}}}(c_{l,\mathcal{M}}) = N \cdot \left[\int_{\omega_{l,0}}^{+\infty} \frac{d_0 2^{c_{l,\mathcal{M}}} \ln 2}{\kappa \overline{P}_l} \mathrm{e}^{-\frac{\omega_l (2^{c_{l,\mathcal{M}}} - 1)}{\overline{P}_l}} \cdot \sqrt[\kappa]{\frac{\omega_l}{\omega_{l,0}}} \cdot f_{Y_l}\left(d_0 \sqrt[\kappa]{\frac{\omega_l}{\omega_{l,0}}} \right) d\omega_l \right] \cdot \left[\int_{\omega_{l,0}}^{+\infty} \mathrm{e}^{-\frac{\omega_l (2^{c_{l,\mathcal{M}}} - 1)}{\overline{P}_l}} \cdot \frac{d_0}{\kappa \omega_l} \sqrt[\kappa]{\frac{\omega_l}{\omega_{l,0}}} \cdot f_{Y_l}\left(d_0 \sqrt[\kappa]{\frac{\omega_l}{\omega_{l,0}}} \right) d\omega_l \right]^{N-1}, \tag{3.81}$$

for $c_{l,\mathcal{M}} > 0$, where $f_{Y_l}(\cdot)$ is the pdf of the random distance Y_l between a transmitter and receiver pair, and $f_{C_{l,\mathcal{M}}}(c_{l,\mathcal{M}}) = 0$, otherwise.

Note that in the scenario that the multipath fading is not taken into consideration, the multicast spectral efficiency $C_{l,\mathcal{M}}$ cannot exceed its upper bound $c_{l,\mathcal{M}}^{\max}$ because the minimum value for the PL is $\omega_{l,0}$ according to the PL model expressed in Eq.(3.39). However, if the multipath fading effect is considered, the uncertainty of the channel's power amplitude might greatly fluctuate the spectral efficiency $C_{l,\mathcal{M}}$ and make it possibly take any value larger than zero.

By substituting the corresponding pdf $f_{Y_b}(y_b)$ into Eqs.(3.80) and (3.81), we may arrive at the cdf and the pdf of the multicast spectral efficiency $C_{b,\mathcal{M}}$ between the BS and N MUs, where the BS plays the role of the multicaster. We assume that a cell is modelled by a circular area having a radius of r and the BS is at the centre of this circular area, while N MUs move within the circular cell independently by obeying the uniform mobility model. Note that since the maximum value for the random distance Y_b is the radius r, the corresponding maximum PL is $\omega_{b,\max} = \omega_{b,0}(r/d_0)^{\kappa}$. As a result, by substituting $f_{Y_b}(y_b)$ of Eq.(3.3) into Eq.(3.80), the cdf $F_{C_{b,\mathcal{M}}}(c_{b,\mathcal{M}})$ can be expressed as

$$F_{C_{b,\mathcal{M}}}(c_{b,\mathcal{M}}) = 1 - \left[\int_{\omega_{b,0}}^{\omega_{b,\max}} \frac{2\mathrm{e}^{-\frac{\omega_b (2^{c_{b,\mathcal{M}}} - 1)}{\overline{P}_b}}}{\kappa \omega_b} \cdot \left(\frac{d_0}{r} \sqrt[\kappa]{\frac{\omega_b}{\omega_{b,0}}} \right)^2 d\omega_b \right]^N, c_{b,\mathcal{M}} > 0, \tag{3.82}$$

and $F_{C_{b,\mathcal{M}}}(c_{b,\mathcal{M}}) = 0$, otherwise.

By substituting $f_{Y_b}(y_b)$ of Eq.(3.3) into Eq.(3.81), the pdf of the multicast spectral efficiency

$C_{b,\mathcal{M}}$ can be formulated as

$$f_{C_{b,\mathcal{M}}}(c_{b,\mathcal{M}}) = N \cdot \left[\int_{\omega_{b,0}}^{\omega_{b,\max}} \frac{2^{c_{b,\mathcal{M}}+1} \ln 2}{\kappa \overline{P}_b} \mathrm{e}^{-\frac{\omega_b (2^{c_{b,\mathcal{M}}}-1)}{\overline{P}_b}} \cdot \left(\frac{d_0}{r} \sqrt[\kappa]{\frac{\omega_b}{\omega_{b,0}}} \right)^2 d\omega_b \right] \cdot \left[\int_{\omega_{b,0}}^{\omega_{b,\max}} \frac{2\mathrm{e}^{-\frac{\omega_b (2^{c_{b,\mathcal{M}}}-1)}{\overline{P}_b}}}{\kappa \omega_b} \cdot \left(\frac{d_0}{r} \sqrt[\kappa]{\frac{\omega_b}{\omega_{b,0}}} \right)^2 d\omega_b \right]^{N-1}, c_{b,\mathcal{M}} > 0 \tag{3.83}$$

and $f_{C_{b,\mathcal{M}}}(c_{b,\mathcal{M}}) = 0$, otherwise.

Similar to the broadcast scenario, if the multicaster also moves within the area studied, the distances between the multicaster to the N receivers are no longer independent random variables. Due to its extreme complexity, we thus omit the derivation of the cdf and pdf for the multicast spectral efficiency.

3.6 Numerical results

After offering the analytical derivation, we move onto the numerical results for both the various distance distribution and the relevant communication metrics. Note that in all the numerical results presented in this section, the solid lines represent the analytical results, which are obtained via the closed-form equations in sections 3.2-3.5, while the markers represent the simulation results, which are obtained via the Monte-Carlo simulation.

3.6.1 Distance distribution

Let us first study the distance distribution between the BS and a specific MU in the typical scenario of cellular communication. In this scenario, the BS is located at the centre of the cellular area, while the MU roam within this cellular area by obeying the uniform mobility model. As shown in Figures.3.9(a) and (b), we plot both the cdf and the pdf of the random distance for the cells in different types of shape, including the triangular cell that is portrayed by the red solid line and the triangle marker, the square cell that is portrayed by the blue solid line and the square marker, and the hexagon cell that is portrayed by the green line and the diamond marker, as well as the circular cell that is portrayed by the pink line and the circle marker. And all these cells share the same radius, which is $r = 1$ km. As shown in Figure.3.9(a), given a specific distance, say $y_b = 0.6$ km, the circular cell achieves the lowest cdf, which indicates that the random distance is more likely to take a higher value than the cells in other shapes. As shown in Figure.3.9(b), except the random distance in the circular cell, the random distance in the polygon cells have two-fold pdfs. These

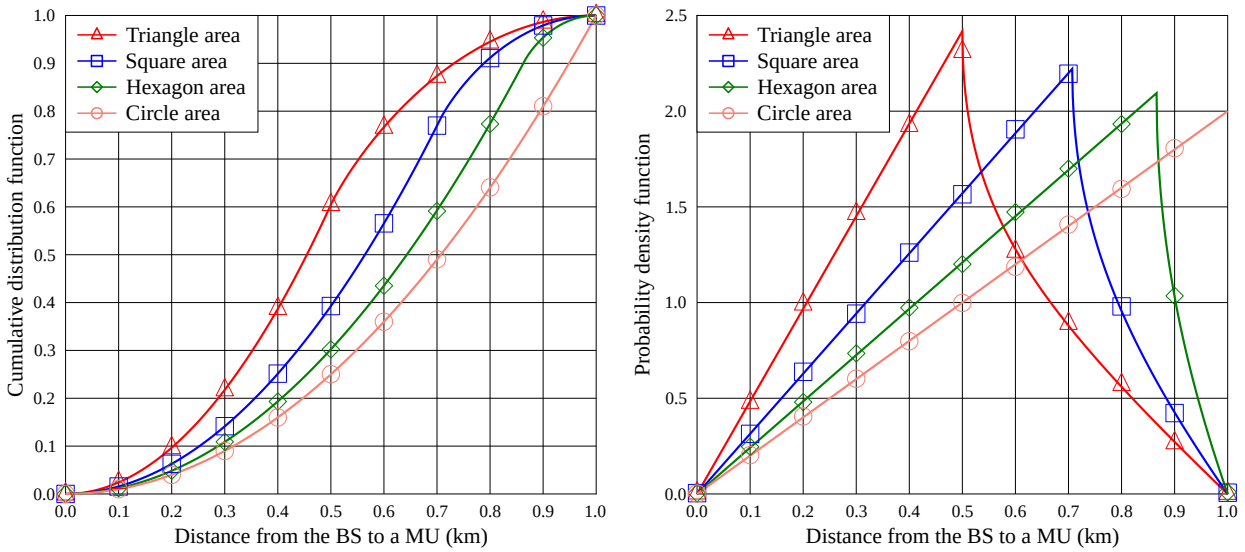

(a) Cumulative distribution function (b) Probability density function

Figure 3.9: The distance distribution between the BS and the MU, when the BS is at the centre of the cell. The radius is $r = 1$ km for all the cells in different types of shape. The analytical results of the cdfs are derived by Eqs.(3.2) and (3.5), while the analytical results of the pdfs are derived by Eqs.(3.3) and (3.6).

pdfs linearly increase and then subside after reaching their peaks. Furthermore, the accuracy of the analytical results expressed in Eqs.(3.2) and (3.3), as well as (3.5) and (3.6) are demonstrated by the Monte-Carlo simulations, as shown in both Figures.3.9(a) and (b).

Then we study the distance distribution between the BS and a specific MU, when the BS is arbitrarily located outside a circular area, while the MU roams within the circular area. The radius of the circular area is $r = 50$ m. Since the BS is outside the circular area, the distance d from the BS to the centre of the circular area should be longer than the radius r. We observe from both Figures.3.10(a) and (b) that the minimum achievable distance from the BS to the MU is $(d - r)$ m, while the maximum achievable distance is $(d + r)$ m. Furthermore, as the BS becomes farther away from the centre of the circular area, which indicates a higher value of d, both the cdf and the pdf are drifted towards the right hand side. Moreover, the accuracy of the analytical results expressed in Eqs.(3.7) and (3.8) are validated by the Monte-Carlo simulation, as shown in both Figures.3.9(a) and (b).

We next study the distance distribution between the BS and a specific MU, when the BS is located at an arbitrary position inside a circular area, while the MU roams within this circular area by following the uniform mobility model. The radius of the circular area is $r = 50$ m, while the distance between the BS and the centre of the circular area varies from $d = 10$ m to $d = 40$

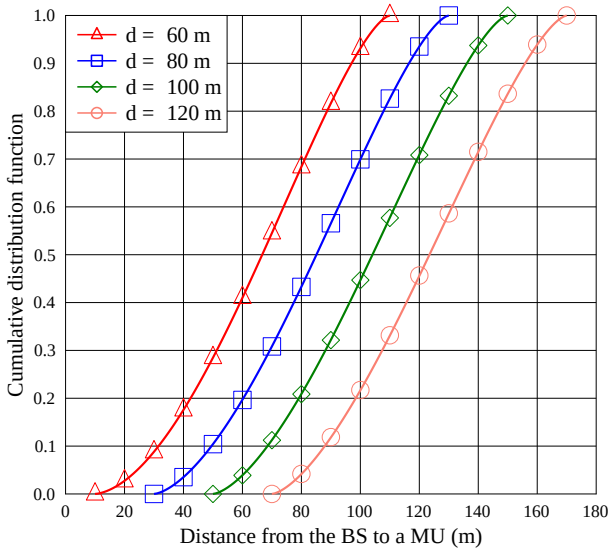

(a) Cumulative distribution function

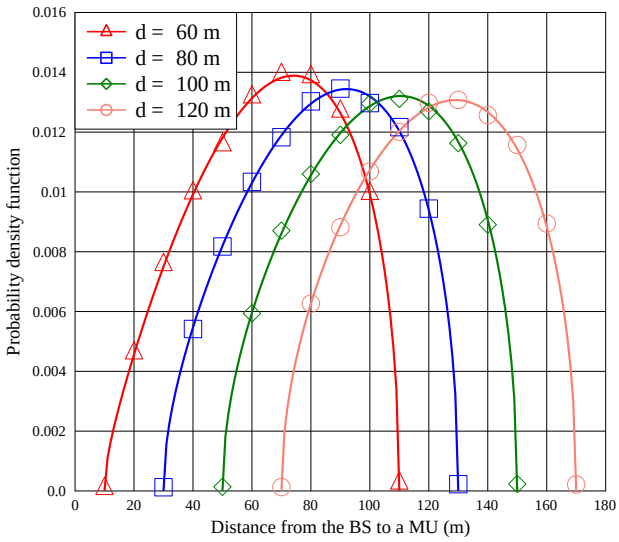

(b) Probability density function

Figure 3.10: The distance distribution between the BS and the MU, when the BS is outside a circular area. The radius of the circular area is $r = 50$ m. The analytical results of the cdfs are derived by Eq.(3.7), while the analytical results of the pdfs are derived by Eq.(3.8).

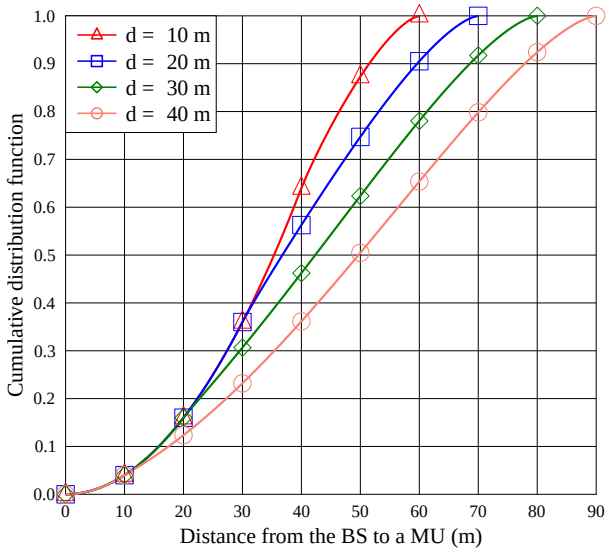

(a) Cumulative distribution function

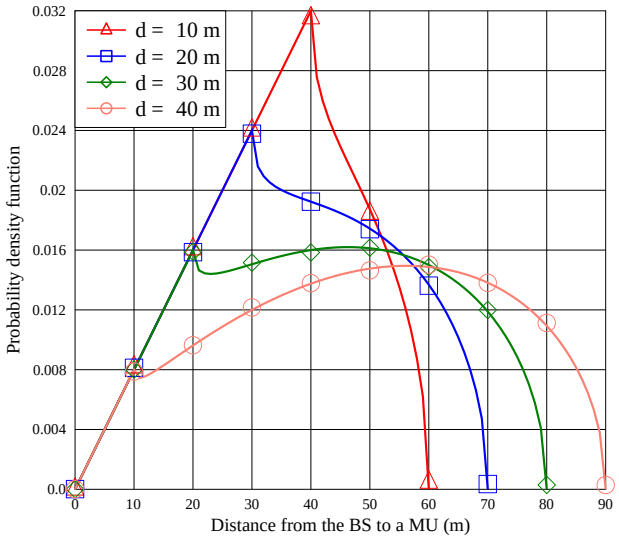

(b) Probability density function

Figure 3.11: The distance distribution between the BS and the MU, when the BS is inside a circular area. The analytical results of the cdfs are derived by Eq.(3.9), while the analytical results of the pdfs are derived by Eq.(3.10). The radius of the circular area is $r = 50$ m.

m. In Figures.3.11(a) and (b), we portrays the cdf and the pdf of the random distance for this scenario, respectively. As shown in Figure.3.11(a), the minimum achievable value for the random

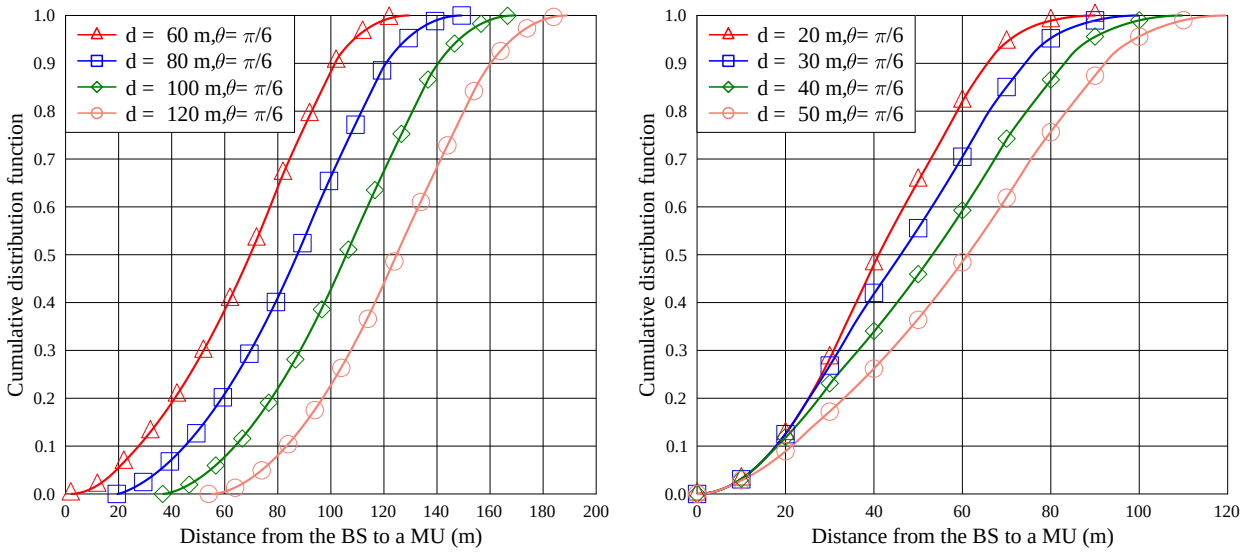

(a) The BS is outside a square area

(b) The BS is inside a square area

Figure 3.12: The distance distribution between the BS and the MU, when the BS is outside/inside a square area. The side length of the square area is $a = 100$ m. The analytical results of the cdfs are derived by Eq.3.16 and Eq.3.16, respectively.

distance are all zeros for all the different values of d. In contrast, the maximum achievable values depends on the specific d and the radius r. For example, if d takes value of 40 m, the maximum distance in this case is $d + r = 90$ m. As apparently shown in Figure.3.11(a), if the BS is farther away from the centre of the circular area, which is indicated by a larger value of d, the random distance may vary in a larger regions. Furthermore, as shown in Figure.3.11(b), the pdfs of the random distance linearly increase at first, and then subside after reaching their peaks. As the BS becomes farther away from the centre of the circular area, the linear parts of the pdfs diminish till completely disappear when the BS is located at the circumference of the circular area. Moreover, the accuracy of the analytical results expressed in Eqs.(3.9) and (3.10) are validated by the Monte-Carlo simulations, as shown in both Figures.3.9(a) and (b).

Let us now study the cdfs of the random distance between the BS and a specific MU, when the BS is arbitrarily located outside/inside a square area, while the MU roams within the square area by obeying the uniform mobility model. The side length of the square area is $a = 100$ m. In both Figures.3.12(a) and (b), the same angle $\theta = \pi/6$ is assumed, while the distance from the BS to the centre of the square varies. As shown in Figure.3.12(a), when the BS is outside the square area, both the minimum and maximum achievable distances depends on the distance d. As the BS becomes farther away from the centre of the square area, the random distance between the BS and the MU may take higher minimum and maximum values, which results in the cdf is drifted

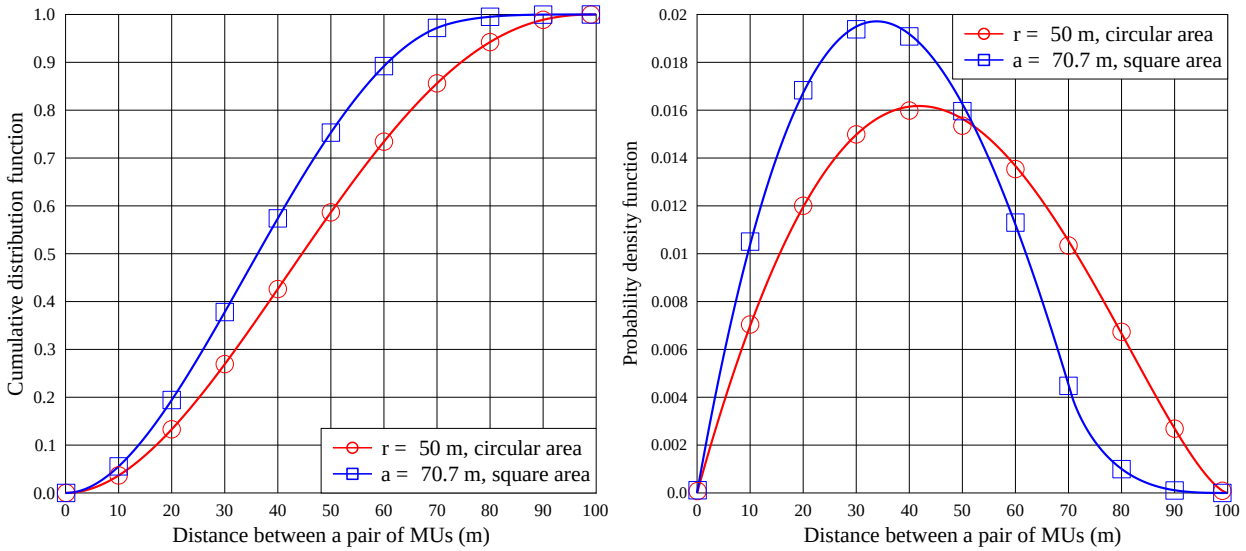

(a) Cumulative distribution function (b) Probability density function

Figure 3.13: The distance distribution between a pair of MUs, when both of the MUs roam within a circular/square area. The analytical results of the cdfs are expressed in Eqs.(3.29), (3.30), (3.35) and (3.36), respectively. The circular area and the square area both have a radius of $r = 50$ m.

towards the right hand side. However, as shown in Figure.3.12(b), only the maximum achievable distance between the BS and the MU depends on d, while the minimum achievable distances are all zeros for different values of d. As the BS becomes farther away from the centre of the square area, the random distance between the BS and the MU is distributed in a larger region. Moreover, the accuracy of the analytical results that we derived in Section 3.3.2 is validated by the Monte-Carlo simulations, as shown in both Figures.3.12(a) and (b).

At last, we evaluate the cdf and the pdf of the random distance between a pair of MUs, who both roam within a circular/square area by obeying the uniform mobility model. The radius of the circular and square areas are both $r = 50$ m. Note that the corresponding side length of the square area is $a = 70.7$ m. As shown in Figure.3.13(a), the cdf of the random distance between a pair of MUs for the square area is higher than that for the circular area. As shown in Figure.3.13(b), both of the pdfs for these two scenarios firstly increase and then subside after achieving their peaks. Furthermore, we also observe from Figure3.13(b) that the random distance for the square area is more likely to take a small value than that for the circular area. Moreover, the accuracy of the analytical results that are expressed in Eqs.(3.29), (3.30), (3.35) and (3.36) are validated by the Monte-Carlo simulation, as shown in both Figures.3.13(a) and (b).

Table 3.1: PARAMETERS OF THE PHY LAYER

	BS to MUs	MUs to MUs
Transmit Power	$P_b = 20 \sim 50$ dBm	$P_s = 0 \sim 15$ dBm
Carrier Freq	$f_{c,b} = 1.8$ GHz	$f_{c,s} = 2.4$ GHz
Bandwidth	$W_b = 10$ MHz	$W_s = 10$ MHz
Noise PSD	$N_0 = -174$ dBm/Hz (20^oC)	
PL Parameters	Exponent: $\kappa = 3$; Ref Distance: $d_0 = 1$ m	

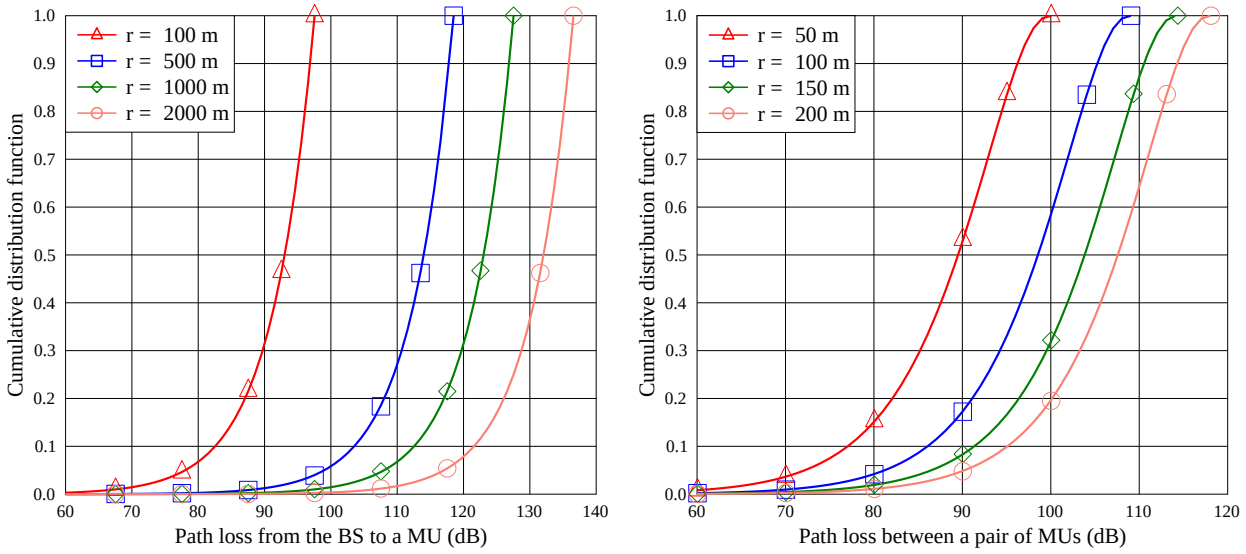

(a) The BS is at the centre of a circular cell

(b) Both of the MUs roam within a circular area

Figure 3.14: The PL between the BS and a specific MU, when the BS is located at the centre of a circular cell, while the MU roam within this cell, and that between a pair of MUs, when both of the MUs roam within a circular area. The analytical results of the cdfs are expressed in Eqs.(3.44) and (3.46), respectively.

3.6.2 Communication metrics evaluation

Now, we focus on the various communication metrics incurred by the movements of the MUs. The physical layer parameters are provided in Table 3.1. Specifically, the parameters for the communications between the BS and the MUs corresponds to the LTE-Advanced system [27], while the parameters for the communications amongst MUs corresponds to the IEEE 802.11 protocol [28]. All the following numerical results concerning the path loss and the spectral efficiency as well as the broadcast outage event are based on these physical layer parameters.

3.6.2.1 Time-varying path loss

Let us first evaluate the cdf of the time-varying PL between the BS and a specific MU in Figure 3.14(a), when the BS is located at the centre of a circular area, while the MU roams within this cell by obeying the uniform mobility model. We vary the radius of the circular cell from $r = 100$ m to $r = 2000$ m. The carrier frequency for the BS's transmission and the reference distance are given by Table 3.1. As shown in Figure 3.14(a), the cdfs of the PL exponentially increase until they reaches the unity. Furthermore, for all different value of r, the minimum achievable PL is around 60 dB because the minimum achievable PL mainly depends on the reference distance d_0. In contrast, the maximum achievable PL depends on the radius of the circular cell. As the radius increases, the maximum achievable PL also increases. For example, when the radius is $r = 2000$ m, the maximum achievable PL is around 137 dB. Then we evaluate the cdf of the time-varying PL between a pair of MUs in Figure 3.14(b), when both of the MUs roam within a circular area. The radius of the circular area varies from $r = 50$ m to $r = 200$m. As shown in Figure 3.14(b), the cdfs of the PL in this scenario firstly increases very fast but then slow down its pace toward the unity. Similarly to Figure 3.14(a), the minimum achievable PL for all different radius is around 60 dB as well. Increasing the radius of the circular area may consequently increase the maximum achievable PL. For example, the maximum achievable PL is 100 dB for $r = 50$ m, but when the radius is increased to $r = 200$ m, the maximum achievable PL also increases to 118 dB. Moreover, the accuracy of the analytical results derived in Eqs.(3.44) and (3.46) is validated by the Monte-Carlo simulations, as shown in both Figures 3.14(a) and (b).

3.6.2.2 Spectral efficiency of a single-hop link

Let us now study the spectral efficiency for the single-hop link connecting a specific MU to the BS, when the BS is located at the centre of the circular cell, while the MU roam within the circular cell by following the uniform mobility model. The radius of the circular cell is $r = 1$ km. The transmit power P_b of the BS varies from 20 dBm to 50 dBm, while all the other physical layer parameters correspond to Table 3.1. We portray the spectral efficiency without considering the multipath fading in Figure 3.15(a). When no multipath fading exists in the transmission, the spectrum efficiency is jointly determined by the time-varying PL and the transmit power. Since the radius of the cell is fixed at $r = 1$ km, the maximum achievable path loss is a constant value. As a result, the minimum achievable spectral efficiency is determined by the transmit power of the BS. We observe from Figure 3.15(a) that the minimum achievable spectral efficiency increases as we increase the transmit power of the BS, which simultaneously results in the right hand drift of the cdf curves. However, when considering the multipath fading, the wireless environment becomes

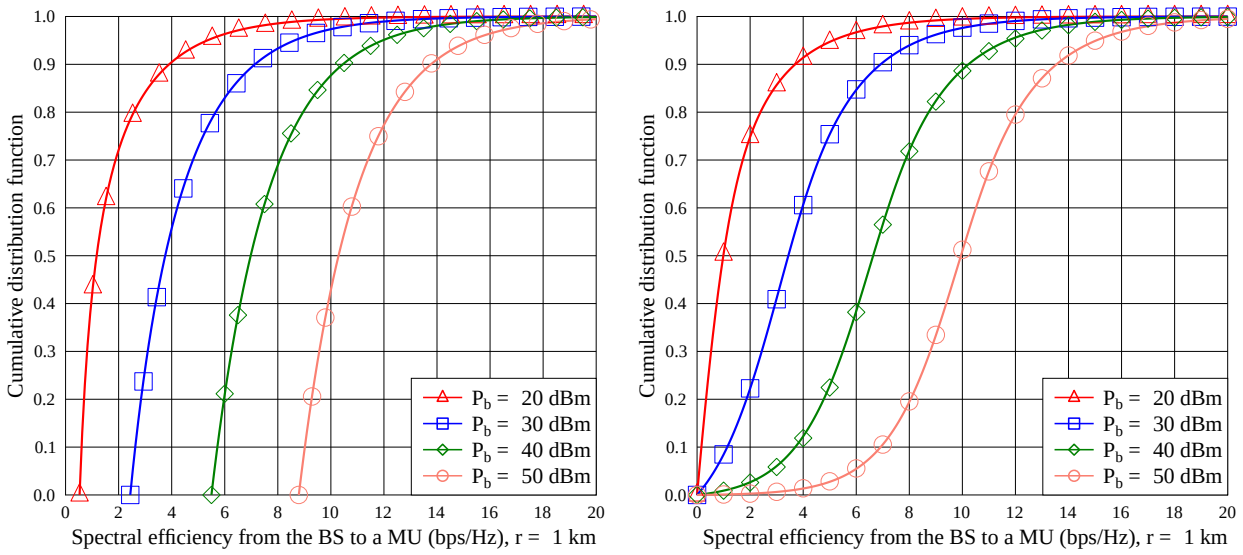

(a) Without the multipath fading

(b) With the Rayleigh fading

Figure 3.15: The single-hop spectral efficiency between the BS and a specific MU, when the BS is located at the centre of a circular cell, while the MU roam within this cell. The radius of the circular cell is $r = 1$ km. The analytical results of the cdfs are formulated in Eqs.(3.54) and (3.63), respectively.

even worse. As a result, the spectral efficiency is no longer bounded by the maximum PL and it is likely to take values very close to zero, as shown in Figure 3.15(b). Furthermore, since the cdf of the spectral efficiency can be interpreted as the outage probability, we can observe from Figure 3.15(b) that given a specific spectral efficiency as the threshold, the channel is less likely in outage state if we have a higher transmit power. Moreover, the accuracy of the analytical results derived in Eqs.(3.54) and (3.63) is validated by the Monte-Carlo simulations, as shown in both Figures 3.15(a) and (b).

We now study the spectral efficiency for the single-hop link connecting a pair of MUs, when both of the MUs roam within a circular area by following the uniform mobility model. The radius of the circular area is $r = 50$ m. The transmit power P_s of the MUs varies from 0 dBm to 15 dBm, while all the other physical layer parameters correspond to Table 3.1. We portray the spectral efficiency without considering the multipath fading in Figure 3.15(a). When no multipath fading exists in the transmission, the spectrum efficiency is jointly determined by the time-varying PL and the transmit power. Since the radius of the circular area is fixed at $r = 50$ m, the maximum achievable path loss is a constant value. As a result, the minimum achievable spectral efficiency is determined by the transmit power of the MUs. We observe from Figure 3.15(a) that the minimum achievable spectral efficiency increases as we increase the transmit power of the MUs, which

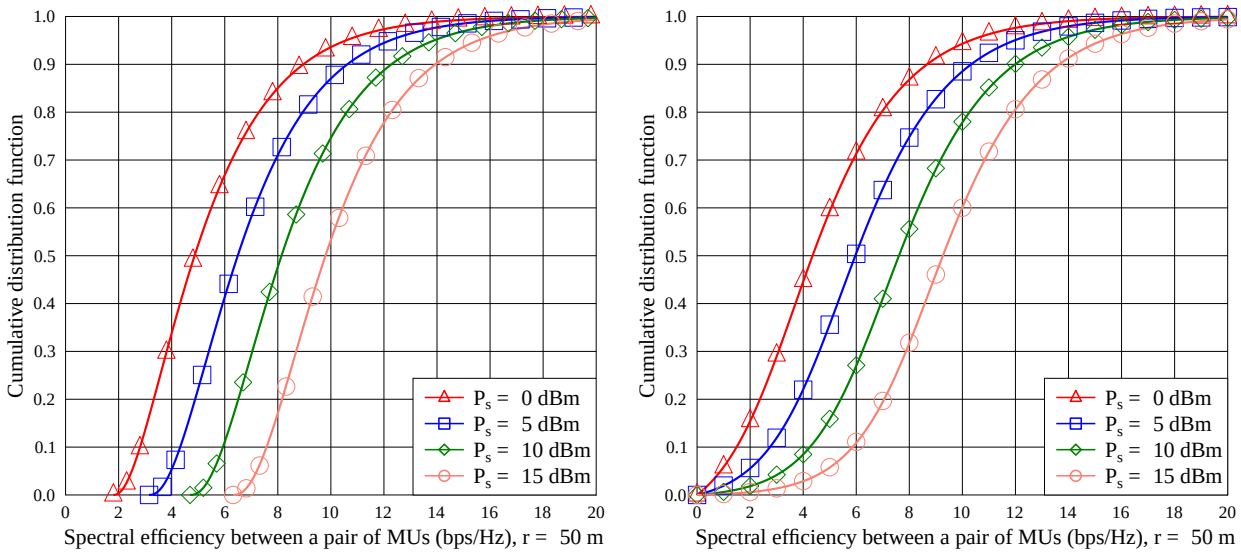

(a) Without the multipath fading

(b) With the Rayleigh fading

Figure 3.16: The single-hop spectral efficiency between a pair of MUs, when both of the MUs roam within a circular area. The radius of the circular cell is $r = 50$ m. The analytical results of the cdfs are formulated in Eqs.(3.57) and (3.65), respectively.

simultaneously results in the right hand drift of the cdf curves. However, when considering the multipath fading, the wireless environment becomes even worse. As a result, the spectral efficiency is no longer bounded by the maximum PL and it is likely to take values very close to zero, as shown in Figure 3.15(b). Furthermore, since the cdf of the spectral efficiency can be interpreted as the outage probability, we can observe from Figure 3.15(b) that given a specific spectral efficiency as the threshold, the channel is less likely in outage state if we have a higher transmit power. Moreover, the accuracy of the analytical results derived in Eqs.(3.57) and (3.65) is validated by the Monte-Carlo simulations, as shown in both Figures 3.16(a) and (b).

3.6.2.3 PMF of the outage MUs in the broadcast

Let us now study the pmf of the outage MUs in the BS-based broadcast, when the BS is located at the centre of a circular cell, while $N = 50$ MUs roam within this cell. The radius of the circular cell is $r = 1$ km. The transmit power of the BS is $P_b = 20$ dBm. We portray the pmf of the outage MUs in the BS-based broadcast in Figure 3.17(a) by only considering the time-varying PL. In this case, the minimum achievable spectral efficiency is around 0.52 bps/Hz. Hence, we set the outage threshold of the spectral efficiency to be $c_{th} = 0.6,\ 0.8,\ 1.2$ bps/Hz so as to quantify their influences on the pmf of the outage MUs. We observe from Figure 3.17(a) that as the outage threshold increases from $c_{th} = 0.6$ bps/Hz to $c_{th} = 1.2$ bps/Hz, more MUs fall to the outage state.

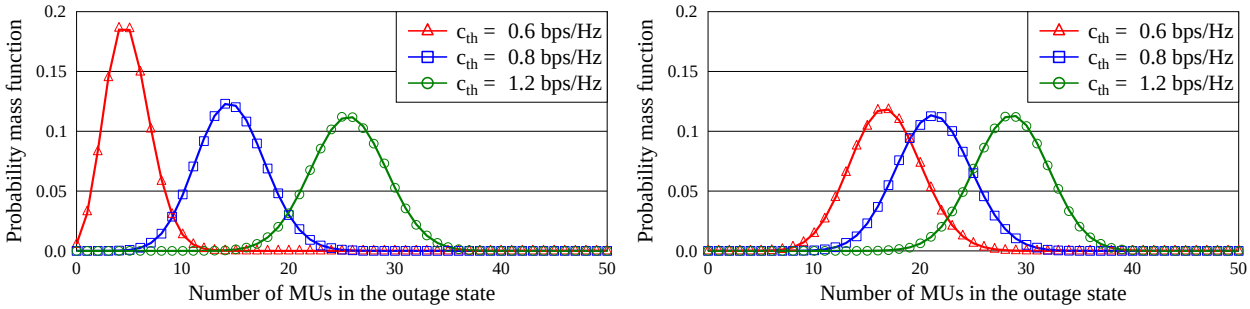

(a) Without the multipath fading

(b) With the Rayleigh fading

Figure 3.17: The pmf of the outage MUs in the BS-based broadcast, when the BS is located at the centre of a circular cell, while $N = 50$ MUs roam within this cell. The radius of the circular cell is $r = 1$ km. The transmit power of the BS is $P_b = 20$ dBm. The analytical results of the cdfs are formulated in Eq.(3.67), respectively.

For example, the average number of outage MUs is increased from 4.5 when $c_{th} = 0.6$ bps/Hz to 25 when $c_{th} = 1.2$ bps/Hz. We also portray the pmf of the outage MUs in Figure 3.17(b) by jointly considering both the time-varying PL and the multipath fading. By comparing the results of Figure 3.17(a) to those of Figure 3.17(b), we observe that when the multipath fading is taken into account, the channels connecting the BS to the MUs become even worse, which results in more MUs falling to the outage state. For example, when the outage threshold is $c_{th} = 0.6$ bps/Hz and we additionally consider the effect of the multipath fading, the average number of outage MUs is 16.5, which is far higher than the average number 4.5 when only the time-varying PL is taken into account. Moreover, the accuracy of the analytical results derived in Eq.(3.67) is demonstrated by the Monte-Carlo simulations, as shown in both Figures 3.17(a) and (b).

3.6.2.4 Spectral efficiency of multicast links

Then we move onto the spectral efficiency of the multicast transmission from the BS to the N MUs, when the BS is located at the centre of a circular cell, while all the N MUs roam within this circular cell. The radius of the circular cell is $r = 1$ km and the transmit power of the BS is $P_b = 30$ dBm. The number of the MUs varies from 1 to 20. Observe from Figure 3.18(a) that there is a common minimum achievable multicast spectral efficiency, which is around 2.5 bps/Hz, since the transmit power and the radius of the cell are the same for all different cases. In contrast, when the multipath fading is taken into consideration, the wireless environment becomes even worse. As a result, the spectral efficiency is no longer bounded by the maximum PL and it is likely to take values vary close to zero, as shown in Figure 3.18(b). Furthermore, observe from both Figures 3.18(a) and (b) that given a specific spectral efficiency value as the threshold, the outage probability for the

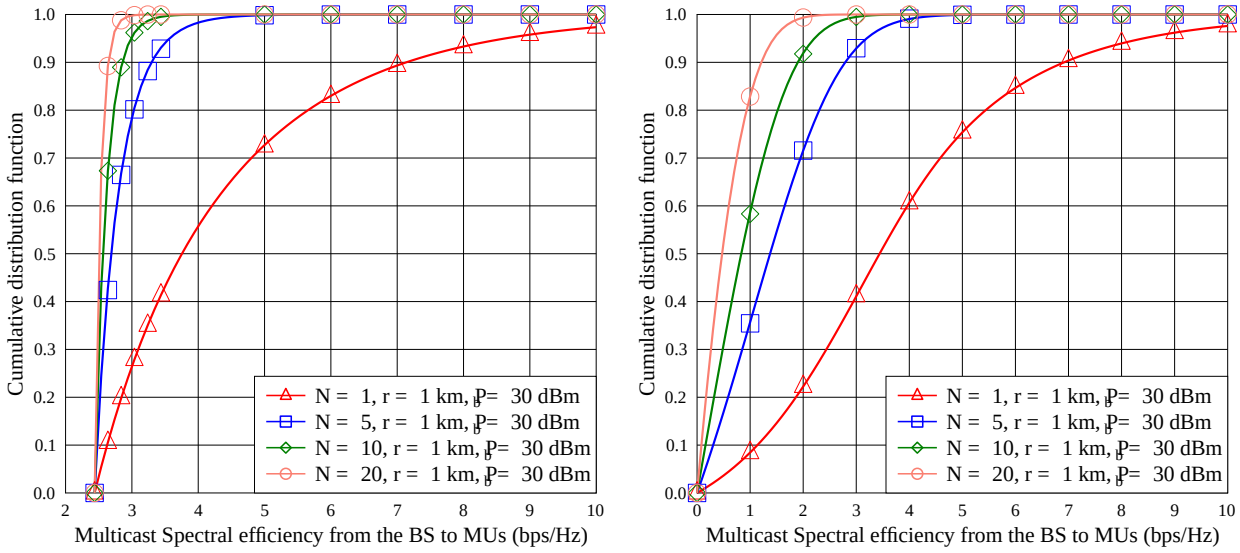

(a) Without the multipath fading

(b) With the Rayleigh fading

Figure 3.18: The multicast spectral efficiency between the BS and N MUs, when the BS is located at the centre of a circular cell, while all of the N MUs roam within this cell. The radius of the circular cell is $r = 1$ km. The transmit power of the BS is $P_b = 30$ dBm. The analytical results of the cdfs are formulated in Eqs.(3.76) and (3.82), respectively.

multicast transmission increases as we increase the number of MUs in the circular area because the outage event in the multicast transmission is dominated by the weakest link. Moreover, the accuracy of the analytical results derived in Eqs.(3.76) and (3.82) is validated by the Monte-Carlo simulations, as shown in both Figures 3.18(a) and (b).

3.7 Conclusions

In this chapter, we derive the distance distribution between the BS (static transmitter) and the MU (mobile transmitter or receiver) as well as the distance distribution between a pair of MUs, when the MUs roam within a bounded area by following the uniform mobility model, as introduced in Definition 3.1. Firstly, we study the scenario of the classic cellular communication, when the BS is located at the centre of the cell while the MU roam within the cell by following the uniform mobility model. The cell is modelled by either a circular area or a l-sided regular polygon area. Both the cdf and the pdf of the random distance between the BS and the MU are derived in closed-form formulas. Then, we focus on the distance distribution between the BS and the MU, when the MU roams within a bounded area, modelled by either a circular area or a square area, while the BS is located at an arbitrary position either outside or inside the bounded area. Again, the

cdf and the pdf of the random distance between the BS and the MU are derived in closed-form formulas for this scenario. At last, we further derive the closed-form cdf and pdf of the random distance between a pair of MUs, when both of the MUs roam within a bounded area, which can be modelled by either a circular area or a square area.

After obtaining the statistical properties of the random distance between the BS and the MU and those of the random distance between a pair of MUs, we are able to evaluate the impact of the varying distance, which is incurred by the movement of both the transmitter and the receiver, on the wireless communication performance metrics. The most straightforward consequence resulted in by the distance variation is the time-varying PL. Distance variations incurred by the movement of transmitters/receivers generate PL fluctuation, which further introduces the fluctuation of the channel gain. As a result, apart from the multipath fading, the fluctuation of the PL can be regarded as another type of fading, which may greatly affect various communication performance metrics. In this chapter, we then obtain the cdf and the pdf for the time-varying PL in closed-form, based on which we further study the statistical properties of the spectral efficiency in single-hop transmission and in multicast transmission as well as the outage MUs in the broadcast scenario. According to our numerical results, the accuracy of our theoretical analysis perfectly match the Monte-Carlo simulation results.

Apart from the time-varying PL and the spectral efficiency, in the following chapters, the statistical properties of the distance distribution between the BS (static transmitter) and the MU (mobile transmitter or receiver) as well as those of the distance distribution between a pair of MUs are further exploited in our research of content dissemination.

Appendix

3.A The proofs for the theorems in Section 3.2

3.A.1 The proof for Theorem 3.1

In this scenario, the cell is modelled by a circular area having point O as its center and having r as its radius, which is denoted as $\odot(O, r)$. The BS is positioned at the centre of this circular area, within which a MU roams by obeying the uniform mobility model, as presented in Definition 3.1. We draw another circle having O as the center and y_b as the radius, which is denoted as $\odot(O, y_b)$, as shown in Figure 3.19. According to the uniform mobility model, the MU might appear at any position in the circular area with equal probability. Therefore, if the MU appears within $\odot(O, y_b)$,

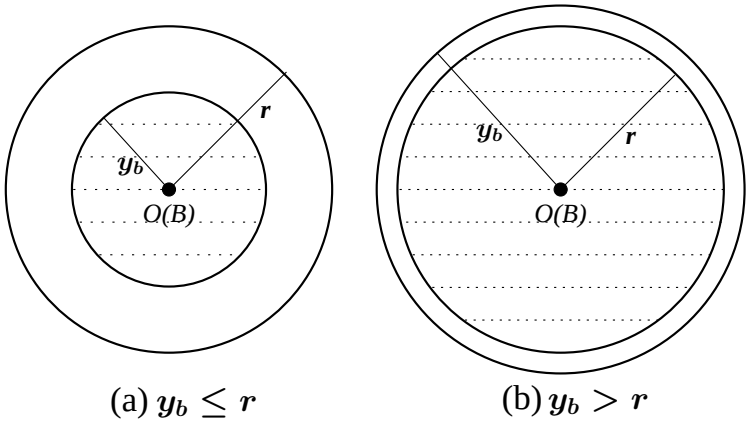

Figure 3.19: Circular cell

the distance between this MU and the BS is shorter than y_b. Furthermore, since the probability of the MU appearing within $\odot(O, y_b)$ is equal to the ratio between the area $S_{\odot(O,y_b)}$ of $\odot(O, y_b)$ and the area $S_{\odot(O,r)}$ of $\odot(O, r)$, the cumulative distribution function (cdf) $F_{Y_b}(y_b)$ of the random distance Y_b between the BS and the MU is derived as

$$F_{Y_b}(y_b) = \frac{S_{\odot(O,y_b)}}{S_{\odot(O,r)}} = \frac{\pi y_b^2}{\pi r^2} = \frac{y_b^2}{r^2}, \tag{3.84}$$

for $0 \leq y_b \leq r$. Since the movement of the MU is bounded within the studied circular area $\odot(O, r)$, the MU is unlikely to appear within the annulus, when y_b is longer than r, as shown in Figure 3.19(b). As a result, for $y_b > r$, the cdf $F_{Y_b}(y_b)$ is apparently equal to one.

Summarising the above cdf results, we finally arrive at the cdf of the random distance Y_b between the centre-positioned BS and the MU obeying the uniform mobility model within a circular cell, as expressed in Eq.(3.2) of Theorem 3.1. Differentiating the cdfs with respect to y_b in different regions, we may obtain the corresponding pdfs, as expressed in Eq.(3.3) of Theorem 3.1. As a result, Theorem 3.1 has been proven.

3.A.2 The proof for Theorem 3.2

In this scenario, the cell is modelled by a l-sided regular polygon having O as the centre and having r as the radius. The radius of a regular polygon is defined as the length of the straight line connecting the centre to one of the vertices. The coverage of this cell is denoted as a triple $\square(O, r, l)$, where l is the number of sides. The BS is positioned at the centre of this l-sided regular polygon, within which a MU roams by obeying the uniform mobility model, as defined in Definition 3.1. We draw an circle having O as the centre and y_b as the radius. This circular area

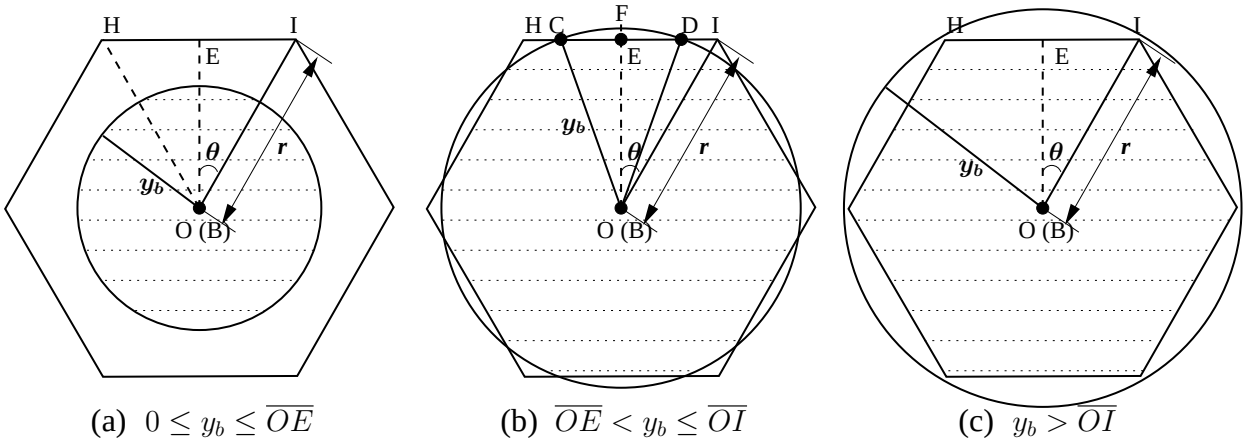

(a) $0 \leq y_b \leq \overline{OE}$ (b) $\overline{OE} < y_b \leq \overline{OI}$ (c) $y_b > \overline{OI}$

Figure 3.20: l-sided regular polygon cell: a regula hexagon example

is denoted as $\odot(O, y_b)$, as shown in Figure 3.20. According to the uniform mobility model, the MU might appear at any locations within the l-sided polygon with equal probability. Therefore, if the MU appears within the overlapped area of the l-sided regular polygon $\square(O, r, l)$ and the circle $\odot(O, y_b)$, the distance between this MU and the BS is shorter than y_b. This overlapped area is denoted as the shaded part in Figure 3.20. As a result, the cdf $F_{Y_b}(y_b)$ for the random distance Y_b between the BS and the MU is expressed as the ratio between the area of the shaded part and the area of the studied l-sided regular polygon.

As shown in Figure 3.20, we assume $\angle EOI = \theta$. Hence, the length of straight line $\overline{OE}$ is equal to $\overline{OE} = \overline{OI} \cos \angle EOI = r \cos\theta$. Furthermore, the length of the side $\overline{HI}$ is derived as $\overline{HI} = 2\overline{EI} = 2\overline{OI} \sin \angle EOI = 2r \sin\theta$. Due to the symmetry of the l-sided regular polygon, the area of $\square(O, r, l)$ can be derived as

$$\begin{aligned} S_{\square(O,r,l)} &= l \cdot S_{\triangle HOI} = l \cdot \frac{1}{2}\overline{HI} \cdot \overline{OE} \\ &= lr^2 \sin\theta \cos\theta \end{aligned} \tag{3.85}$$

where the angle θ is determined by the number of sides that the regular polygon have, which should be derived as $\theta = \frac{1}{2} \cdot \frac{2\pi}{l} = \frac{\pi}{l}$.

In order to further obtain the cdf for the random distance Y_b, we need to derive the overlapped area of the l-sided polygon $\square(O, r, l)$ and the circle $\odot(O, y_b)$. However, given different value of y_b, we have to discuss the following cases for calculating the overlapped area and the cdf $F_{Y_b}(y_b)$:

Case I: $0 \leq y_b \leq \overline{OE}$

In this case, the circle $\odot(O, y_b)$ is surrounded by the l-sided regular polygon $\square(O, a)$, as shown

in Figure 3.20(a). Hence, the overlapped area is equal to the circular area of $\odot(O, y_b)$, which is shaded in Figure 3.20(b) and derived as $S_{shade} = \pi y_b^2$. As a result, the cdf of the random distance Y_b in this case is expressed as

$$F_{Y_b}(y_b) = \frac{S_{shade}}{S_{\square(O,r,l)}} = \frac{\pi}{l \tan\theta} \left(\frac{y_b}{r\cos\theta}\right)^2, \ 0 \leq y_b \leq r\cos\theta \tag{3.86}$$

Case II: $\overline{OE} \leq y_b \leq \overline{OI}$

In this case, the overlapped area is an irregular shape, which is shaded in Figure 3.20(b). Apparently, the circle $\odot(O, y_b)$ is intersected by each side of the l-sided regular polygon $\square(O, r, l)$, which produces a small segment, such as segment $CFDE$. The number of this small segment is equal to the number l of sides. Let us see how to derive the area of this small segment. As shown in Figure 3.20(b), the area of segment $CFDE$ can be derived by subtracting the triangular area $S_{\triangle COD}$ from the sector area $S_{\widehat{CODF}}$. The key to the areas of both $\triangle COD$ and sector $\widehat{CODF}$ is the value of the angle $\angle EOD$. Since point D is on the circumference of $\odot(O, y_b)$, we have $\overline{OD} = y_b$. Given $\overline{OE} = r\cos\theta$, the cosine of $\angle EOD$ is $\cos\angle EOD = \frac{\overline{OE}}{\overline{OD}} = \frac{r\cos\theta}{y_b}$. With the aid of inverse trigonometric functions, we can express the value of $\angle EOD$ as $\angle EOD = \arccos\frac{r\cos\theta}{y_b}$. Furthermore, according to Pythagorean theorem, the length of $\overline{ED}$ is expressed as

$$\overline{ED} = \sqrt{\overline{OD}^2 - \overline{OE}^2} = \sqrt{y_b^2 - r^2\cos^2\theta}. \tag{3.87}$$

As a result, the area of segment $CFDE$ is derived as

$$\begin{aligned} S_{CFDE} &= S_{\widehat{COD}} - S_{\triangle COD} = \frac{1}{2}\cdot 2\angle EOD \cdot \overline{OD}^2 - \frac{1}{2}\cdot 2\overline{ED}\cdot\overline{OE} \\ &= y_b^2 \arccos\frac{r\cos\theta}{y_b} - r\cos\theta\sqrt{y_b^2 - r^2\cos^2\theta}. \end{aligned} \tag{3.88}$$

Furthermore, the area of the shaded part is derived by subtracting the number l of identical segments like segment $CFDE$ from the area of the circle $\odot(O, y_b)$, which is expressed as

$$\begin{aligned} S_{shaded} &= S_{\odot(O,y_b)} - l\cdot S_{CFDE} \\ &= \pi y_b^2 - y_b^2 l \arccos\frac{r\cos\theta}{y_b} + lr\cos\theta\sqrt{y_b^2 - r^2\cos^2\theta}. \\ &= y_b^2\left(\pi - l\arccos\frac{r\cos\theta}{y_b}\right) + lr\cos\theta\sqrt{y_b^2 - r^2\cos^2\theta} \end{aligned} \tag{3.89}$$

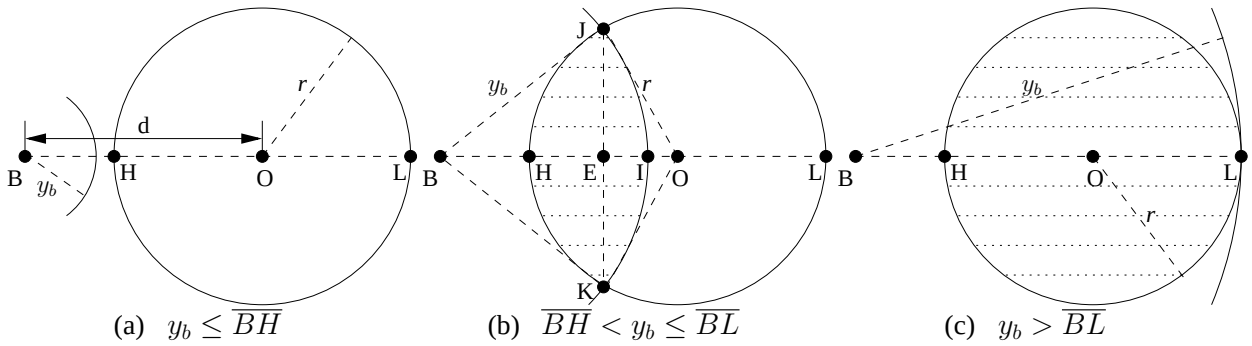

Figure 3.21: BS is outside the bounded circular area

As a result, the cdf of the random distance Y_b in this case is expressed as

$$\begin{aligned} F_{y_b}(y_b) &= \frac{S_{shaded}}{S_{\square(O,r,l)}} \\ &= \frac{1}{l\tan\theta}\left(\frac{y_b}{r\cos\theta}\right)^2\left(\pi - l\arccos\left(\frac{y_b}{r\cos\theta}\right)^{-1}\right) + \frac{1}{\tan\theta}\sqrt{\left(\frac{y_b}{r\cos\theta}\right)^2 - 1}, \end{aligned} \quad (3.90)$$

for $r\cos\theta < y_b \leq r$.

Case III: $y_b > \overline{OI}$

For this case, the l-sided regular polygon $\square(O, r, l)$ is completed surrounded by the circle $\odot(O, y_b)$. As a result, the random distance between the BS and the MU is surely shorter than y_b with a unity probability, which indicates that the cdf of the random distance Y_b is $F_{Y_b}(y_b) = 1$ for $y_b > r$.

Summarising the above-derived cdfs in different cases, we are able to obtain Eq.(3.5) in Theorem 3.2. Differentiating the above-derived cdfs in different cases with respect to y_b, we may arrive at the corresponding pdf of the distance Y_b between the centre-positioned BS and the MU obeying the uniform mobility model within a l-sided regular polygon, as expressed in Eq.(3.6). As a result, Theorem 3.2 has been proven.

3.B The proofs for the theorems in Section 3.3

3.B.1 The proof for Theorem 3.3

The bounded area, which restricts the movement of the MU, is modelled by the circular area $\odot(O, r)$, as shown in Figure 3.21. The BS is at the position B, which is d m away from the centre O. Since the BS is outside $\odot(O, r)$, we have $d > r$. We draw another circle, whose centre is

at point B and whose radius is y_b. This circle is denoted as $\odot(B, y_b)$. If the MU is within the overlapped area of $\odot(B, y_b)$ and $\odot(O, r)$, the distance between the MU and the BS is shorter than y_b. Since the studied MU may appear at any positions within the circular area $\odot(O, r)$, the cdf of the random distance Y is the ratio between the overlapped area and the whole area of $\odot(O, r)$. When the BS is outside the studied circular area, namely $d > r$, the following cases need to be specifically considered:

Case I: $0 \leq y_b \leq \overline{BH}$

In this case, as shown in Figure 3.21(a), $\overline{BH} = d - r$ and $\odot(B, y_b)$ does not overlap with $\odot(O, r)$. As a result the area of the overlapped part is zero, which indicates that the cdf $F_{Y_b}(y_b)$ is also zero when $0 \leq y_b \leq d - r$.

Case II: $\overline{BH} < y_b \leq \overline{BL}$

In this case, $\odot(B, y_b)$ intersects $\odot(O, r)$ at points I and K, as shown in Figure 3.21. We connect points B and O with a straight line $\overline{OB}$, which intersects $\odot(B, y_b)$ and $\odot(O, r)$ at points H , I and L, respectively, and we therefore have $\overline{BH} = d - r$ and $\overline{BL} = d + r$. We also connect points I and K with a straight line $\overline{IK}$, which intersects $\overline{OB}$ at point E. In order to derive the cdf $F_{Y_b}(y_b)$, we have to derive the area of the overlapped part of $\odot(O, r)$ and $\odot(B, y_b)$, which is denoted as the shaded part in Figure 3.21(b). Apparently, the area of the shaded part can be derived by the following expression:

$$\begin{aligned} S_{shaded} &= (S_{\widehat{JOKH}} - S_{\triangle JOK}) + (S_{\widehat{JBKI}} - S_{\triangle JBK}) \\ &= (S_{\widehat{JOKH}} + S_{\widehat{JBKI}}) - (S_{\triangle JOK} + S_{\triangle JBK}) \\ &= (S_{\widehat{JOKH}} + S_{\widehat{JBKI}}) - S_{\square BJOK}, \end{aligned} \tag{3.91}$$

where $S_{\widehat{JOKH}}$ and $S_{\widehat{JBKI}}$ denote the areas of sectors $\widehat{JOKH}$ and $\widehat{JBKI}$, respectively, whereas $S_{\triangle JOK}$ and $S_{\triangle JBK}$ denote the areas of triangles $\triangle JOK$ and $\triangle JBK$, respectively, and $S_{\square BJOK}$ denotes the area of polygon $\square BJOK$. Afterwards, we will derive these areas.

According to the law of cosines, given that $\overline{OJ} = r$, $\overline{BJ} = y_b$ and $\overline{OB} = d$, we have the following two equations for evaluating the values of cosines for the angles $\angle JOB$ and $\angle JBO$:

$$\cos(\angle JOB) = \frac{\overline{OJ}^2 + \overline{OB}^2 - \overline{BJ}^2}{2\overline{OJ} \cdot \overline{OB}} = \frac{r^2 + d^2 - y_b^2}{2rd} \tag{3.92}$$

$$\cos(\angle JBO) = \frac{\overline{BJ}^2 + \overline{BO}^2 - \overline{OJ}^2}{2\overline{BJ} \cdot \overline{BO}} = \frac{y_b^2 + d^2 - r^2}{2y_b d}. \tag{3.93}$$

Furthermore, we can express the exact values for $\angle JOB$ and $\angle JBO$ in terms of inverse cosine

function as

$$\angle JOB = \arccos\left(\frac{r^2 + d^2 - y_b^2}{2rd}\right), \tag{3.94}$$

$$\angle JBO = \arccos\left(\frac{y_b^2 + d^2 - r^2}{2y_b d}\right) \tag{3.95}$$

respectively. Given the exact values of $\angle JOB$ and $\angle JBO$, the area of sector $\widehat{JOKH}$ and that of sector $\widehat{JBKI}$ can be derived as

$$S_{\widehat{JOKH}} = \frac{1}{2} \cdot r^2 \cdot 2\angle JOB = r^2 \cdot \arccos\left(\frac{r^2 + d^2 - y_b^2}{2rd}\right), \tag{3.96}$$

$$S_{\widehat{JBKI}} = \frac{1}{2} \cdot y_b^2 \cdot 2\angle JBO = y_b^2 \cdot \arccos\left(\frac{y^2 + d^2 - r^2}{2y_b d}\right). \tag{3.97}$$

In order to derive $S_{\square BJOK}$ we must decide the length of vertical line $\overline{JE}$. According to Pythagorean theorem, the length of $\overline{JE}$ is derived as

$$\begin{aligned}\overline{JE} &= \sqrt{\overline{JO}^2 - \overline{OE}^2} = \sqrt{\overline{JO}^2 - \overline{JO}^2 \cdot \cos^2(\angle JOB)} \\ &= \sqrt{r^2 - r^2\frac{(r^2 + d^2 - y_b^2)^2}{4r^2d^2}} \\ &= \frac{\sqrt{4r^2d^2 - (r^2 + d^2 - y_b^2)^2}}{2d}.\end{aligned} \tag{3.98}$$

Furthermore, $S_{\square BJOK}$ can be derived as

$$\begin{aligned}S_{\square BJOK} &= 2S_{\triangle JBO} = |JE| \cdot |OB| \\ &= \frac{1}{2}\sqrt{4r^2d^2 - (r^2 + d^2 - y_b^2)^2}\end{aligned} \tag{3.99}$$

Substituting $S_{\widehat{JOKH}}$, $S_{\widehat{JBKI}}$ and $S_{\square BJOK}$ into (3.91), the area of the shaded part is expressed as

$$\begin{aligned}S_{shaded} = r^2 \arccos&\left(\frac{r^2 + d^2 - y_b^2}{2rd}\right) + y_b^2 \arccos\left(\frac{y_b^2 + d^2 - r^2}{2y_b d}\right) \\ &- \frac{1}{2}\sqrt{4r^2d^2 - (r^2 + d^2 - y_b^2)^2}.\end{aligned} \tag{3.100}$$

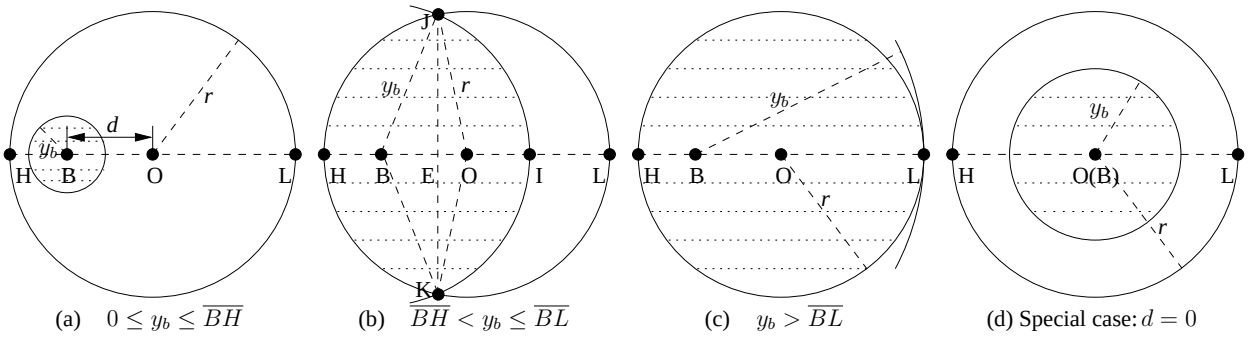

Figure 3.22: BS is inside the bounded circular area

Hence, the cdf of Y_b can be obtained as

$$\begin{aligned} F_Y(y) &= S_{shaded}/S_{\odot(O,r)} \\ &= \frac{1}{\pi}\left[\arccos\left(\frac{r^2+d^2-y_b^2}{2rd}\right) + \frac{y_b^2}{r^2}\arccos\left(\frac{y_b^2+d^2-r^2}{2y_bd}\right)\right. \\ &\quad \left. -\frac{1}{2r^2}\sqrt{4r^2d^2-(r^2+d^2-y_b^2)^2}\right], \end{aligned} \tag{3.101}$$

for $d - r < y_b \leq d + r$.

Case III: $y_b > \overline{BL}$

In this case, as shown in Figure 3.21, we have $\overline{BL} = d + r$ and the overlapped part between $\odot(O, r)$ and $\odot(B, y_b)$ is the whole area of $\odot(O, r)$, within which the movement of the studied MU is restricted. Therefore, the cdf $F_{Y_b}(y_b)$ of the random distance Y_b is expressed as $F_{Y_b}(y_b) = S_{\odot(O,r)}/S_{\odot(O,r)} = 1$ for $y_b > d + r$.

Summarising the above-derived cdfs in different cases, we are able to obtain Eq.(3.7) in Theorem 3.3. Differentiating the above-derived cdfs in different cases with respect to y_b, we may arrive at the corresponding pdf of the distance Y_b between the BS positioned outside the circular area and the MU obeying the uniform mobility model within the circular area, as expressed in Eq.(3.8). As a result, Theorem 3.3 has been proven.

3.B.2 The proof for Theorem 3.4

We draw another circle, whose centre is at point B and whose radius is y_b, as shown in Figure 3.22. This circle is denoted as $\odot(B, y_b)$. If the MU is within the overlapped area of $\odot(B, y_b)$ and $\odot(O, r)$, the distance between the MU and the BS is shorter than y_b. Since the studied MU may appear at any position within the circular area $\odot(O, r)$, the cdf of the random distance Y_b is the

ratio between the overlapped area and the whole area of $\odot(O,r)$. When the BS is inside the studied circular area and not at the centre, namely $0 < d \leq r$, the following cases need to be specifically considered:

Case I: $0 \leq y_b \leq \overline{BH}$

In this case, as shown in Figure 3.22(a), we have $\overline{BH} = r - d$ and the overlapped area is the whole circular area of $\odot(B, y_b)$. Hence, the cdf of the random distance Y should be expressed as

$$F_{Y_b}(y_b) = \frac{S_{shaded}}{S_{\odot(O,r)}} = \frac{y_b^2}{r^2}, \tag{3.102}$$

for $0 \leq y_b \leq r - d$.

Case II: $\overline{BH} < y_b \leq \overline{BL}$

As shown in Figure 3.22(b), we have $\overline{BH} = r-d$ and $\overline{HL} = r+d$. In this case, the overlapped area is denoted as the shaded part of Figure 3.22, which can be calculated by the same equation as presented in Eq.(3.101) for $r - d < y_b \leq r + d$.

Case III: $y_b > \overline{BL}$

As shown in Figure 3.22(c), we have $\overline{HL} = r + d$. In this case, the overlapped part between $\odot(O,r)$ and $\odot(B, y_b)$ is the whole area of $\odot(O,r)$, within which the movement of the studied MU is restricted. Therefore, the cdf $F_{Y_b}(y_b)$ of the random distance Y_b is expressed as $F_{Y_b}(y_b) = S_{\odot(O,r)}/S_{\odot(O,r)} = 1$.

Summarising the above-derived cdfs in different cases, we are able to obtain Eq.(3.9) in Theorem 3.4. Differentiating the above-derived cdfs in different cases with respect to y_b, we may arrive at the corresponding pdf of the distance Y_b between the BS positioned inside the circular area and the MU obeying the uniform mobility model within the circular area, as expressed in Eq.(3.10). As a result, Theorem 3.4 has been proven.

3.B.3 The proof for Theorem 3.5

The cdf $F_{Y_b}(y_b)$ is defined as the probability of the random distance Y_b being shorter than a specific value y_b. We draw a circle having point B as the centre and having y_b as the radius. This circle is denoted as $\odot(B, y_b)$. The overlapped area between $\square HIJK$ and $\odot(B, y_b)$ is shaded in Figure 3.23. Since the position of the MU is uniformly distributed within $\square HIJK$ according to the uniform mobility model, the cdf $F_{Y_b}(y_b)$ can be further expressed as the ratio of the area of the shaded part to the area of $\square HIJK$. Given different values of y_b, the following cases need to be discussed in order to derive $F_{Y_b}(y_b)$.

CASE I: $0 \leq y_b \leq \overline{BE}$.

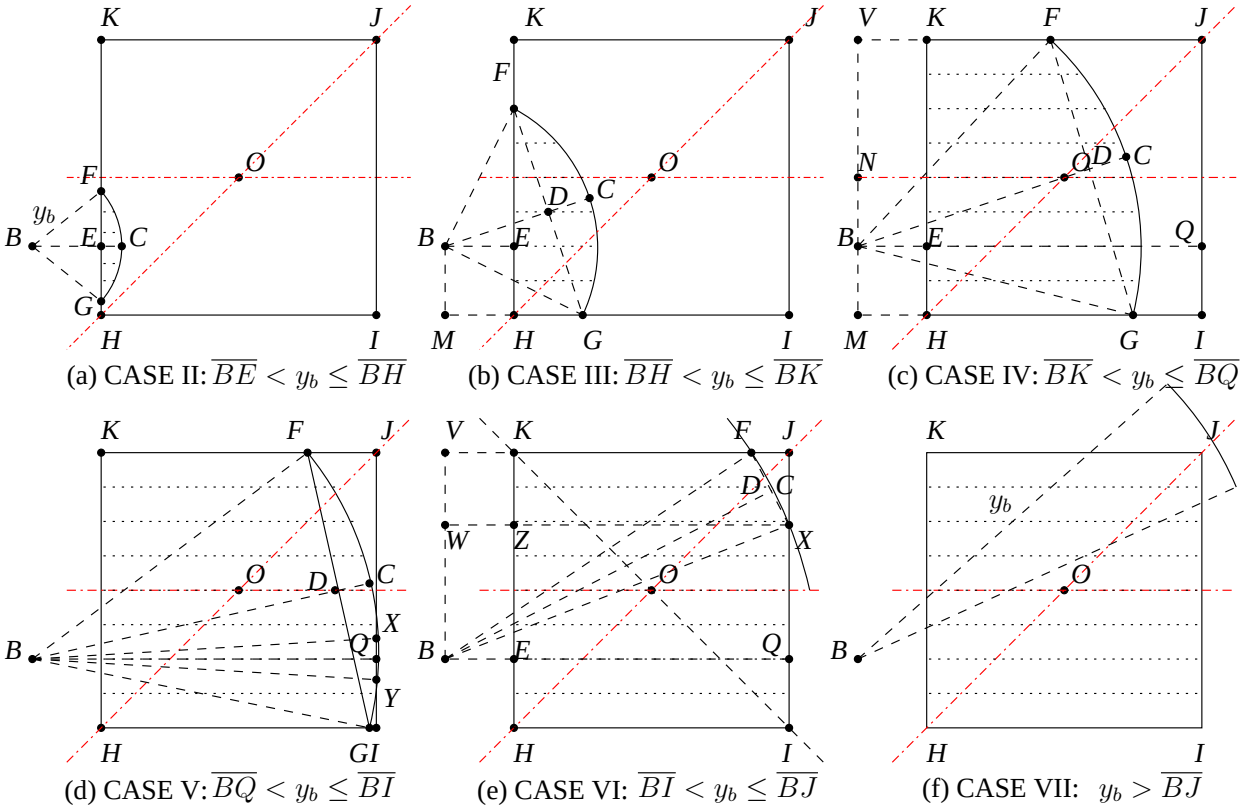

(a) CASE II: $\overline{BE} < y_b \leq \overline{BH}$ (b) CASE III: $\overline{BH} < y_b \leq \overline{BK}$ (c) CASE IV: $\overline{BK} < y_b \leq \overline{BQ}$

(d) CASE V: $\overline{BQ} < y_b \leq \overline{BI}$ (e) CASE VI: $\overline{BI} < y_b \leq \overline{BJ}$ (f) CASE VII: $y_b > \overline{BJ}$

Figure 3.23: BS is outside the bounded square area

In this case, the circle $\odot(B, y_b)$ does not overlap the square $\square HIJK$. As a result the area of the overlapped part is zero, which indicates that the cdf $F^I_{Y_b}(y_b)$ is also zero when $0 \leq y_b \leq d\cos\theta - a/2$.

CASE II: $\overline{BE} < y_b \leq \overline{BH}$

In this case, as shown in Figure 3.23(a), the circle $\odot(B, y_b)$ intersects the side $\overline{KH}$ at points F and G. Extending the straight line $\overline{BE}$, it intersects the circle $\odot(B, y_b)$ at point C. As a result, the overlapped area is a small segment, which is shaded in Figure 3.23(a). The area of this shaded part can be calculated by $S_{shade} = S_{\widehat{FBGC}} - S_{\triangle FBG}$, where $S_{\widehat{FBGC}}$ is the area of sector $\widehat{FBGC}$ and $S_{\triangle FBG}$ is the area of the triangle $\triangle FBG$.

In order to derive both $S_{\widehat{FBGC}}$ and $S_{\triangle FBG}$, we have to calculate the value of angle $\angle FBC$. Since point F is on the circumference of $\odot(B, y_b)$, we have $\overline{BF} = y_b$. Since we have obtained the length of $\overline{BE}$ as $\overline{BE} = d\cos\theta - a/2$, the cosine value of $\angle FBC$ is expressed as

$$\cos\angle FBC = \frac{\overline{BE}}{\overline{BF}} = \frac{d\cos\theta - \frac{a}{2}}{y_b}. \tag{3.103}$$

With the aid of the inverse trigonometric function, the value of angle $\angle FBC$ is expressed as

$$\angle FBC = \arccos \frac{d\cos\theta - \frac{a}{2}}{y_b}. \tag{3.104}$$

As a result, the area of sector $\widehat{FBGC}$ is derived as

$$S_{\widehat{FBGC}} = \frac{1}{2} \cdot 2\angle FBC \cdot \overline{BF}^2 = y_b^2 \arccos \frac{d\cos\theta - \frac{a}{2}}{y_b}. \tag{3.105}$$

Furthermore, according to Pythagorean theorem, the length of straight line $\overline{FG}$ is expressed as

$$\overline{FG} = 2\overline{EF} = 2\sqrt{\overline{BF}^2 - \overline{BE}^2} = 2\sqrt{y_b^2 - \left(d\cos\theta - \frac{a}{2}\right)^2}. \tag{3.106}$$

Hence the area of triangle $\triangle FBG$ is derived as

$$S_{\triangle FBG} = \frac{1}{2}\overline{FG} \cdot \overline{BE} = \left(d\cos\theta - \frac{a}{2}\right)\sqrt{y_b^2 - \left(d\cos\theta - \frac{a}{2}\right)^2}. \tag{3.107}$$

As a result, the area of the shaded part can be derived as

$$\begin{aligned} S_{shade}^{II} &= S_{\widehat{FBGC}} - S_{\triangle FBG} \\ &= y_b^2 \arccos \frac{d\cos\theta - \frac{a}{2}}{y_b} - \left(d\cos\theta - \frac{a}{2}\right)\sqrt{y_b^2 - \left(d\cos\theta - \frac{a}{2}\right)^2}. \end{aligned} \tag{3.108}$$

Finally, in this case, the cdf of the random distance Y_b is the ratio between S_{shade}^{II} and $S_{\square HIJK}$, which is presented as

$$\begin{aligned} F_{Y_b}^{II}(y_b) &= \frac{S_{shade}^{II}}{S_{\square HIJK}} \\ &= \frac{1}{a^2}\left[y_b^2 \arccos \frac{d\cos\theta - \frac{a}{2}}{y_b} - \left(d\cos\theta - \frac{a}{2}\right)\sqrt{y_b^2 - \left(d\cos\theta - \frac{a}{2}\right)^2}\right] \end{aligned} \tag{3.109}$$

for $(d\cos\theta - a/2) < y_b \leq \sqrt{a^2/2 + d^2 - ad(\sin\theta + \cos\theta)}$, where $S_{\square HIJK} = a^2$.

CASE III: $\overline{BH} < y_b \leq \overline{BK}$

In this case, as shown in Figure 3.23(b), the circle $\odot(B, y_b)$ intersects the side $\overline{KH}$ of the square $\square HIJK$ at point F and intersects the side $\overline{HI}$ of the square $\square HIJK$ at point G. $\overline{BC}$ is perpendicular to $\overline{FG}$ and they intersect at point D. The overlapped area of $\odot(B, y_b)$ and $\square HIJK$ is denoted as the shaded part in Figure 3.23(b). Apparently, the area of the shaded part can be

expressed as the following equation:

$$S_{shade}^{III} = S_{\widehat{FBGC}} - S_{\triangle FBG} + S_{\triangle FHG}, \tag{3.110}$$

where $S_{\widehat{FBGC}}$ denotes the area of the sector $\widehat{FBGC}$, $S_{\triangle FBG}$ denotes the area of the triangle $\triangle FBG$ and $S_{\triangle FHG}$ denotes the area of the triangle $\triangle FHG$. Next, we will derive these areas, respectively.

Since points F and G are both on the circumference of $\odot(B, y_b)$, we have $\overline{BF} = \overline{BG} = y_b$. In Figure 3.23(b), $\overline{BE}$ is parallel to $\overline{HI}$. Hence, we have $\angle EBG = \angle BGM$. Furthermore, the sine value of $\angle EBG$ is given by

$$\sin\angle EBG = \sin\angle BGM = \frac{\overline{BM}}{\overline{BG}} = \frac{\frac{a}{2} - d\sin\theta}{y_b}. \tag{3.111}$$

Therefore, with the aid of the inverse trigonometric function, the value of $\angle EBG$ is derived as

$$\angle EBG = \arcsin\frac{\frac{a}{2} - d\sin\theta}{y_b}. \tag{3.112}$$

Similarly, the cosine value of $\angle FBE$ is derived as

$$\cos\angle FBE = \frac{\overline{BE}}{\overline{BF}} = \frac{d\cos\theta - \frac{a}{2}}{y_b}. \tag{3.113}$$

Therefore, with the aid of the inverse trigonometric function, the value of $\angle FBE$ is derived as

$$\angle FBE = \arccos\frac{d\cos\theta - \frac{a}{2}}{y_b}. \tag{3.114}$$

As shown in Figure 3.23(b), given $\angle EBG$ and $\angle FBE$, we can obtain $\angle FBG$ as

$$\angle FBG = \angle EBG + \angle FBE = \arcsin\frac{\frac{a}{2} - d\sin\theta}{y_b} + \arccos\frac{d\cos\theta - \frac{a}{2}}{y_b}. \tag{3.115}$$

Now, we are able to express $S_{\widehat{FBGC}}$ as

$$\begin{aligned} S_{\widehat{FBGC}} &= \frac{1}{2}\cdot\overline{BF}^2\cdot\angle FBG \\ &= \frac{y_b^2}{2}\left(\arcsin\frac{\frac{a}{2} - d\sin\theta}{y_b} + \arccos\frac{d\cos\theta - \frac{a}{2}}{y_b}\right). \end{aligned} \tag{3.116}$$

Before deriving $S_{\triangle FBG}$, we must know the sine value of $\angle FBG$, which can be derived as

$$\begin{aligned}\sin\angle FBG &= \sin(\angle EBG + \angle FBE) = \sin\angle EBG\cos\angle FBE + \cos\angle EBG\sin\angle FBE \\ &= \sin\angle EBG\cos\angle FBE + \sqrt{1-\sin^2\angle EBG}\sqrt{1-\cos^2\angle FBE} \\ &= \frac{1}{y_b^2}\left[(\frac{a}{2} - d\sin\theta)(d\cos\theta - \frac{a}{2})\right. \\ &\qquad \left. + \sqrt{y_b^2 - (\frac{a}{2} - d\sin\theta)^2}\sqrt{y_b^2 - (d\cos\theta - \frac{a}{2})^2}\right]. \end{aligned} \tag{3.117}$$

As a result, we can calculate $S_{\triangle FBG}$ as

$$\begin{aligned} S_{\triangle FBG} &= \frac{1}{2}\cdot\overline{BF}\cdot\overline{BG}\cdot\sin\angle FBG \\ &= \frac{1}{2}\left[(\frac{a}{2} - d\sin\theta)(d\cos\theta - \frac{a}{2})\right. \\ &\qquad \left. + \sqrt{y_b^2 - (\frac{a}{2} - d\sin\theta)^2}\sqrt{y_b^2 - (d\cos\theta - \frac{a}{2})^2}\right]. \end{aligned} \tag{3.118}$$

In order to derive $S_{\triangle FHG}$, we have to first obtain the length of $\overline{FH}$ and $\overline{HG}$. According to Pythagorean theorem, $\overline{FE}$ can be expressed as

$$\overline{FE} = \sqrt{\overline{BF}^2 - \overline{BE}^2} = \sqrt{y_b^2 - (d\cos\theta - \frac{a}{2})^2}. \tag{3.119}$$

Since $\overline{EH} = \overline{BM} = \frac{a}{2} - d\sin\theta$, the length of $\overline{FH}$ can be derived as

$$\overline{FH} = \overline{FE} + \overline{EH} = \sqrt{y_b^2 - (d\cos\theta - \frac{a}{2})^2} + (\frac{a}{2} - d\sin\theta). \tag{3.120}$$

Furthermore, according to Pythagorean theorem, $\overline{MG}$ is calculated by

$$\overline{MG} = \sqrt{\overline{BG}^2 - \overline{BM}^2} = \sqrt{y_b^2 - (\frac{a}{2} - d\sin\theta)^2}. \tag{3.121}$$

Since the length of $\overline{MH}$ is expressed as $\overline{MH} = \overline{BE} = d\cos\theta - \frac{a}{2}$, the length of $\overline{HG}$ is derived as

$$\overline{HG} = \overline{MG} - \overline{MH} = \sqrt{y_b^2 - (\frac{a}{2} - d\sin\theta)^2} - (d\cos\theta - \frac{a}{2}). \tag{3.122}$$

Therefore, the area of the triangle $\triangle FHG$ can be derived as

$$\begin{aligned} S_{\triangle FHG} &= \frac{1}{2} \cdot \overline{FH} \cdot \overline{HG} \\ &= \frac{1}{2}\left[\sqrt{y_b^2 - (d\cos\theta - \frac{a}{2})^2}\sqrt{y_b^2 - (\frac{a}{2} - d\sin\theta)^2} - (d\cos\theta - \frac{a}{2})\sqrt{y_b^2 - (d\cos\theta - \frac{a}{2})^2}\right. \\ &\quad \left. +(\frac{a}{2} - d\sin\theta)\sqrt{y_b^2 - (\frac{a}{2} - d\sin\theta)^2} - (d\cos\theta - \frac{a}{2})(\frac{a}{2} - d\sin\theta)\right] \end{aligned} \tag{3.123}$$

As a result, the area of the shaded part can be derived as

$$\begin{aligned} S_{shade}^{III} &= S_{\widehat{FBGC}} - S_{\triangle FBG} + S_{\triangle FHG} \\ &= \frac{y_b^2}{2}\left(\arcsin\frac{\frac{a}{2} - d\sin\theta}{y_b} + \arccos\frac{d\cos\theta - \frac{a}{2}}{y_b}\right) \\ &\quad + \frac{1}{2}\left[(\frac{a}{2} - d\sin\theta)\sqrt{y_b^2 - (\frac{a}{2} - d\sin\theta)^2} - (d\cos\theta - \frac{a}{2})\sqrt{y_b^2 - (d\cos\theta - \frac{a}{2})^2}\right. \\ &\quad \left. -2(d\cos\theta - \frac{a}{2})(\frac{a}{2} - d\sin\theta)\right]. \end{aligned} \tag{3.124}$$

Finally, in this case, the cdf of the random distance Y_b is the ratio between S_{shade}^{III} and $S_{\square HIJK} = a^2$, which is presented as

$$\begin{aligned} F_{Y_b}^{III}(y_b) &= \frac{S_{shade}^{III}}{S_{\square HIJK}} \\ &= \frac{y_b^2}{2a^2}\left(\arcsin\frac{\frac{a}{2} - d\sin\theta}{y_b} + \arccos\frac{d\cos\theta - \frac{a}{2}}{y_b}\right) \\ &\quad + \frac{1}{2a^2}\left[(\frac{a}{2} - d\sin\theta)\sqrt{y_b^2 - (\frac{a}{2} - d\sin\theta)^2} - (d\cos\theta - \frac{a}{2})\sqrt{y_b^2 - (d\cos\theta - \frac{a}{2})^2}\right. \\ &\quad \left. -2(d\cos\theta - \frac{a}{2})(\frac{a}{2} - d\sin\theta)\right], \end{aligned} \tag{3.125}$$

for $\sqrt{a^2/2 + d^2 - ad(\sin\theta + \cos\theta)} < y_b \leq \sqrt{a^2/2 + d^2 - ad(\cos\theta - \sin\theta)}$.

CASE IV: $\overline{BK} < y_b \leq \overline{BQ}$

In this case, as shown in Figure 3.23(c), the circle $\odot(B, y_b)$ intersects the side $\overline{JK}$ of the square $\square HIJK$ at point F and intersects the side $\overline{HI}$ of the square $\square HIJK$ at point G. $\overline{BC}$ and $\overline{FG}$ are vertical lines and they intersect at point D. The overlapped area of $\odot(B, y_b)$ and $\square HIJK$ is denoted as the shaded part in Figure 3.23(c). Apparently, the area of the shaded part can be expressed as the following equation:

$$S_{shade}^{IV} = S_{\widehat{FBGC}} - S_{\triangle FBG} + S_{\square HGFK}, \tag{3.126}$$

where $S_{\widehat{FBGC}}$ denotes the area of the sector $\widehat{FBGC}$, $S_{triangleFBG}$ denotes the area of the triangle $\triangle FBG$ and $S_{\square HGFK}$ denotes the area of the trapezium $\square HGFK$. Next, we will derive these areas, respectively.

Since points F and G are both on the circumference of $\odot(B, y_b)$, we have $\overline{BF} = \overline{BG} = y_b$. In Figure 3.23(c), $\overline{BE}$ and $\overline{HI}$ are parallel lines. Hence, we have $\angle EBG = \angle BGM$. Furthermore, the sine value of $\angle EBG$ is given by

$$\sin\angle EBG = \sin\angle BGM = \frac{\overline{BM}}{\overline{BG}} = \frac{\frac{a}{2} - d\sin\theta}{y_b}. \tag{3.127}$$

Therefore, with the aid of the inverse trigonometric function, the value of $\angle EBG$ is derived as

$$\angle EBG = \arcsin\frac{\frac{a}{2} - d\sin\theta}{y_b}. \tag{3.128}$$

In Figure 3.23(c), $\overline{BE}$ and $\overline{JK}$ are parallel lines. Hence, we have $\angle FBE = \angle BFV$. Furthermore, given $\overline{BV} = \overline{EK} = \frac{a}{2} + d\sin\theta$, the sine value of $\angle FBE$ is given by

$$\sin\angle FBE = \sin\angle BFV = \frac{\overline{BV}}{\overline{BF}} = \frac{\frac{a}{2} + d\sin\theta}{y_b} \tag{3.129}$$

Therefore, with the aid of the inverse trigonometric function, the value of $\angle FBE$ is derived as

$$\angle FBE = \arcsin\frac{\frac{a}{2} + d\sin\theta}{y_b}. \tag{3.130}$$

As shown in Figure 3.23(c), given $\angle EBG$ and $\angle FBE$, we can obtain $\angle FBG$ as

$$\angle FBG = \angle EBG + \angle FBE = \arcsin\frac{\frac{a}{2} - d\sin\theta}{y_b} + \arcsin\frac{\frac{a}{2} + d\sin\theta}{y_b}. \tag{3.131}$$

Now, we are able to express $S_{\widehat{FBGC}}$ as

$$\begin{aligned} S_{\widehat{FBGC}} &= \frac{1}{2}\cdot\overline{BF}^2\cdot\angle FBG \\ &= \frac{y_b^2}{2}\left(\arcsin\frac{\frac{a}{2} - d\sin\theta}{y_b} + \arcsin\frac{\frac{a}{2} + d\sin\theta}{y_b}\right). \end{aligned} \tag{3.132}$$

Before deriving $S_{\triangle FBG}$, we must know the sine value of $\angle FBG$, which can be derived as

$$\begin{aligned}\sin\angle FBG &= \sin(\angle EBG + \angle FBE) = \sin\angle EBG\cos\angle FBE + \cos\angle EBG\sin\angle FBE \\ &= \sin\angle EBG\sqrt{1-\sin^2\angle FBE} + \sin\angle FBE\sqrt{1-\sin^2\angle EBG} \\ &= \frac{\frac{a}{2}-d\sin\theta}{y_b^2}\sqrt{y_b^2-(\frac{a}{2}+d\sin\theta)^2} + \frac{\frac{a}{2}+d\sin\theta}{y_b^2}\sqrt{y_b^2-(\frac{a}{2}-d\sin\theta)^2} \end{aligned} \tag{3.133}$$

As a result, we can calculate $S_{\triangle FBG}$ as

$$\begin{aligned}S_{\triangle FBG} &= \frac{1}{2}\cdot\overline{BF}\cdot\overline{BG}\cdot\sin\angle FBG \\ &= \frac{1}{2}\left[(\frac{a}{2}-d\sin\theta)\sqrt{y_b^2-(\frac{a}{2}+d\sin\theta)^2} + (\frac{a}{2}+d\sin\theta)\sqrt{y^2-(\frac{a}{2}-d\sin\theta)^2}\right]\end{aligned} \tag{3.134}$$

In order to derive $S_{\square HGFK}$, we have to first obtain the length of $\overline{FK}$ and $\overline{HG}$. According to Pythagorean theorem, $\overline{FV}$ can be expressed as

$$\overline{FV} = \sqrt{\overline{BF}^2-\overline{BV}^2} = \sqrt{y_b^2-(\frac{a}{2}+d\sin\theta)^2}. \tag{3.135}$$

Given $\overline{KV} = \overline{EB} = d\cos\theta - \frac{a}{2}$, we have

$$\overline{FK} = \overline{FV} - \overline{KV} = \sqrt{y_b^2-(\frac{a}{2}+d\sin\theta)^2} - (d\cos\theta-\frac{a}{2}). \tag{3.136}$$

Furthermore, according to Pythagorean theorem, $\overline{MG}$ is calculated by

$$\overline{MG} = \sqrt{\overline{BG}^2-\overline{BM}^2} = \sqrt{y_b^2-(\frac{a}{2}-d\sin\theta)^2}. \tag{3.137}$$

Since the length of $\overline{MH}$ is expressed as $\overline{MH} = \overline{BE} = d\cos\theta - \frac{a}{2}$, the length of $\overline{HG}$ is derived as

$$\overline{HG} = \overline{MG} - \overline{MH} = \sqrt{y_b^2-(\frac{a}{2}-d\sin\theta)^2} - (d\cos\theta-\frac{a}{2}). \tag{3.138}$$

Therefore, given $\overline{KH} = a$, the area of the trapezium $\square HGFK$ can be derived as

$$\begin{aligned} S_{\square HGFK} &= \frac{1}{2} \cdot \overline{KH} \cdot (\overline{HG} + \overline{FK}) \\ &= \frac{a}{2}\left[\sqrt{y_b^2 - (\frac{a}{2} + d\sin\theta)^2} + \sqrt{y_b^2 - (\frac{a}{2} - d\sin\theta)^2} - 2(d\cos\theta - \frac{a}{2})\right] \end{aligned} \tag{3.139}$$

As a result, the area of the shaded part can be derived as

$$\begin{aligned} S^{IV}_{shade} &= S_{\widehat{FBGC}} - S_{\triangle FBG} + S_{\square HGFK} \\ &= \frac{y_b^2}{2}\left(\arcsin\frac{\frac{a}{2} - d\sin\theta}{y_b} + \arcsin\frac{\frac{a}{2} + d\sin\theta}{y_b}\right) \\ &\quad + \frac{1}{2}\left[(\frac{a}{2} - d\sin\theta)\sqrt{y_b^2 - (\frac{a}{2} - d\sin\theta)^2} + (\frac{a}{2} + d\sin\theta)\sqrt{y_b^2 - (\frac{a}{2} + d\sin\theta)^2}\right. \\ &\qquad \left. -2a(d\cos\theta - \frac{a}{2})\right]. \end{aligned} \tag{3.140}$$

Finally, in this case, the cdf of the random distance Y_b is the ratio of S^{IV}_{shade} to $S_{\square HIJK} = a^2$, which is expressed as

$$\begin{aligned} F^{IV}_{Y_b}(y_b) &= \frac{S^{IV}_{shade}}{S_{\square HIJK}} \\ &= \frac{y_b^2}{2a^2}\left(\arcsin\frac{\frac{a}{2} - d\sin\theta}{y_b} + \arcsin\frac{\frac{a}{2} + d\sin\theta}{y_b}\right) \\ &\quad + \frac{1}{2a^2}\left[(\frac{a}{2} - d\sin\theta)\sqrt{y_b^2 - (\frac{a}{2} - d\sin\theta)^2} + (\frac{a}{2} + d\sin\theta)\sqrt{y_b^2 - (\frac{a}{2} + d\sin\theta)^2}\right. \\ &\qquad \left. -2a(d\cos\theta - \frac{a}{2})\right]. \end{aligned} \tag{3.141}$$

for $\sqrt{a^2/2 + d^2 - ad(\cos\theta - \sin\theta)} < y_b \leq (d\cos\theta + a/2)$.

CASE V: $\overline{BQ} < y_b \leq \overline{BI}$

In this case, as shown in Figure 3.23(d), the circle $\odot(B, y_b)$ intersects the side $\overline{JK}$ of the square $\square HIJK$ at point F and intersects the side $\overline{HI}$ at point G. Moreover, the side $\overline{IJ}$ has two intersection points with the circle $\odot(B, y_b)$, namely points X and J, as shown in Figure 3.23(d). The straight line $\overline{BQ}$ is perpendicular to the side $\overline{IJ}$ and intersect $\overline{IJ}$ at point Q, whose length is $\overline{BQ} = d\cos\theta + a/2$.

The shaded part in Figure 3.23(d) is slightly different from that in Figure 3.23(d). In order to derive the area S^{V}_{shade} of the shaded part in Figure 3.23(d), we have to subtract the area of a small segment, which is formed by the arc $\widehat{XY}$ and the straight line $\overline{XY}$, from the sum of the area of a trapezium $\square HGFK$ and the area of a segment formed by the arc $\widehat{FCG}$ and the line $\overline{FG}$.

Let us first derive the area of the small segment that is formed by the the arc $\widehat{XY}$ and the straight line $\overline{XY}$. The area of this small segment can be expressed as

$$S_{seg} = S_{\widehat{XBY}} - S_{\triangle XBY}, \tag{3.142}$$

where $S_{\widehat{XBY}}$ denotes the area of the sector $\widehat{XBY}$ and $S_{\triangle XBY}$ denotes the area of the triangle $\triangle XBY$. The cosine value of $\angle XBQ$ is expressed as

$$\cos\angle XBQ = \frac{\overline{BQ}}{\overline{BX}} = \frac{d\cos\theta + \frac{a}{2}}{y_b}, \tag{3.143}$$

where $\overline{BX} = y_b$ because point X is on the circumference of $\odot(B, y_b)$. With the aid of the inverse trigonometric function, $\angle XBQ$ is derived as

$$\angle XBQ = \arccos\frac{d\cos\theta + \frac{a}{2}}{y_b}. \tag{3.144}$$

As a result, the area of the sector $\widehat{XBY}$ can be expressed as

$$S_{\widehat{XBY}} = \frac{1}{2}\cdot\overline{BX}^2\cdot\angle XBY = \frac{1}{2}\cdot\overline{BX}^2\cdot 2\angle XBQ = y_b^2\arccos\frac{d\cos\theta + \frac{a}{2}}{y_b}. \tag{3.145}$$

According to Pythagorean theorem, the length of $\overline{XQ}$ can be expressed as

$$\overline{XQ} = \sqrt{\overline{BX}^2 - \overline{BQ}^2} = \sqrt{y_b^2 - (d\cos\theta + \frac{a}{2})^2}. \tag{3.146}$$

As a result, the area of the triangle $\triangle XBY$ can be expressed as

$$S_{\triangle XBY} = \frac{1}{2}\cdot\overline{BQ}\cdot 2\overline{XQ} = (d\cos\theta + \frac{a}{2})\sqrt{y_b^2 - (d\cos\theta + \frac{a}{2})^2}. \tag{3.147}$$

Therefore, the area of the small segment that is formed by the the arc $\widehat{XY}$ and the straight line $\overline{XY}$ can be expressed as

$$\begin{aligned} S_{seg} &= S_{\widehat{XBY}} - S_{\triangle XBY} \\ &= y_b^2\arccos\frac{d\cos\theta + \frac{a}{2}}{y_b} - (d\cos\theta + \frac{a}{2})\sqrt{y_b^2 - (d\cos\theta + \frac{a}{2})^2}. \end{aligned} \tag{3.148}$$

Since the sum of the area of a trapezium $\square HGFK$ and the area of a segment formed by the arc $\widehat{FCG}$ and the line $\overline{FG}$ has the same shape with the shaded part in CASE IV, as shown in Figure

3.23(c)(d), this area can be calculated by Eq.3.140, which is derived for calculating the area of the shaded part in CASE IV. As a result, the area of the shaded part in CASE V can be derived as

$$\begin{aligned}
S^V_{shade} &= S^{IV}_{shade} - S_{seq} \\
&= \frac{y_b^2}{2}\left(\arcsin\frac{\frac{a}{2}-d\sin\theta}{y_b} + \arcsin\frac{\frac{a}{2}+d\sin\theta}{y_b} - 2\arccos\frac{d\cos\theta+\frac{a}{2}}{y_b}\right) \\
&\quad + \frac{1}{2}\left[(\frac{a}{2}-d\sin\theta)\sqrt{y_b^2-(\frac{a}{2}-d\sin\theta)^2} + (\frac{a}{2}+d\sin\theta)\sqrt{y_b^2-(\frac{a}{2}+d\sin\theta)^2}\right. \\
&\qquad \left. +2(d\cos\theta+\frac{a}{2})\sqrt{y_b^2-(d\cos\theta+\frac{a}{2})^2} - 2a(d\cos\theta-\frac{a}{2})\right]. \qquad (3.149)
\end{aligned}$$

Finally, in this case, the cdf of the random distance Y_b is the ratio between S^V_{shade} and $S_{\square HIJK} = a^2$, which is presented as

$$\begin{aligned}
F^V_{Y_b}(y_b) &= \frac{S^V_{shade}}{S_{\square HIJK}} \\
&= \frac{y_b^2}{2a^2}\left(\arcsin\frac{\frac{a}{2}-d\sin\theta}{y_b} + \arcsin\frac{\frac{a}{2}+d\sin\theta}{y_b} - 2\arccos\frac{d\cos\theta+\frac{a}{2}}{y_b}\right) \\
&\quad + \frac{1}{2a^2}\left[(\frac{a}{2}-d\sin\theta)\sqrt{y_b^2-(\frac{a}{2}-d\sin\theta)^2} + (\frac{a}{2}+d\sin\theta)\sqrt{y_b^2-(\frac{a}{2}+d\sin\theta)^2}\right. \\
&\qquad \left. +2(d\cos\theta+\frac{a}{2})\sqrt{y_b^2-(d\cos\theta+\frac{a}{2})^2} - 2a(d\cos\theta-\frac{a}{2})\right], \qquad (3.150)
\end{aligned}$$

for $(d\cos\theta + a/2) < y_b \leq \sqrt{a^2/2 + d^2 + ad(\cos\theta - \sin\theta)}$.

CASE VI: $\overline{BI} < y_b \leq \overline{BJ}$

In this case, as shown in Figure 3.23(e), the circle $\odot(B, y_b)$ intersects the side $\overline{JK}$ at point F and intersects the side $\overline{IJ}$ at point X. The straight line $\overline{BC}$ is perpendicular to the line $\overline{FX}$ and intersects $\overline{FX}$ at point D and intersect the circle $\odot(B, y_b)$ at point C. $\overline{WX}$ is a horizontal line and intersect the side KH of $\square HIJK$ at point Z. The overlapped area between the circle $\odot(B, y_b)$ and the square $\square HIJK$ is denoted as the shaded part in Figure 3.23(e). This shaded part comprise three different areas, namely a trapezium $\square KFXZ$, a rectangular $\square HIXZ$, and a small segment surrounded by an arc $\widehat{FCX}$ and a straight line $\overline{FX}$. Since the area of the small segment can be derived as $S_{seg} = S_{\widehat{FBXC}} - S_{\triangle FBX}$, the area of the shaded part can be expressed as

$$S_{shade} = S_{\widehat{FBXC}} - S_{\triangle FBX} + S_{\square KFXZ} + S_{\square HIKZ}, \qquad (3.151)$$

where $S_{\widehat{FBXC}}$ denotes the area of the sector $\widehat{FBXC}$, $S_{\triangle FBX}$ denotes the area of the triangle $\triangle FBX$, $S_{\square KFXZ}$ denotes the area of the trapezium $\square KFXZ$ and $S_{\square HIKZ}$ denotes the area of

the rectangular $\square HIKZ$. Let us derive these areas, respectively.

As shown in Figure 3.23(e), point F is on the circumference of $\odot(B, y_b)$. Hence, we have $\overline{BF} = y_b$. Given $\overline{BV} = \overline{EQ} = a/2 + d\sin\theta$, we may derive the sine value of $\angle VFB$. Since $\overline{BQ}$ is parallel to $\overline{JK}$, we have $\angle QBF = \angle VFB$. hence, the sine value of $\angle QBF$ can be derived as

$$\sin\angle QBF = \sin\angle VBF = \frac{\overline{BF}}{\overline{BV}} = \frac{\frac{a}{2} + d\sin\theta}{y_b}. \tag{3.152}$$

With the aid of the inverse trigonometric function, the value of $\angle QBF$ can be expressed as

$$\angle QBF = \arcsin\frac{\frac{a}{2} + d\sin\theta}{y_b}. \tag{3.153}$$

Given $\overline{WZ} = \overline{BE} = d\cos\theta - a/2$ and $\overline{ZX} = \overline{HI} = a$, the length of $\overline{WX}$ can be derived as

$$\overline{WX} = \overline{WZ} + \overline{ZX} = \overline{BE} + \overline{HI} = \frac{a}{2} + d\cos\theta. \tag{3.154}$$

Since point X is on the circumference of $\odot(B, y)$, we have $\overline{BX} = y_b$. As shown in Figure 3.23(e), $\overline{WX}$ is parallel to $\overline{BQ}$. Therefore, the value of $\angle QBX$ is equal to the value of $\angle WXB$. As a result, the cosine value of $\angle QBX$ can be expressed as

$$\cos\angle QBX = \cos\angle WXB = \frac{\overline{WX}}{\overline{BX}} = \frac{\frac{a}{2} + d\cos\theta}{y_b}. \tag{3.155}$$

With the aid of the inverse trigonometric function, the value of $\angle QBX$ can be expressed as

$$\angle QBX = \arccos\frac{\frac{a}{2} + d\cos\theta}{y_b}. \tag{3.156}$$

As a result, the value of $\angle FBX$ can be expressed as

$$\angle FBX = \angle QBF - \angle QBX = \arcsin\frac{\frac{a}{2} + d\sin\theta}{y_b} - \arccos\frac{\frac{a}{2} + d\cos\theta}{y_b}. \tag{3.157}$$

Then, the area of the sector $\widehat{FBXC}$ can be expressed as

$$\begin{aligned} S_{\widehat{FBXC}} &= \frac{1}{2}\cdot\overline{BF}^2\cdot\angle FBX \\ &= \frac{y_b^2}{2}\left(\arcsin\frac{\frac{a}{2} + d\sin\theta}{y_b} - \arccos\frac{\frac{a}{2} + d\cos\theta}{y_b}\right). \end{aligned} \tag{3.158}$$

Furthermore, in order to derive the area of $\triangle FBX$, we have to obtain the sine value of $\angle FBX$,

which can be calculated as

$$\begin{aligned}
&\sin\angle FBX = \sin\angle QBF\cos\angle QBX - \cos\angle QBF\sin\angle QBX \\
&= \sin\angle QBF\cos\angle QBX - \sqrt{1-\sin^2\angle QBF}\sqrt{1-\cos^2\angle QBX} \\
&= \frac{\frac{a}{2}+d\sin\theta}{y_b}\cdot\frac{\frac{a}{2}+d\cos\theta}{y_b} - \sqrt{1-\left(\frac{\frac{a}{2}+d\sin\theta}{y_b}\right)^2}\sqrt{1-\left(\frac{\frac{a}{2}+d\cos\theta}{y_b}\right)^2}.
\end{aligned} \tag{3.159}$$

Hence, the area of $\triangle FBX$ can be derived as

$$\begin{aligned}
S_{\triangle FBX} &= \frac{1}{2}\cdot\overline{BF}\cdot\overline{BX}\cdot\sin\angle FBX \\
&= \frac{1}{2}\left[(\frac{a}{2}+d\sin\theta)(\frac{a}{2}+d\cos\theta)\right. \\
&\qquad \left.-\sqrt{y_b^2-(\frac{a}{2}+d\sin\theta)^2}\sqrt{y_b^2-(\frac{a}{2}+d\cos\theta)^2}\right].
\end{aligned} \tag{3.160}$$

According to Pythagorean theorem, the length of $\overline{BW}$ can be expressed as

$$\overline{BW} = \sqrt{\overline{BX}^2-\overline{WX}^2} = \sqrt{y_b^2-(\frac{a}{2}+d\cos\theta)^2}. \tag{3.161}$$

As a result, the length of $\overline{KZ}$ can be derived as

$$\overline{KZ} = \overline{VW} = \overline{BV}-\overline{BW} = (\frac{a}{2}+d\sin\theta) - \sqrt{y_b^2-(\frac{a}{2}+d\cos\theta)^2}. \tag{3.162}$$

Similarly, according to Pythagorean theorem, the length of $\overline{FV}$ can be obtained as

$$\overline{VF} = \sqrt{\overline{BF}^2-\overline{BV}^2} = \sqrt{y_b^2-(\frac{a}{2}+d\sin\theta)^2}. \tag{3.163}$$

As a result, the length of $\overline{KF}$ can be derived as

$$\overline{KF} = \overline{VF}-\overline{VK} = \overline{VF}-\overline{BE} = \sqrt{y^2-(\frac{a}{2}+d\sin\theta)^2}-(d\cos\theta-\frac{a}{2}). \tag{3.164}$$

Therefore, the area of the trapezium $\square KFXZ$ is derived as

$$\begin{aligned}
&S_{\square KFXZ} = \frac{1}{2} \cdot \overline{KZ} \cdot (\overline{KF} + \overline{ZX}) \\
&= \frac{1}{2}\left[(\frac{a}{2} + d\sin\theta)\sqrt{y_b^2 - (\frac{a}{2} + d\sin\theta)^2} + (d\cos\theta - \frac{3}{2}a)\sqrt{y^2 - (\frac{a}{2} + d\cos\theta)^2}\right. \\
&\left.-(\frac{a}{2} + d\sin\theta)(d\cos\theta - \frac{3}{2}a) - \sqrt{y_b^2 - (\frac{a}{2} + d\sin\theta)^2}\sqrt{y_b^2 - (\frac{a}{2} + d\cos\theta)^2}\right].
\end{aligned} \tag{3.165}$$

Furthermore, the length of $\overline{HZ}$ is expressed as

$$\overline{HZ} = \overline{HK} - \overline{KZ} = (\frac{a}{2} - d\sin\theta) + \sqrt{y_b^2 - (\frac{a}{2} + d\cos\theta)^2}. \tag{3.166}$$

Hence, the area of the rectangular $\square HIXZ$ can be obtained as

$$S_{\square HIXZ} = \overline{HI} \cdot \overline{HZ} = a\left[(\frac{a}{2} - d\sin\theta) + \sqrt{y_b^2 - (\frac{a}{2} + d\cos\theta)^2}\right]. \tag{3.167}$$

Then, we arrive at the expression of the shaded part in Figure 3.4(g), which is derived as

$$\begin{aligned}
&S_{shade}^{VI} = S_{\widehat{FBXC}} - S_{\triangle FBX} + S_{\square KFXZ} + S_{\square HIKZ} \\
&= \frac{y^2}{2}\left(\arcsin\frac{\frac{a}{2} + d\sin\theta}{y_b} - \arccos\frac{\frac{a}{2} + d\cos\theta}{y_b}\right) \\
&\quad + \frac{1}{2}\left[(\frac{a}{2} + d\sin\theta)\sqrt{y_b^2 - (\frac{a}{2} + d\sin\theta)^2} + (d\cos\theta + \frac{a}{2})\sqrt{y_b^2 - (\frac{a}{2} + d\cos\theta)^2}\right. \\
&\quad \left.+2a(\frac{a}{2} - d\sin\theta) - 2(\frac{a}{2} + d\sin\theta)(d\cos\theta - \frac{a}{2})\right]
\end{aligned} \tag{3.168}$$

Finally, in this case, the cdf of the random distance Y_b is the ratio between S_{shade}^{VI} and $S_{\square HIJK} = a^2$, which is expressed as

$$\begin{aligned}
&F_{Y_b}^{VI}(y_b) = \frac{S_{shade}^{VI}}{S_{\square HIJK}} \\
&= \frac{y_b^2}{2a^2}\left(\arcsin\frac{\frac{a}{2} + d\sin\theta}{y_b} - \arccos\frac{\frac{a}{2} + d\cos\theta}{y_b}\right) \\
&\quad + \frac{1}{2a^2}\left[(\frac{a}{2} + d\sin\theta)\sqrt{y_b^2 - (\frac{a}{2} + d\sin\theta)^2} + (d\cos\theta + \frac{a}{2})\sqrt{y_b^2 - (\frac{a}{2} + d\cos\theta)^2}\right. \\
&\quad \left.+2a(\frac{a}{2} - d\sin\theta) - 2(\frac{a}{2} + d\sin\theta)(d\cos\theta - \frac{a}{2})\right],
\end{aligned} \tag{3.169}$$

for $\sqrt{a^2/2 + d^2 + ad(\cos\theta - \sin\theta)} < y_b \leq \sqrt{a^2/2 + d^2 + ad(\cos\theta + \sin\theta)}$.

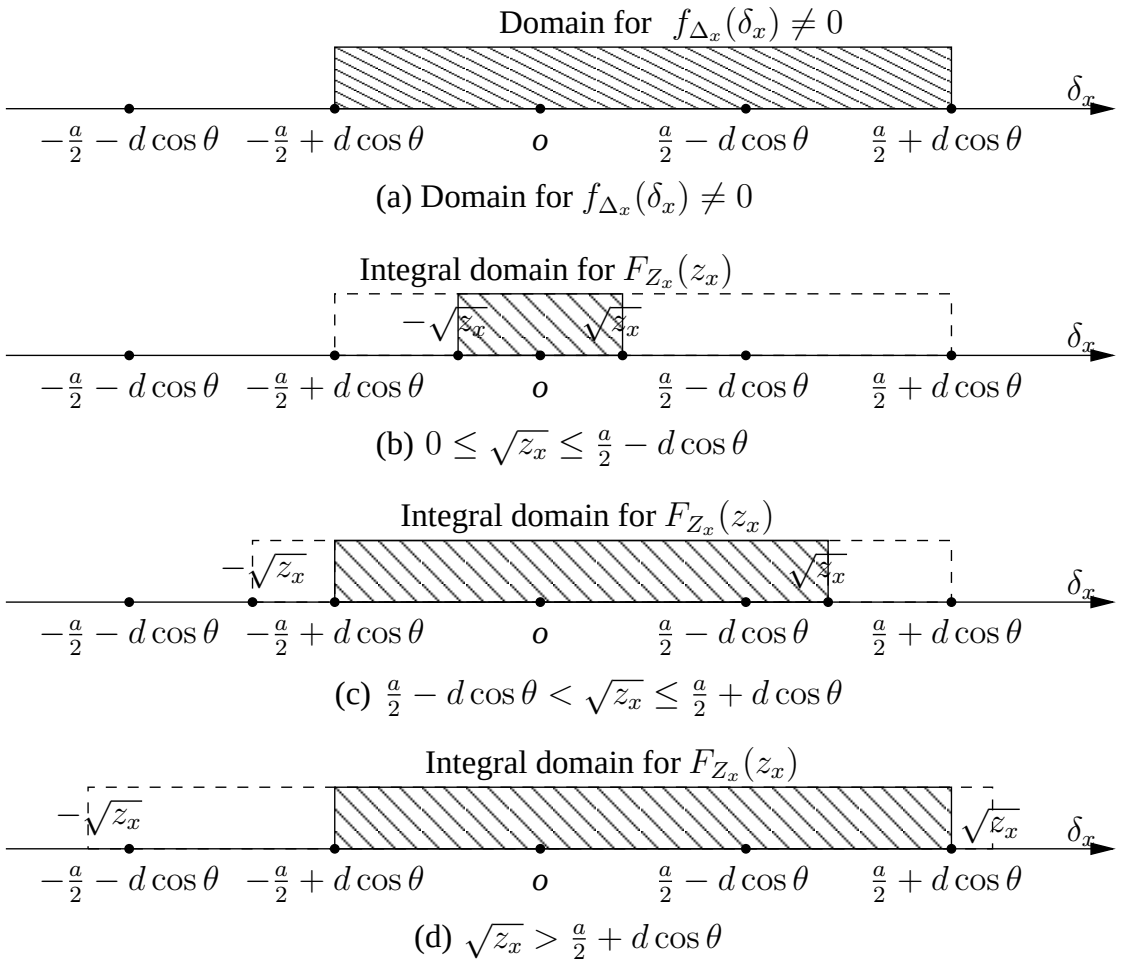

Figure 3.24: The integral area for different values of $\sqrt{z_x}$.

CASE VII: $y_b > \overline{BJ}$

In this case, as shown in Figure 3.23(f), the whole square area of $\square HIJK$ is completely surrounded by the circle $\odot(B, y_b)$. As a result, the overlapped area, which is denoted as the shaded part in Figure 3.23(f), is equal to the area $S_{\square HIJK} = a^2$. In this case, the cdf of the random distance Y_b is the ratio between S^{VII}_{shade} and $S_{\square HIJK}$, which is presented as $F^{VII}_{Y_b}(y_b) = 1$ for $y_b > \sqrt{a^2/2 + d^2 + ad(\cos\theta + \sin\theta)}$.

3.B.4 The proof for Lemma 3.3

Since the random variable Z_x is defined as $Z_x = \Delta_x^2$, the cdf of Z_x should be expressed as

$$\begin{aligned} F_{Z_x}(z_x) &= \Pr(Z_x \le z_x) = \Pr(\Delta_x^2 \le z_x) = \Pr(-\sqrt{z_x} \le \Delta_x \le \sqrt{z_x}) \\ &= \int_{-\sqrt{z_x}}^{\sqrt{z_x}} f_{\Delta_x}(\delta_x) d\delta_x. \end{aligned} \tag{3.170}$$

Jointly considering Eq.(3.170) and Eq.(3.19), we can see that the integral domain of Eq.(3.170) is determined by the specific value of $\sqrt{z_x}$. When we have $0 \le \sqrt{z_x} \le \frac{a}{2} - d\cos\theta$, the integral domain is $[-\sqrt{z_x}, \sqrt{z_x}]$, as shown in Figure 3.24(b). As a result, the cdf $F_{Z_x}(z_x)$ can be expressed as

$$F_{Z_x}(z_x) = \int_{-\sqrt{z_x}}^{\sqrt{z_x}} f_{\Delta_x}(\delta_x) d\delta_x = \int_{-\sqrt{z_x}}^{\sqrt{z_x}} \frac{1}{a} \cdot d\delta_x = \frac{2\sqrt{z_x}}{a}. \tag{3.171}$$

When we have $\frac{a}{2} - d\cos\theta < \sqrt{z_x} \le \frac{a}{2} + d\cos\theta$, the integral domain is $[\frac{a}{2} - d\cos\theta, \sqrt{z_x}]$, as shown in Figure 3.24(c). As a result, the cdf $F_{Z_x}(z_x)$ can be expressed as

$$F_{Z_x}(z_x) = \int_{\frac{a}{2}-d\cos\theta}^{\sqrt{z_x}} f_{\Delta_x}(\delta_x) d\delta_x = \int_{\frac{a}{2}-d\cos\theta}^{\sqrt{z_x}} \frac{1}{a} \cdot d\delta_x = \frac{\sqrt{z_x} + \frac{a}{2} - d\cos\theta}{a}. \tag{3.172}$$

When we have $\sqrt{z_x} > \frac{a}{2} + d\cos\theta$, the integral domain is $[-\frac{a}{2} + d\cos\theta, \frac{a}{2} + d\cos\theta]$, as shown in Figure 3.24(d). As a result, the cdf $F_{Z_x}(z_x)$ can be expressed as

$$F_{Z_x}(z_x) = \int_{-\frac{a}{2}+d\cos\theta}^{\frac{a}{2}+d\cos\theta} f_{\Delta_x}(\delta_x) d\delta_x = \int_{-\frac{a}{2}+d\cos\theta}^{\frac{a}{2}+d\cos\theta} \frac{1}{a} \cdot d\delta_x = 1. \tag{3.173}$$

In a nutshell, the cdf of Z_x can be expressed as

$$F_{Z_x}(z_x) = \begin{cases} \dfrac{2\sqrt{z_x}}{a}, & 0 \le z_x \le (\dfrac{a}{2} - d\cos\theta)^2, \\ \dfrac{\sqrt{z_x} + \frac{a}{2} - d\cos\theta}{a}, & (\dfrac{a}{2} - d\cos\theta)^2 < z_x \le (\dfrac{a}{2} + d\cos\theta)^2 \\ 1, & z_x > (\dfrac{a}{2} + d\cos\theta)^2. \end{cases} \tag{3.174}$$

Differentiating $F_{Z_x}(z_x)$ with respect to z_x both in the domains $[0, (\frac{a}{2} - d\cos\theta)^2]$ and $((\frac{a}{2} - d\cos\theta)^2, (\frac{a}{2} + d\cos\theta)^2]$, the pdf of Z_x can be expressed as Eq.(3.21) in Lemma 3.3.

Similarly, by following the same methodology, we may derive the cdf $F_{Z_Y}(z_y)$ for the random

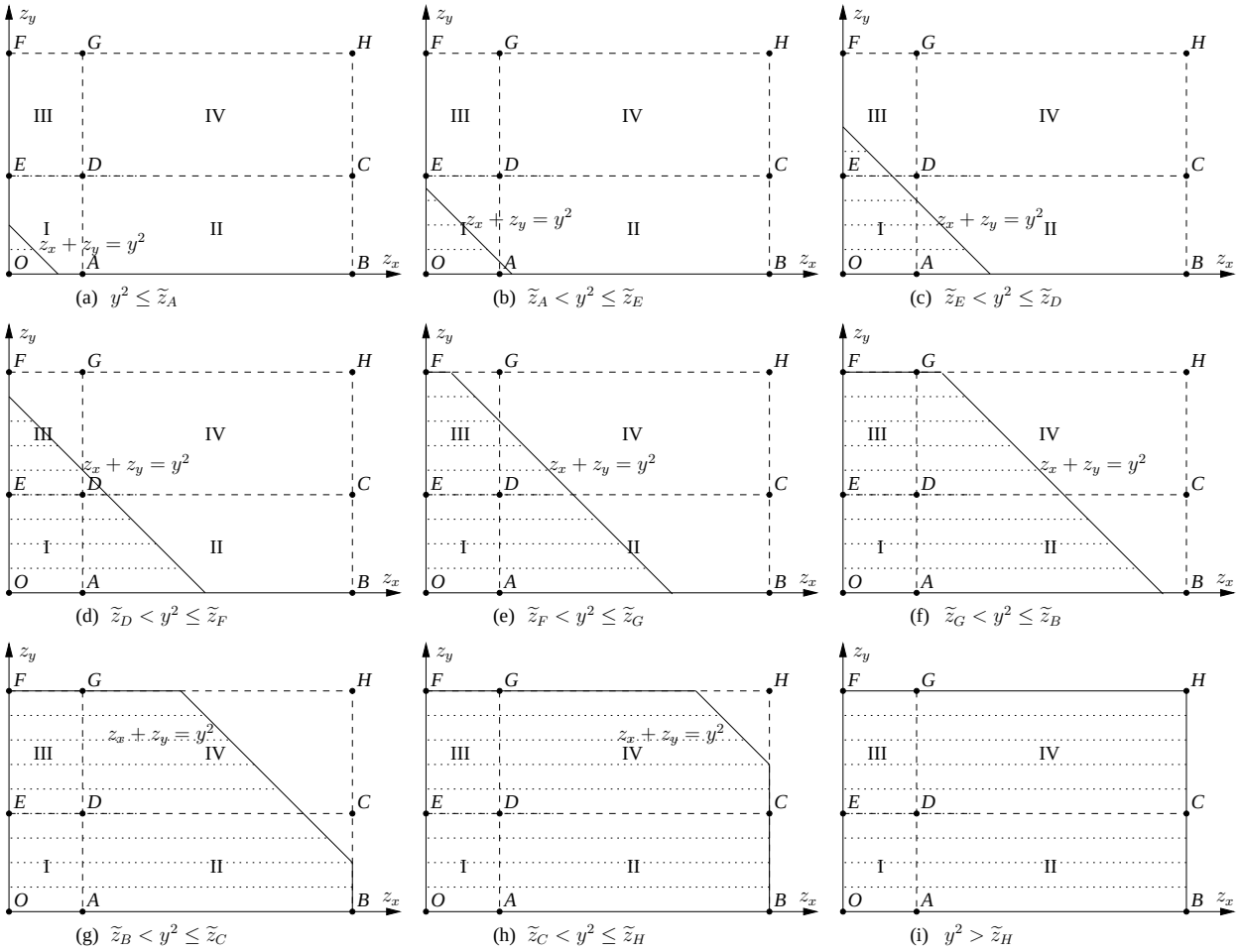

Figure 3.25: The integral area $\mathcal{S}$ given different value of y^2

variable $Z_Y = \widetilde{y} + d\sin\theta$, which is expressed as

$$F_{Z_y}(z_y) = \begin{cases} \dfrac{2\sqrt{z_y}}{a}, & 0 \leq z_y \leq (\dfrac{a}{2} - d\sin\theta)^2, \\ \dfrac{\sqrt{z_y} + \frac{a}{2} - d\sin\theta}{a}, & (\dfrac{a}{2} - d\sin\theta)^2 < z_y \leq (\dfrac{a}{2} + d\sin\theta)^2 \\ 1, & z_y > (\dfrac{a}{2} + d\sin\theta)^2. \end{cases} \tag{3.175}$$

Hence, the corresponding pdf for Z_y can be expressed as Eq.3.22 in Lemma 3.3. The lemma has been proven.

$$F_{Y_b}(y_b) = \iint_{\mathcal{S}} f_{Z_xZ_y}(z_x, z_y)dz_xdz_y = \iint_{\mathcal{S}_I} f^{(I)}_{Z_xZ_y}(z_x, z_y)dz_xdz_y,$$
$$= \int_0^{y_b^2} dz_x \int_0^{y_b^2-z_x} \frac{1}{a^2\sqrt{z_xz_y}}dz_y = \pi\left(\frac{y_b}{a}\right)^2. \tag{3.176}$$

$$\begin{aligned} F_{Y_b}(y_b) &= \iint_{\mathcal{S}} f_{Z_xZ_y}(z_x, z_y)dz_xdz_y \\ &= \iint_{\mathcal{S}_I} f^{(I)}_{Z_xZ_y}(z_x, z_y)dz_xdz_y + \iint_{\mathcal{S}_{II}} f^{(II)}_{Z_xZ_y}(z_x, z_y)dz_xdz_y \\ &= \underbrace{\int_0^{(\frac{a}{2}-d\cos\theta)^2} dz_x \int_0^{y_b^2-z_x} \frac{1}{a^2\sqrt{z_xz_y}}dz_y}_{\text{Double integral on } \mathcal{S}_I} + \underbrace{\int_{(\frac{a}{2}-d\cos\theta)^2}^{y_b^2} dz_x \int_0^{y_b^2-z_x} \frac{1}{2a^2\sqrt{z_xz_y}}dz_y}_{\text{Double integral on } \mathcal{S}_{II}} \\ &= \frac{1}{a^2}\left[\frac{\pi}{2}y_b^2 + y_b^2\arcsin\frac{\frac{a}{2}-d\cos\theta}{y_b} + (\frac{a}{2}-d\cos\theta)\sqrt{y_b^2-(\frac{a}{2}-d\cos\theta)^2}\right] \end{aligned} \tag{3.177}$$

3.B.5 The proof for Theorem 3.6

This ascending sort $\overline{OA} \le \overline{OE} \le \overline{EF} \le \overline{OF} \le \overline{AB} \le \overline{OB}$, assumed in Theorem 3.6, indicates $(\frac{a}{2}-d\cos\theta)^2 \le (\frac{a}{2}-d\sin\theta)^2 \le 2ad\sin\theta \le (\frac{a}{2}+d\sin\theta)^2 \le 2ad\cos\theta \le (\frac{a}{2}+d\cos\theta)^2$. As a result, the ascending sort of the array $\{\widetilde{z}_i | i \in \{A, B, C, D, E, F, G, H\}\}$ in this case is given by $\widetilde{z}_A \le \widetilde{z}_E \le \widetilde{z}_D \le \widetilde{z}_F \le \widetilde{z}_G \le \widetilde{z}_B \le \widetilde{z}_C \le \widetilde{z}_H$.

Since the joint pdf $f_{Z_xZ_y}(z_x, z_y)$ has different expressions in different domains, as shown in Eq.(3.24) and Figure 3.5, we have to generally divide the integral area $\mathcal{S}$ into four parts, namely $\mathcal{S}_I = \mathcal{S} \cap$ Domain I, $\mathcal{S}_{II} = \mathcal{S} \cap$ Domain II, $\mathcal{S}_{III} = \mathcal{S} \cap$ Domain III and $\mathcal{S}_{IV} = \mathcal{S} \cap$ Domain IV.

When $0 \le y_b^2 \le \widetilde{z}_A$, we have $y_b \le (\frac{a}{2}-d\cos\theta)$ and the integral area $\mathcal{S}$ is shown by the shaded part in Figure 3.25(a). As a result, the double integral given by Eq.(3.23) can be further derived as Eq.(3.176).

When $\widetilde{z}_A < y_b^2 \le \widetilde{z}_E$, we have $(\frac{a}{2}-d\cos\theta) < y_b \le (\frac{a}{2}-d\sin\theta)$ and the integral area $\mathcal{S}$ is shown by the shaded part in Figure 3.25(b). As a result, the double integral given by Eq.(3.23) can be further derived as Eq.(3.177).

When $\widetilde{z}_E < y_b^2 \le \widetilde{z}_D$, we have $(\frac{a}{2}-d\sin\theta) < y_b \le \sqrt{(\frac{a}{2}-d\cos\theta)^2+(\frac{a}{2}-d\sin\theta)^2}$ and the integral area $\mathcal{S}$ is shown by the shaded part in Figure 3.25(c). As a result, the double integral given by Eq.(3.23) can be further derived as Eq.(3.178).

When $\widetilde{z}_D < y_b^2 \le \widetilde{z}_F$, we have $\sqrt{(\frac{a}{2}-d\cos\theta)^2+(\frac{a}{2}-d\sin\theta)^2} < y_b \le (\frac{a}{2}+d\sin\theta)$ and the

$$
\begin{aligned}
F_{Y_b}(y_b) &= \iint_{\mathcal{S}} f_{Z_x Z_y}(z_x, z_y) dz_x dz_y \\
&= \iint_{\mathcal{S}_I} f^{(I)}_{Z_x Z_y}(z_x, z_y) dz_x dz_y + \iint_{\mathcal{S}_{II}} f^{(II)}_{Z_x Z_y}(z_x, z_y) dz_x dz_y + \iint_{\mathcal{S}_{III}} f^{(III)}_{Z_x Z_y}(z_x, z_y) dz_x dz_y \\
&= \underbrace{\int_0^{y_b^2-(\frac{a}{2}-d\sin\theta)^2} dz_x \int_0^{(\frac{a}{2}-d\sin\theta)^2} \frac{1}{a^2\sqrt{z_x z_y}} dz_y + \int_{y_b^2-(\frac{a}{2}-d\sin\theta)^2}^{(\frac{a}{2}-d\cos\theta)^2} dz_x \int_0^{y_b^2-z_x} \frac{1}{a^2\sqrt{z_x z_y}} dz_y}_{\text{Double integral on } \mathcal{S}_I} \\
&\quad + \underbrace{\int_{(\frac{a}{2}-d\cos\theta)^2}^{y_b^2} dz_x \int_0^{y_b^2-z_x} \frac{1}{2a^2\sqrt{z_x z_y}} dz_y}_{\text{Double integral on } \mathcal{S}_{II}} + \underbrace{\int_0^{y_b^2-(\frac{a}{2}-d\sin\theta)^2} dz_x \int_{(\frac{a}{2}-d\sin\theta)^2}^{y_b^2-z_x} \frac{1}{2a^2\sqrt{z_x z_y}} dz_y}_{\text{Double integral on } \mathcal{S}_{III}} \\
&= \frac{1}{a^2}\left[\frac{\pi}{2}y_b^2 + y_b^2 \arcsin\frac{\frac{a}{2}-d\cos\theta}{y_b} - y_b^2 \arcsin\frac{\sqrt{y_b^2-(\frac{a}{2}-d\sin\theta)^2}}{y_b}\right. \\
&\qquad \left. +(\frac{a}{2}-d\sin\theta)\sqrt{y_b^2-(\frac{a}{2}-d\sin\theta)^2} + (\frac{a}{2}-d\cos\theta)\sqrt{y_b^2-(\frac{a}{2}-d\cos\theta)^2}\right]. \quad (3.178)
\end{aligned}
$$

integral area $\mathcal{S}$ is shown by the shaded part in Figure 3.25(d). As a result, the double integral given by Eq.(3.23) can be further derived as Eq.(3.179).

When $\widetilde{z}_F < y_b^2 \leq \widetilde{z}_G$, we have $(\frac{a}{2}+d\sin\theta) < y_b \leq (\frac{a}{2}+d\cos\theta)$ and the integral area $\mathcal{S}$ is shown by the shaded part in Figure Figure 3.25(e). As a result, the double integral given by Eq.(3.23) can be further derived as Eq.(3.180).

When $\widetilde{z}_G < y_b^2 \leq \widetilde{z}_B$, we have $(\frac{a}{2}+d\cos\theta) < y_b \leq \sqrt{(\frac{a}{2}+d\sin\theta)^2+(\frac{a}{2}-d\cos\theta)^2}$ and the integral area $\mathcal{S}$ is shown by the shaded part in Figure Figure 3.25(f). As a result, the double integral given by Eq.(3.23) can be further derived as Eq.(3.181).

When $\widetilde{z}_B < y_b^2 \leq \widetilde{z}_C$, we have

$$\sqrt{(\frac{a}{2}+d\sin\theta)^2+(\frac{a}{2}-d\cos\theta)^2} < y_b \leq \sqrt{(\frac{a}{2}-d\sin\theta)^2+(\frac{a}{2}+d\cos\theta)^2}$$

and the integral area $\mathcal{S}$ is shown by the shaded part in Figure Figure 3.25(g). As a result, the double integral given by Eq.(3.23) can be further derived as Eq.(3.182).

When $\widetilde{z}_C < y_b^2 \leq \widetilde{z}_H$, we have

$$\sqrt{(\frac{a}{2}-d\sin\theta)^2+(\frac{a}{2}+d\cos\theta)^2} < y_b \leq \sqrt{(\frac{a}{2}+d\sin\theta)^2+(\frac{a}{2}+d\cos\theta)^2}$$

and the integral area $\mathcal{S}$ is shown by the shaded part in Figure Figure 3.25(h). As a result, the double

$$
\begin{aligned}
F_{Y_b}(y_b) &= \iint_{\mathcal{S}_I} f^{(I)}_{Z_xZ_y}(z_x,z_y)dz_xdz_y + \iint_{\mathcal{S}_{II}} f^{(II)}_{Z_xZ_y}(z_x,z_y)dz_xdz_y + \iint_{\mathcal{S}_{III}} f^{(III)}_{Z_xZ_y}(z_x,z_y)dz_xdz_y \\
&\quad + \iint_{\mathcal{S}_{IV}} f^{(IV)}_{Z_xZ_y}(z_x,z_y)dz_xdz_y \\
&= \underbrace{\int_0^{(\frac{a}{2}-d\cos\theta)^2} dz_x \int_0^{(\frac{a}{2}-d\sin\theta)^2} \frac{1}{a^2\sqrt{z_xz_y}}dz_y}_{\text{Double integral on } \mathcal{S}_I} + \underbrace{\int_0^{(\frac{a}{2}-d\cos\theta)^2} dz_x \int_{(\frac{a}{2}-d\sin\theta)^2}^{y_b^2-z_x} \frac{1}{2a^2\sqrt{z_xz_y}}dz_y}_{\text{Double integral on } \mathcal{S}_{III}} \\
&\quad + \underbrace{\int_{(\frac{a}{2}-d\cos\theta)^2}^{y_b^2-(\frac{a}{2}-d\sin\theta)^2} dz_x \int_0^{(\frac{a}{2}-d\sin\theta)^2} \frac{1}{2a^2\sqrt{z_xzy}}dz_y + \int_{y_b^2-(\frac{a}{2}-d\sin\theta)^2}^{y_b^2} dz_x \int_0^{y_b^2-z_x} \frac{1}{2a^2\sqrt{z_xz_y}}dz_y}_{\text{Double integral on } \mathcal{S}_{II}} \\
&\quad + \underbrace{\int_{(\frac{a}{2}-d\cos\theta)^2}^{y_b^2-(\frac{a}{2}-d\sin\theta)^2} dz_x \int_{(\frac{a}{2}-d\sin\theta)^2}^{y_b^2-z_x} \frac{1}{4a^2\sqrt{z_xz_y}}dz_y}_{\text{Double integral on } \mathcal{S}_{IV}} \\
&= \frac{1}{2a^2}\Bigg[\pi y_b^2 + y_b^2\arcsin\frac{\frac{a}{2}-d\cos\theta}{y_b} - y_b^2\arcsin\frac{\sqrt{y_b^2-(\frac{a}{2}-d\sin\theta)^2)}}{y_b} \\
&\qquad + (\frac{a}{2}-d\sin\theta)\sqrt{y_b^2-(\frac{a}{2}-d\sin\theta)^2} + (\frac{a}{2}-d\cos\theta)\sqrt{y_b^2-(\frac{a}{2}-d\cos\theta)^2} \\
&\qquad + 2(\frac{a}{2}-d\cos\theta)(\frac{a}{2}-d\sin\theta)\Big]
\end{aligned}
\tag{3.179}
$$

integral given by Eq.(3.23) can be further derived as Eq.(3.183).

At last, when $y_b^2 > \widetilde{z}_H$, we have $y_b > \sqrt{(\frac{a}{2}+d\sin\theta)^2+(\frac{a}{2}+d\cos\theta)^2}$ and the integral area $\mathcal{S}$ is the whole domain of the joint pdf $f_{Z_xZ_y}(z_x,z_y)$, as shown in Figure 3.25(i). As a result, the double integral given by Eq.(3.23) can be further derived as Eq.(3.184).

Differentiating the corresponding cdfs of different regions with respect to y_b, we may get the pdf $f_{Y_b}(y_b)$ in different regions for the random distance Y_b between the BS and a MU roaming in a bounded square area, when the position of the BS is defined by the tuple $B(d,\theta)$.

The cdfs of other cases from ii) to viii) can be derived by obeying the similar methodology. Another particular case that the position B of the BS is placed at the centre O of the square area $\square HIJK$ needs our further attention. The radius r of $\square HIJK$, which is defined as the distance from the centre O of $\square HIJK$ to any of the four vertices, can be obtained as $r = \overline{HI}/\cos\frac{\pi}{4} = \sqrt{2}a/2$. Buy substituting r into Eq.(3.5) and Eq.(3.6) of Section 1.2.2 and letting $l = 4$, we may obtain the cdf and the pdf of the random distance Y_b between the BS, which is placed at the centre of the square area $\square HIJK$, and the MU, which moves within $\square HIJK$.

$$
\begin{aligned}
F_{Y_b}(y_b) &= \iint_{\mathcal{S}_I} f^{(I)}_{Z_xZ_y}(z_x,z_y)dz_xdz_y + \iint_{\mathcal{S}_{II}} f^{(II)}_{Z_xZ_y}(z_x,z_y)dz_xdz_y + \iint_{\mathcal{S}_{III}} f^{(III)}_{Z_xZ_y}(z_x,z_y)dz_xdz_y \\
&\quad + \iint_{\mathcal{S}_{IV}} f^{(IV)}_{Z_xZ_y}(z_x,z_y)dz_xdz_y \\
&= \underbrace{\int_0^{(\frac{a}{2}-d\cos\theta)^2} dz_x \int_0^{(\frac{a}{2}-d\sin\theta)^2} \frac{1}{a^2\sqrt{z_xz_y}}dz_y}_{\text{Double integral on } \mathcal{S}_I} + \underbrace{\int_{(\frac{a}{2}-d\cos\theta)^2}^{y_b^2-(\frac{a}{2}-d\sin\theta)^2} dz_x \int_{(\frac{a}{2}-d\sin\theta)^2}^{y_b^2-z_x} \frac{1}{4a^2\sqrt{z_xz_y}}dz_y}_{\text{Double integral on } \mathcal{S}_{IV}} \\
&\quad + \underbrace{\int_{(\frac{a}{2}-d\cos\theta)^2}^{y_b^2-(\frac{a}{2}-d\sin\theta)^2} dz_x \int_0^{(\frac{a}{2}-d\sin\theta)^2} \frac{1}{2a^2\sqrt{z_xzy}}dz_y + \int_{y_b^2-(\frac{a}{2}-d\sin\theta)^2}^{y^2} dz_x \int_0^{y_b^2-z_x} \frac{1}{2a^2\sqrt{z_xz_y}}dz_y}_{\text{Double integral on } \mathcal{S}_{II}} \\
&\quad + \underbrace{\int_0^{y_b^2-(\frac{a}{2}+d\sin\theta)^2} dz_x \int_{(\frac{a}{2}-d\sin\theta)^2}^{(\frac{a}{2}+d\sin\theta)^2} \frac{1}{2a^2\sqrt{z_xz_y}}dz_y + \int_{y_b^2-(\frac{a}{2}+d\sin\theta)^2}^{(\frac{a}{2}-d\cos\theta)^2} dz_x \int_{(\frac{a}{2}-d\sin\theta)^2}^{y_b^2-z_x} \frac{1}{2a^2\sqrt{z_xz_y}}dz_y}_{\text{Double integral on } \mathcal{S}_{III}} \\
&= \frac{1}{2a^2}\Bigg[\pi y_b^2 + y_b^2\arcsin\frac{\frac{a}{2}-d\cos\theta}{y_b} - y_b^2\arcsin\frac{\sqrt{y_b^2-(\frac{a}{2}-d\sin\theta)^2)}}{y_b} \\
&\qquad - 2y_b^2\arcsin\frac{\sqrt{y_b^2-(\frac{a}{2}+d\sin\theta)^2}}{y_b} + (\frac{a}{2}-d\sin\theta)\sqrt{y_b^2-(\frac{a}{2}-d\sin\theta)^2} \\
&\qquad + (\frac{a}{2}-d\cos\theta)\sqrt{y_b^2-(\frac{a}{2}-d\cos\theta)^2} + 2(\frac{a}{2}+d\sin\theta)\sqrt{y_b^2-(\frac{a}{2}+d\sin\theta)^2} \\
&\qquad + 2(\frac{a}{2}-d\cos\theta)(\frac{a}{2}-d\sin\theta)\Bigg]. \qquad (3.180)
\end{aligned}
$$

3.C The proofs for the theorems in Section 3.4

3.C.1 The proof for Theorem 3.9

Let us discuss how to derive the pdf of the random distance Y_s between a pair of MUs roaming within a circular area $\odot(O,r)$ by exploiting the Crofton's fixed points theorem, as introduced in Theorem 3.7. For solving this problem, we define the set $\mathcal{S}_2$ as a two-dimensional plane containing all possible points on it, whose $\sigma-$algebra is denoted as $\Psi_{\mathcal{S}_2}$. A measure over a subset $\mathcal{A}$ that belongs to $\Psi_{\mathcal{S}_2}$ can be defined as the area covered by $\mathcal{A}$. For the scenario that a pair of MUs roam within a circular area $\odot(O,r)$, $\mathcal{A}$ is defined as a subset containing all possible points within a circular area $\odot(O,r)$, whose measure should be defined as $\varphi(\mathcal{A}) = \pi r^2$. As a result, the differential of $\varphi(\mathcal{A})$ can be derived as $d\varphi(\mathcal{A}) = 2\pi r dr$. We uniformly distribute two points $\{\epsilon_1, \epsilon_2\}$, representing two MUs, within the points subset $\mathcal{A}$. Furthermore, we let $\delta\mathcal{A}$ be the subsets containing all the

$$
\begin{aligned}
F_{Y_b}(y_b) &= \iint_{\mathcal{S}_I} f^{(I)}_{Z_xZ_y}(z_x,z_y)dz_xdz_y + \iint_{\mathcal{S}_{II}} f^{(II)}_{Z_xZ_y}(z_x,z_y)dz_xdz_y + \iint_{\mathcal{S}_{III}} f^{(III)}_{Z_xZ_y}(z_x,z_y)dz_xdz_y \\
&\quad + \iint_{\mathcal{S}_{IV}} f^{(IV)}_{Z_xZ_y}(z_x,z_y)dz_xdz_y \\
&= \underbrace{\int_0^{(\frac{a}{2}-d\cos\theta)^2} dz_x \int_0^{(\frac{a}{2}-d\sin\theta)^2} \frac{1}{a^2\sqrt{z_xz_y}}dz_y}_{\text{Double integral on } \mathcal{S}_I} + \underbrace{\int_0^{(\frac{a}{2}-d\cos\theta)^2} dz_x \int_{(\frac{a}{2}-d\sin\theta)^2}^{(\frac{a}{2}+d\sin\theta)^2} \frac{1}{2a^2\sqrt{z_xz_y}}dz_y}_{\text{Double integral on } \mathcal{S}_{III}} \\
&\quad + \underbrace{\int_{(\frac{a}{2}-d\cos\theta)^2}^{y_b^2-(\frac{a}{2}-d\sin\theta)^2} dz_x \int_0^{(\frac{a}{2}-d\sin\theta)^2} \frac{1}{2a^2\sqrt{z_xzy}}dz_y + \int_{y_b^2-(\frac{a}{2}-d\sin\theta)^2}^{y_b^2} dz_x \int_0^{y_b^2-z_x} \frac{1}{2a^2\sqrt{z_xz_y}}dz_y}_{\text{Double integral on } \mathcal{S}_{II}} \\
&\quad + \underbrace{\int_{(\frac{a}{2}-d\cos\theta)^2}^{y_b^2-(\frac{a}{2}+d\sin\theta)^2} dz_x \int_{(\frac{a}{2}-d\sin\theta)^2}^{(\frac{a}{2}+d\sin\theta)^2} \frac{1}{4a^2\sqrt{z_xz_y}}dz_y + \int_{y_b^2-(\frac{a}{2}+d\sin\theta)^2}^{y_b^2-(\frac{a}{2}-d\sin\theta)^2} dz_x \int_{(\frac{a}{2}-d\sin\theta)^2}^{y_b^2-z_x} \frac{1}{4a^2\sqrt{z_xz_y}}dz_y}_{\text{Double integral on } \mathcal{S}_{IV}} \\
&= \frac{1}{2a^2}\left[\pi y_b^2 - y_b^2\arcsin\frac{\sqrt{y_b^2-(\frac{a}{2}-d\sin\theta)^2}}{y_b} - y_b^2\arcsin\frac{\sqrt{y_b^2-(\frac{a}{2}+d\sin\theta)^2}}{y_b}\right. \\
&\quad + (\frac{a}{2}-d\sin\theta)\sqrt{y_b^2-(\frac{a}{2}-d\sin\theta)^2} + (\frac{a}{2}+d\sin\theta)\sqrt{y_b^2-(\frac{a}{2}+d\sin\theta)^2} \\
&\quad \left.+2a(\frac{a}{2}-d\cos\theta)\right] \qquad (3.181)
\end{aligned}
$$

points on the circumference of $\odot(O,r)$. We define $\mathcal{H}$ as an event that two points are separated by a distance between y_s and (y_s+dy_s). Let us first derive the term of $\Pr(H|\epsilon_1 \in \delta\mathcal{A})$ in Eq.(3.27).

$\Pr(H|\epsilon_1 \in \delta\mathcal{A})$ is the probability that, when point ϵ_1 is placed on the circumference of $\odot(O,r)$, ϵ_1 and ϵ_2 is separated by a distance between y_s and (y_s+dy_s). As shown in Figure 3.26, we draw a circle $\odot(\epsilon_1,y_s)$ having ϵ_1 as the centre and having y_s as the radius. $\odot(\epsilon_1,y_s)$ intersects $\odot(O,r)$ at points A and B. We draw another circle $\odot(\epsilon_1,y_s+dy_s)$ having ϵ_1 as the centre and having (y_s+dy_s) as the radius. If point ϵ_2 appears within the shaded annulus of Figure 3.26, the distance separating ϵ_1 from ϵ_2 is between y_s and (y_s+dy_s). Since ϵ_2 is uniformly distributed within $\odot(O,r)$, $\Pr(H|\epsilon_1 \in \delta\mathcal{A})$ can be derived as the ratio of the area of the annulus to the area of $\odot(O,r)$.

In order to derive the area of the annulus, we have to obtain the length of the arc $\widehat{ACB}$ first. According to the law of cosine, the cosine value of $\angle A\epsilon_1 O$ can be expressed as

$$\cos\angle A\epsilon_1 O = \frac{\overline{\epsilon_1 A}^2 + \overline{\epsilon_1 O}^2 - \overline{AO}^2}{2\overline{\epsilon_1 A}\overline{\epsilon_1 O}} = \frac{y_s^2+r^2-r^2}{2y_sr} = \frac{y_s}{2r}. \qquad (3.185)$$

$$
\begin{aligned}
F_{Y_b}(y_b) &= \iint_{\mathcal{S}_I} f^{(I)}_{Z_xZ_y}(z_x,z_y)dz_xdz_y + \iint_{\mathcal{S}_{II}} f^{(II)}_{Z_xZ_y}(z_x,z_y)dz_xdz_y + \iint_{\mathcal{S}_{III}} f^{(III)}_{Z_xZ_y}(z_x,z_y)dz_xdz_y \\
&\quad + \iint_{\mathcal{S}_{IV}} f^{(IV)}_{Z_xZ_y}(z_x,z_y)dz_xdz_y \\
&= \underbrace{\int_0^{(\frac{a}{2}-d\cos\theta)^2} dz_x \int_0^{(\frac{a}{2}-d\sin\theta)^2} \frac{1}{a^2\sqrt{z_xz_y}}dz_y}_{\text{Double integral on } \mathcal{S}_I} + \underbrace{\int_0^{(\frac{a}{2}-d\cos\theta)^2} dz_x \int_{(\frac{a}{2}-d\sin\theta)^2}^{(\frac{a}{2}+d\sin\theta)^2} \frac{1}{2a^2\sqrt{z_xz_y}}dz_y}_{\text{Double integral on } \mathcal{S}_{III}} \\
&\quad + \underbrace{\int_{(\frac{a}{2}-d\cos\theta)^2}^{y_b^2-(\frac{a}{2}-d\sin\theta)^2} dz_x \int_0^{(\frac{a}{2}-d\sin\theta)^2} \frac{1}{2a^2\sqrt{z_xzy}}dz_y + \int_{y_b^2-(\frac{a}{2}-d\sin\theta)^2}^{(\frac{a}{2}+d\cos\theta)^2} dz_x \int_0^{y_b^2-z_x} \frac{1}{2a^2\sqrt{z_xz_y}}dz_y}_{\text{Double integral on } \mathcal{S}_{II}} \\
&\quad + \underbrace{\int_{(\frac{a}{2}-d\cos\theta)^2}^{y_b^2-(\frac{a}{2}+d\sin\theta)^2} dz_x \int_{(\frac{a}{2}-d\sin\theta)^2}^{(\frac{a}{2}+d\sin\theta)^2} \frac{1}{4a^2\sqrt{z_xz_y}}dz_y + \int_{y_b^2-(\frac{a}{2}+d\sin\theta)^2}^{y_b^2-(\frac{a}{2}-d\sin\theta)^2} dz_x \int_{(\frac{a}{2}-d\sin\theta)^2}^{y_b^2-z_x} \frac{1}{4a^2\sqrt{z_xz_y}}dz_y}_{\text{Double integral on } \mathcal{S}_{IV}} \\
&= \frac{1}{2a^2}\left[2a(\frac{a}{2}-d\cos\theta) + 2y_b^2\arcsin\frac{\frac{a}{2}+\cos\theta}{y_b} - y_b^2\arcsin\frac{\sqrt{y_b^2-(\frac{a}{2}-d\sin\theta)^2)}}{y_b}\right. \\
&\quad - y_b^2\arcsin\frac{\sqrt{y_b^2-(\frac{a}{2}+d\sin\theta)^2}}{y_b} + (\frac{a}{2}-d\sin\theta)\sqrt{y_b^2-(\frac{a}{2}-d\sin\theta)^2} \\
&\quad \left. +2(\frac{a}{2}+d\cos\theta)\sqrt{y_b^2-(\frac{a}{2}+\cos\theta)^2} + (\frac{a}{2}+d\sin\theta)\sqrt{y_b^2-(\frac{a}{2}+d\sin\theta)^2}\right]. \quad (3.182)
\end{aligned}
$$

With the aid of inverse trigonometric function, we can obtain the exact value of the angle $\angle A\epsilon_1 B$ as

$$\angle A\epsilon_1 B = 2\angle A\epsilon_1 O = 2\arccos\frac{y_s}{2r}. \quad (3.186)$$

Therefore, the length of the arc $\widehat{ACB}$ can be derived as $\widehat{ACB} = y_s\angle A\epsilon_1 B = 2y_s\arccos(y_s/2r)$. Furthermore, the area of the shaded annulus is expressed as $S_{annulus} = \widehat{ACB}dy_s = 2y_sdy_s \cdot \arccos(y_s/2r)$. Thus, $\Pr(H|\epsilon_1 \in \delta\mathcal{A})$ can be expressed as

$$\Pr(H|\epsilon_1 \in \delta\mathcal{A}) = \frac{S_{annulus}}{S_{\odot(O,r)}} = \frac{2y_sdy_s}{\pi r^2}\arccos\frac{y_s}{2r}. \quad (3.187)$$

Substituting $\Pr(H|\epsilon_1 \in \delta\mathcal{A})$, $n = 2$, $\varphi(\mathcal{A}) = \pi r^2$ and $d\varphi(\mathcal{A}) = 2\pi r dr$ into Eq.(3.27), we may

$$
\begin{aligned}
F_{Y_b}(y_b) &= \iint_{\mathcal{S}_I} f^{(I)}_{Z_xZ_y}(z_x,z_y)dz_xdz_y + \iint_{\mathcal{S}_{II}} f^{(II)}_{Z_xZ_y}(z_x,z_y)dz_xdz_y + \iint_{\mathcal{S}_{III}} f^{(III)}_{Z_xZ_y}(z_x,z_y)dz_xdz_y \\
&\quad + \iint_{\mathcal{S}_{IV}} f^{(IV)}_{Z_xZ_y}(z_x,z_y)dz_xdz_y \\
&= \underbrace{\int_{(\frac{a}{2}-d\cos\theta)^2}^{y_b^2-(\frac{a}{2}+d\sin\theta)^2} dz_x \int_{(\frac{a}{2}-d\sin\theta)^2}^{(\frac{a}{2}+d\sin\theta)^2} \frac{1}{4a^2\sqrt{z_xz_y}}dz_y + \int_{y_b^2-(\frac{a}{2}+d\sin\theta)^2}^{(\frac{a}{2}+d\cos\theta)^2} dz_x \int_{(\frac{a}{2}-d\sin\theta)^2}^{y_b^2-z_x} \frac{1}{4a^2\sqrt{z_xz_y}}dz_y}_{\text{Double integral on } \mathcal{S}_{IV}} \\
&\quad + \underbrace{\int_0^{(\frac{a}{2}-d\cos\theta)^2} dz_x \int_0^{(\frac{a}{2}-d\sin\theta)^2} \frac{1}{a^2\sqrt{z_xz_y}}dz_y}_{\text{Double integral on } \mathcal{S}_I} + \underbrace{\int_{(\frac{a}{2}-d\cos\theta)^2}^{(\frac{a}{2}+d\cos\theta)^2} dz_x \int_0^{(\frac{a}{2}-d\sin\theta)^2} \frac{1}{2a^2\sqrt{z_xz_y}}}_{\text{Double integral on } \mathcal{S}_{II}} \\
&\quad + \underbrace{\int_0^{(\frac{a}{2}-d\cos\theta)^2} dz_x \int_{(\frac{a}{2}-d\sin\theta)^2}^{(\frac{a}{2}+d\sin\theta)^2} \frac{1}{2a^2\sqrt{z_xz_y}}dz_y}_{\text{Double integral on } \mathcal{S}_{III}} \\
&= \frac{1}{2a^2}\left[y_b^2 \arcsin\frac{\frac{a}{2}+\cos\theta}{y_b} - y_b^2\arcsin\frac{\sqrt{y_b^2-(\frac{a}{2}+d\sin\theta)^2)}}{y_b}\right. \\
&\qquad + (\frac{a}{2}+d\cos\theta)\sqrt{y_b^2-(\frac{a}{2}+\cos\theta)^2} + (\frac{a}{2}+d\sin\theta)\sqrt{y_b^2-(\frac{a}{2}+d\sin\theta)^2} \\
&\qquad \left. +\frac{3}{2}a^2 - ad(\sin\theta+\cos\theta) - 2d^2\sin\theta\cos\theta\right].
\end{aligned} \tag{3.183}
$$

$$
\begin{aligned}
F_{Y_b}(y_b) &= \iint_{\mathcal{S}_I} f^{(I)}_{Z_xZ_y}(z_x,z_y)dz_xdz_y + \iint_{\mathcal{S}_{II}} f^{(II)}_{Z_xZ_y}(z_x,z_y)dz_xdz_y + \iint_{\mathcal{S}_{III}} f^{(III)}_{Z_xZ_y}(z_x,z_y)dz_xdz_y \\
&\quad + \iint_{\mathcal{S}_{IV}} f^{(IV)}_{Z_xZ_y}(z_x,z_y)dz_xdz_y \\
&= \underbrace{\int_0^{(\frac{a}{2}-d\cos\theta)^2} dz_x \int_0^{(\frac{a}{2}-d\sin\theta)^2} \frac{1}{a^2\sqrt{z_xz_y}}dz_y}_{\text{Double integral on } \mathcal{S}_I} + \underbrace{\int_{(\frac{a}{2}-d\cos\theta)^2}^{(\frac{a}{2}+d\cos\theta)^2} dz_x \int_0^{(\frac{a}{2}-d\sin\theta)^2} \frac{1}{2a^2\sqrt{z_xz_y}}}_{\text{Double integral on } \mathcal{S}_{II}} \\
&\quad + \underbrace{\int_0^{(\frac{a}{2}-d\cos\theta)^2} dz_x \int_{(\frac{a}{2}-d\sin\theta)^2}^{(\frac{a}{2}+d\sin\theta)^2} \frac{1}{2a^2\sqrt{z_xz_y}}dz_y}_{\text{Double integral on } \mathcal{S}_{III}} + \underbrace{\int_{(\frac{a}{2}-d\cos\theta)^2}^{(\frac{a}{2}+d\cos\theta)^2} dz_x \int_{(\frac{a}{2}-d\sin\theta)^2}^{(\frac{a}{2}+d\sin\theta)^2} \frac{1}{4a^2\sqrt{z_xz_y}}dz_x}_{\text{Double integral on } \mathcal{S}_{IV}} \\
&= 1
\end{aligned} \tag{3.184}
$$

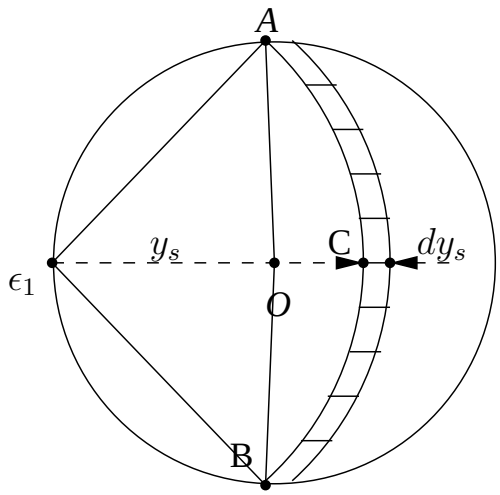

Figure 3.26: Calculate $\text{Pr}(H|\epsilon_1 \in \delta\mathcal{A})$ in the circular area $\odot(O, r)$ considered

obtain the following differential formula:

$$d\text{Pr}(\mathcal{H}) = 2\left(\frac{2y_s dy_s}{\pi r^2}\arccos\frac{y_s}{2r} - \text{Pr}(\mathcal{H})\right)\cdot\frac{2\pi r dr}{\pi r^2}. \tag{3.188}$$

Rearranging the terms in Eq.(3.188), we have the following formula:

$$r^4 d\text{Pr}(\mathcal{H}) + 4\text{Pr}(\mathcal{H})r^3 dr = \frac{8y_s dy_s}{\pi}\cdot r\arccos\frac{y_s}{2r}dr. \tag{3.189}$$

Integrating both side with respect to r, we arrive at

$$\begin{aligned} r^4\text{Pr}(\mathcal{H}) &= \frac{8y_s dy_s}{\pi}\cdot\int r\arccos\frac{y_s}{2r}dr \\ &= \frac{8y_s dy_s}{\pi}\cdot\frac{y_s^2}{8}\left[\left(\frac{2r}{y_s}\right)^2\arccos\frac{y_s}{2r} - \frac{2r}{y_s}\sqrt{1-\left(\frac{y_s}{2r}\right)^2}\right] \\ &= \frac{8r^3 dy_s}{\pi}\cdot\frac{y_s}{2r}\left[\arccos\frac{y_s}{2r} - \frac{y_s}{2r}\sqrt{1-\left(\frac{y_s}{2r}\right)^2}\right]. \end{aligned} \tag{3.190}$$

Based on the definition of the event $\mathcal{H}$, $\text{Pr}(\mathcal{H})$ can be further derived as $\text{Pr}(\mathcal{H}) = F_{Y_s}(y_s + dy_s) - F_{Y_s}(y_s)$, where $F_{Y_s}(y_s)$ is the cdf of the random distance Y_s representing the probability of Y_s being shorter than y_s. As a result, with the aid of Eq.(3.190), the pdf of the random distance Y_s can be

derived as

$$f_{Y_s}(y_s) = \lim_{dy_s \to 0} \frac{F_{Y_s}(y_s + dy_s) - F_{Y_s}(y_s)}{dy_s} = \lim_{dy_s \to 0} \frac{\Pr(\mathcal{H})}{dy_s}$$
$$= \frac{8}{\pi r} \cdot \frac{y_s}{2r} \left[\arccos \frac{y_s}{2r} - \frac{y_s}{2r} \sqrt{1 - \left(\frac{y_s}{2r}\right)^2} \right], \tag{3.191}$$

for $0 \leq y_s \leq 2r$. The theorem has been proven.

3.C.2 The proof for Lemma 3.4

The cdfs of the random variable $\Delta_{\widetilde{x}} = \widetilde{X}_1 - \widetilde{X}_2$ can be expressed as

$$F_{\Delta_{\widetilde{x}}}(\delta_{\widetilde{x}}) = \Pr(\widetilde{X}_1 - \widetilde{X}_2 \leq \delta_{\widetilde{x}}) = \iint_{\mathcal{S}} f_{\widetilde{X}_1 \widetilde{X}_2}(\widetilde{x}_1, \widetilde{x}_2) d\widetilde{x}_1 d\widetilde{x}_2, \tag{3.192}$$

where $f_{\widetilde{X}_1 \widetilde{X}_2}(\widetilde{x}_1, \widetilde{x}_2)$ is the joint pdf of $\widetilde{X}_1$ and $\widetilde{X}_2$ and $\mathcal{S}$ is the integral area surrounded by the domain of $f_{\widetilde{X}_1 \widetilde{X}_2}(\widetilde{x}_1, \widetilde{x}_2)$ and the upper part of straight line $\widetilde{x}_1 - \widetilde{x}_2 = \delta_{\widetilde{x}}$. Since $\widetilde{X}_1$ and $\widetilde{X}_2$ are independent and identical random variables, whose pdfs are both given by Eq.(3.31), $f_{\widetilde{X}_1 \widetilde{X}_2}(\widetilde{x}_1, \widetilde{x}_2)$ can be expressed as

$$f_{\widetilde{X}_1 \widetilde{X}_2}(\widetilde{x}_1, \widetilde{x}_2) = f_{\widetilde{X}_1}(\widetilde{x}_1) f_{\widetilde{X}_2}(\widetilde{x}_2) = \begin{cases} \dfrac{1}{a^2}, & 0 \leq \widetilde{x}_1, \widetilde{x}_2 \leq a, \\ 0, & \text{otherwise.} \end{cases} \tag{3.193}$$

Let us now discuss the result of the double integral Eq.(3.192) given different value of $\delta_{\widetilde{x}}$. If $\delta_{\widetilde{x}} < -a$, as shown in Figure 3.27(a), the straight line $\widetilde{x}_1 - \widetilde{x}_2 = \delta_{\widetilde{x}}$ does not intersect the square domain of the joint pdf $f_{\widetilde{X}_1 \widetilde{X}_2}(\widetilde{x}_1, \widetilde{x}_2)$. Therefore, the cdf of $\Delta_{\widetilde{x}}$ is derived as $F_{\Delta_{\widetilde{x}}}(\delta_{\widetilde{x}}) = 0$.

If $-a \leq \delta_{\widetilde{x}} < 0$, the integral area $\mathcal{S}$ is shown as the shaded part in Figure 3.27(b). Hence, the cdf of the random variable $\Delta_{\widetilde{x}}$ can be further derived from Eq.(3.192) as

$$F_{\Delta_{\widetilde{x}}}(\delta_{\widetilde{x}}) = \int_0^{\delta_{\widetilde{x}}+a} d\widetilde{x}_1 \int_{\widetilde{x}_1 - \delta_{\widetilde{x}}}^{a} \frac{1}{a^2} d\widetilde{x}_2 = \frac{(\delta_{\widetilde{x}} + a)^2}{2a^2}. \tag{3.194}$$

If $0 \leq \delta_{\widetilde{x}} < a$, the integral area $\mathcal{S}$ is shown as the shaded part in Figure 3.27(c). Hence, the cdf of the random variable $\Delta_{\widetilde{x}}$ can be further derived from Eq.(3.192) as

$$F_{\Delta_{\widetilde{x}}}(\delta_{\widetilde{x}}) = \int_0^{\delta_{\widetilde{x}}} d\widetilde{x}_1 \int_0^{a} \frac{1}{a^2} d\widetilde{x}_2 + \int_{\delta_{\widetilde{x}}}^{a} d\widetilde{x}_1 \int_{\widetilde{x}_1 - \delta_{\widetilde{x}}}^{a} \frac{1}{a^2} d\widetilde{x}_2 = \frac{a^2 + 2a\delta_{\widetilde{x}} - \delta_{\widetilde{x}}^2}{2a^2} \tag{3.195}$$

If $\delta_{\widetilde{x}} \geq a$, the integral area $\mathcal{S}$ is the whole domain of the joint pdf $f_{\widetilde{X}_1 \widetilde{X}_2}(\widetilde{x}_1, \widetilde{x}_2)$, as shown in

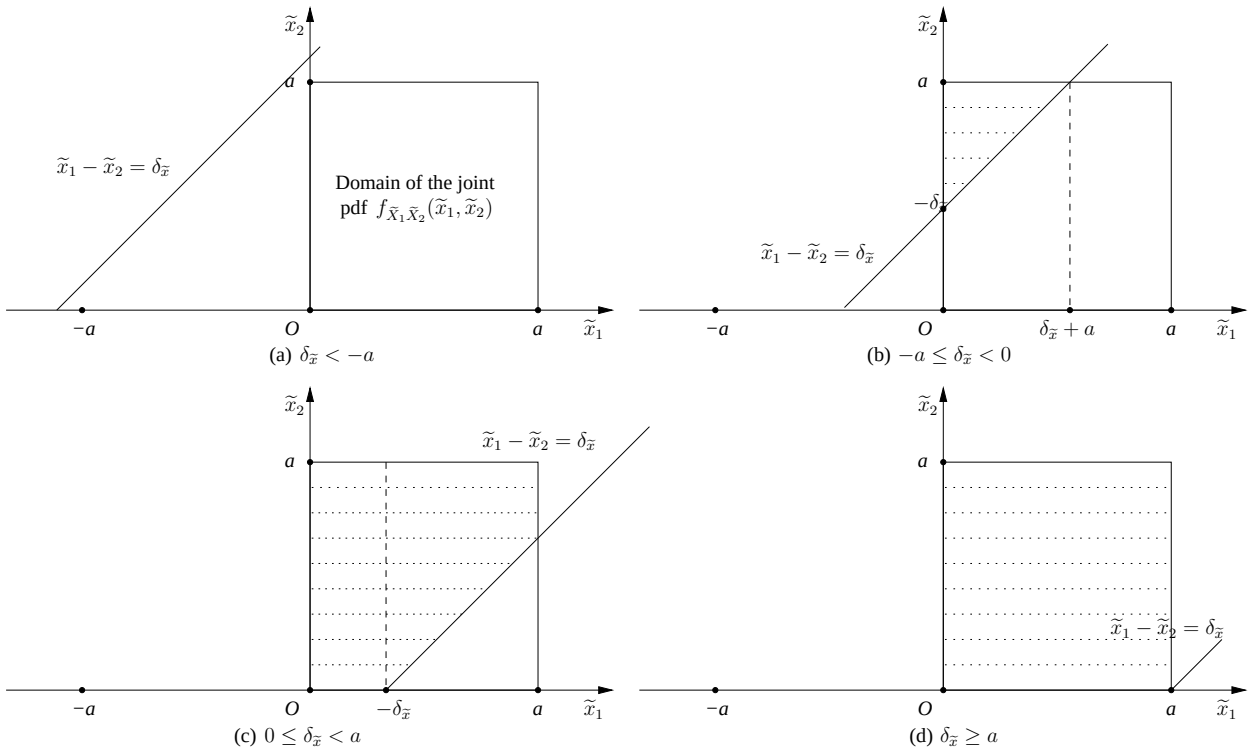

Figure 3.27: Different integral area $\mathcal{S}$ for the derivation of $F_{\Delta_{\widetilde{x}}}(\delta_{\widetilde{x}})$ given different $\delta_{\widetilde{x}}$.

Figure 3.27(d). Hence, the cdf of the random variable $\Delta_{\widetilde{x}}$ can be further derived as $F_{\Delta_{\widetilde{x}}}(\delta_{\widetilde{x}}) = 1$.

After differentiating both Eqs.(3.194) and (3.195) with respect to $\delta_{\widetilde{x}}$, we arrive at the pdf of the random variable $\Delta_{\widetilde{x}}$, as expressed in Eq.(3.33). The lemma has been proven.

3.C.3 The proof for Lemma 3.5

Given that $Z_{\widetilde{x}} = \Delta_{\widetilde{x}}^2$, the cdf of $Z_{\widetilde{x}}$ should be derived as

$$\begin{aligned} F_{Z_{\widetilde{x}}}(z_{\widetilde{x}}) &= \Pr(Z_{\widetilde{x}} \leq z_{\widetilde{x}}) = \Pr(\Delta_{\widetilde{x}}^2 \leq z_{\widetilde{x}}) = \Pr(-\sqrt{z_{\widetilde{x}}} \leq \Delta_{\widetilde{x}} \leq \sqrt{z_{\widetilde{x}}}) \\ &= F_{\Delta_{\widetilde{x}}}(\sqrt{z_{\widetilde{x}}}) - F_{\Delta_{\widetilde{x}}}(-\sqrt{z_{\widetilde{x}}}). \end{aligned} \tag{3.196}$$

If $0 \leq \sqrt{z_{\widetilde{x}}} \leq a$, which also indicates that $-a \leq \sqrt{z_{\widetilde{x}}} \leq 0$, the cdf of the random variable can be further derived from Eq.(3.196) as

$$\begin{aligned} F_{Z_{\widetilde{x}}}(z_{\widetilde{x}}) &= F_{\Delta_{\widetilde{x}}}(\sqrt{z_{\widetilde{x}}}) - F_{\Delta_{\widetilde{x}}}(-\sqrt{z_{\widetilde{x}}}) \\ &= \frac{a^2 + 2a\sqrt{z_{\widetilde{x}}} - z_{\widetilde{x}}}{2a^2} - \frac{(a - \sqrt{z_{\widetilde{x}}})^2}{2a^2} = \frac{2\sqrt{z_{\widetilde{x}}}}{a} - \frac{z_{\widetilde{x}}}{a^2}. \end{aligned} \tag{3.197}$$

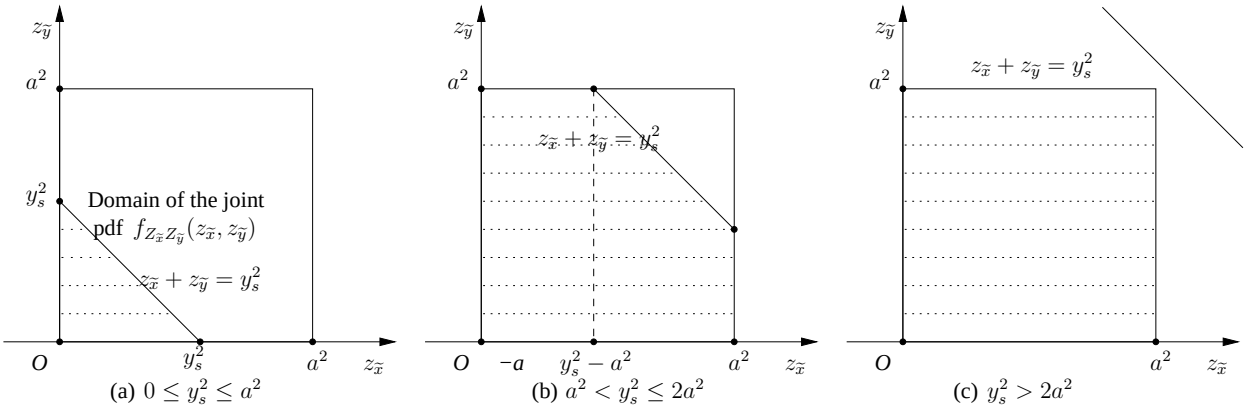

Figure 3.28: Different integral area $\mathcal{S}$ for the derivation of $F_{Y_s}(y_s)$ given different y_s.

If $\sqrt{z_{\widetilde{x}}} > a$, which also indicates that $-\sqrt{z_{\widetilde{x}}} < -a$, the cdf of the random variable can be further derived Eq.(3.196) as

$$F_{Z_{\widetilde{x}}}(z_{\widetilde{x}}) = F_{\Delta_{\widetilde{x}}}(\sqrt{z_{\widetilde{x}}}) - F_{\Delta_{\widetilde{x}}}(-\sqrt{z_{\widetilde{x}}}) = 1 - 0 = 1. \tag{3.198}$$

After differentiating both Eqs.(3.197) and (3.198) with respect to $z_{\widetilde{x}}$, we arrive at the pdf of the random variable $Z_{\widetilde{x}}$, as expressed in Eq.3.5. The lemma has been proven.

3.C.4 The proof for Theorem 3.10

Given that $Y_s = \sqrt{Z_{\widetilde{x}} + Z_{\widetilde{y}}}$, its cdf can be formulated as

$$\begin{aligned} F_{Y_s}(y_s) &= \text{Pr}(Y_s \leq y_s) = \text{Pr}(\sqrt{Z_{\widetilde{x}} + Z_{\widetilde{y}}} \leq y_s) = \text{Pr}(Z_{\widetilde{x}} + Z_{\widetilde{y}} \leq y_s^2) \\ &= \iint_{\mathcal{S}} f_{Z_{\widetilde{x}}Z_{\widetilde{y}}}(z_{\widetilde{x}}, z_{\widetilde{y}}) dz_{\widetilde{x}} dz_{\widetilde{y}}, \end{aligned} \tag{3.199}$$

where $f_{Z_{\widetilde{x}}Z_{\widetilde{y}}}(z_{\widetilde{x}}, z_{\widetilde{y}})$ is the joint pdf of the random variables $Z_{\widetilde{x}}$ and $Z_{\widetilde{x}}$, and $\mathcal{S}$ is the integral area surrounded by the domain of $f_{Z_{\widetilde{x}}Z_{\widetilde{y}}}(z_{\widetilde{x}}, z_{\widetilde{y}})$ and the lower part of the straight line $z_{\widetilde{x}} + z_{\widetilde{y}} = y_s$. Since $Z_{\widetilde{x}}$ and $Z_{\widetilde{x}}$ are independent and identical random variables, their joint pdf can be expressed as

$$f_{Z_{\widetilde{x}}Z_{\widetilde{y}}}(z_{\widetilde{x}}, z_{\widetilde{y}}) = \begin{cases} \dfrac{1}{a^2}\left(\dfrac{1}{\sqrt{z_{\widetilde{x}}}} - \dfrac{1}{a}\right)\left(\dfrac{1}{\sqrt{z_{\widetilde{y}}}} - \dfrac{1}{a}\right), & 0 \leq z_{\widetilde{x}}, z_{\widetilde{y}} \leq a^2, \\ 0, & \text{otherwise.} \end{cases} \tag{3.200}$$

Given different value of y_s^2, we have different integral area $\mathcal{S}$ for calculating the cdf of Y_s. If we have $0 \leq y_s^2 \leq a^2$, as shown in Figure 3.28(a), which indicates that $0 \leq y_s \leq a$, the double integral of Eq.(3.199) can be further derived as

$$\begin{aligned} F_{Y_s}(y_s) &= \int_0^{y_s^2} dz_{\widetilde{x}} \int_0^{y_s^2 - z_{\widetilde{x}}} \frac{1}{a^2} \left(\frac{1}{\sqrt{z_{\widetilde{x}}}} - \frac{1}{a} \right) \left(\frac{1}{\sqrt{z_{\widetilde{y}}}} - \frac{1}{a} \right) dz_{\widetilde{y}} \\ &= \frac{1}{a^2} \left(\pi y_s^2 - \frac{8y_s^3}{3a} + \frac{y_s^4}{2a^2} \right). \end{aligned} \tag{3.201}$$

If we have $a^2 < y_s^2 \leq 2a^2$, as shown in Figure 3.28(b), which indicates that $a < y_s \leq \sqrt{2}a$, the double integral of Eq.(3.199) can be further derived as

$$\begin{aligned} F_{Y_s}(y_s) &= \int_0^{y_s^2 - a^2} dz_{\widetilde{x}} \int_0^{a^2} \frac{1}{a^2} \left(\frac{1}{\sqrt{z_{\widetilde{x}}}} - \frac{1}{a} \right) \left(\frac{1}{\sqrt{z_{\widetilde{y}}}} - \frac{1}{a} \right) dz_{\widetilde{y}} \\ &\quad + \int_{y_s^2 - a^2}^{a^2} dz_{\widetilde{x}} \int_0^{y_s^2 - z_{\widetilde{x}}} \frac{1}{a^2} \left(\frac{1}{\sqrt{z_{\widetilde{x}}}} - \frac{1}{a} \right) \left(\frac{1}{\sqrt{z_{\widetilde{y}}}} - \frac{1}{a} \right) dz_{\widetilde{y}} \\ &= \frac{1}{a^2} \left[2y^2 \arcsin \frac{2a^2 - y_s^2}{y_s^2} + \left(\frac{4}{3}a + \frac{8}{3a} y_s^2 \right) \sqrt{y_s^2 - a^2} - 2y_s^2 - \frac{y^4}{2a^2} + \frac{a^2}{3} \right] \end{aligned} \tag{3.202}$$

If we have $y_s^2 > 2a^2$, as shown in Figure 3.28(c), which indicates that $y_s > \sqrt{2}a$, the integral area is the whole domain of the joint pdf $f_{Z_{\widetilde{x}} Z_{\widetilde{y}}}(z_{\widetilde{x}}, z_{\widetilde{y}})$. As a result, the cdf of the random distance Y_s is derived as $F_{Y_s}(y_s) = 1$.

In a nutshell, the cdf of the random distance Y_s between a pair of MUs that move within a square area by obeying the uniform mobility model can be summarised as Eq.(3.35). After differentiating the cdf $F_{Y_s}(y_s)$ of Eq.(3.35) with respect to y_s, we arrive at the pdf of the random distance Y_s, which is expressed as Eq.(3.36). The theorem has been proven.

Bibliography

[1] Y. S. Soh, T. Q. S. Quek, M. Kountouris, and H. Shin, "Energy Efficient Heterogeneous Cellular Networks," *IEEE Journal on Selected Areas in Communications*, vol. 31, pp. 840–850, May 2013.

[2] Shanzhi Chen and Jian Zhao, "The requirements, challenges, and technologies for 5G of terrestrial mobile telecommunication," *IEEE Communications Magazine*, vol. 52, pp. 36–43, May 2014.

[3] C. Shin, H. Park, and H. M. Kwon, "PHY-Supported Frame Aggregation for Wireless Local Area Networks," *IEEE Transactions on Mobile Computing*, vol. 13, pp. 2369–2381, Oct. 2014.

[4] D. Fooladivanda and C. Rosenberg, "Joint Resource Allocation and User Association for Heterogeneous Wireless Cellular Networks," *IEEE Transactions on Wireless Communications*, vol. 12, pp. 248–257, Jan. 2013.

[5] K. Shen and W. Yu, "Distributed Pricing-Based User Association for Downlink Heterogeneous Cellular Networks," *IEEE Journal on Selected Areas in Communications*, vol. 32, pp. 1100–1113, June 2014.

[6] S. Singh and J. G. Andrews, "Joint Resource Partitioning and Offloading in Heterogeneous Cellular Networks," *IEEE Transactions on Wireless Communications*, vol. 13, pp. 888–901, Feb. 2014.

[7] B. H. Jung, N.-O. Song, and D. K. Sung, "A Network-Assisted User-Centric WiFi-Offloading Model for Maximizing Per-User Throughput in a Heterogeneous Network," *IEEE Transactions on Vehicular Technology*, vol. 63, pp. 1940–1945, May 2014.

[8] R. L. Streit, *Poisson Point Processes*. Boston, MA: Springer US, 2010.

[9] H. Zhuang and T. Ohtsuki, "A Model Based on Poisson Point Process for Analyzing MIMO Heterogeneous Networks Utilizing Fractional Frequency Reuse," *IEEE Transactions on Wireless Communications*, vol. 13, pp. 1–1, Dec. 2014.

[10] J. Wen, M. Sheng, X. Wang, J. Li, and H. Sun, "On the Capacity of Downlink Multi-Hop Heterogeneous Cellular Networks," *IEEE Transactions on Wireless Communications*, vol. 13, pp. 4092–4103, Aug. 2014.

[11] R. W. Heath, M. Kountouris, and T. Bai, "Modeling Heterogeneous Network Interference Using Poisson Point Processes," *IEEE Transactions on Signal Processing*, vol. 61, pp. 4114–4126, Aug. 2013.

[12] C.-h. Lee and M. Haenggi, "Interference and Outage in Poisson Cognitive Networks," *IEEE Transactions on Wireless Communications*, vol. 11, pp. 1392–1401, Apr. 2012.

[13] H. S. Chiu and K. L. Yeung, "J-CAR: An efficient joint channel assignment and routing protocol for IEEE 802.11-based multi-channel multi-interface mobile Ad Hoc networks," *IEEE Transactions on Wireless Communications*, vol. 8, pp. 1706–1715, Apr. 2009.

[14] J. Haartsen and S. Mattisson, "Bluetooth-a new low-power radio interface providing short-range connectivity," *Proceedings of the IEEE*, vol. 88, pp. 1651–1661, Oct. 2000.

[15] N. Lee, X. Lin, J. Andrews, and R. Heath, "Power Control for D2D Underlaid Cellular Networks: Modeling, Algorithms and Analysis," *IEEE Journal on Selected Areas in Communications*, vol. PP, no. 99, pp. 1–1, 2014.

[16] M. Neely and E. Modiano, "Capacity and Delay Tradeoffs for Ad Hoc Mobile Networks," *IEEE Transactions on Information Theory*, vol. 51, pp. 1917–1937, June 2005.

[17] G. Sharma, R. Mazumdar, and N. Shroff, "Delay and Capacity Trade-Offs in Mobile Ad Hoc Networks: A Global Perspective," *IEEE/ACM Transactions on Networking*, vol. 15, pp. 981–992, Oct. 2007.

[18] T. Rappaport, *Wireless Communications: Principles and Practice*. Upper Saddle River, NJ, USA: Prentice Hall PTR, 2nd ed., 2001.

[19] Z. Gong and M. Haenggi, "Interference and Outage in Mobile Random Networks: Expectation, Distribution, and Correlation," *IEEE Transactions on Mobile Computing*, vol. 13, pp. 337–349, Feb. 2014.

[20] N. Abramson, "THE ALOHA SYSTEM," in *Proceedings of the November 17-19, 1970, fall joint computer conference on - AFIPS '70 (Fall)*, (New York, New York, USA), p. 281, ACM Press, Nov. 1970.

[21] C. E. Shannon, "A mathematical theory of communication," *The Bell System Technical Journal*, vol. 27, p. 3, July 1948.

[22] J. M. Bernardo and A. F. Smith, *Bayesian theory*. Chichester : John Wiley, 2000.

[23] W. Gander and W. Gautschi, "Adaptive QuadratureRevisited," *BIT Numerical Mathematics*, vol. 40, pp. 84–101, Mar. 2000.

[24] C.-h. Liu and J. Andrews, "Multicast outage probability and transmission capacity of multihop wireless networks," *IEEE Transactions on Information Theory*, vol. 57, no. 7, pp. 4344–4358, 2011.

[25] L. E. Miller, "Joint Distribution of Link Distances," in *2003 Conference on Information Sciences and Systems*, pp. 1–2, The Johns Hopkins University, Mar. 2003.

[26] Chih-Cheng Tseng, Hsuan-Tsang Chen, and Kwang-Cheng Chen, "On The Distance Distributions of The Wireless Ad Hoc Networks," in *2006 IEEE 63rd Vehicular Technology Conference*, vol. 2, pp. 772–776, IEEE, May 2006.

[27] R. Zhang, Z. Zheng, M. Wang, X. Shen, and L.-L. Xie, "Equivalent Capacity in Carrier Aggregation-Based LTE-A Systems: A Probabilistic Analysis," *IEEE Transactions on Wireless Communications*, vol. 13, pp. 6444–6460, Nov. 2014.

[28] "Information technology–telecommunications and information exchange between systems local and metropolitan area networks–specific requirements part 11: Wireless LAN Medium Access Control (MAC) and Physical Layer (PHY) Specifications," *ISO/IEC/IEEE 8802-11:2012(E)*, pp. 1–2798, November 2012.